Aus dem
Helmholtz-Zentrum München
Institute of Lung Health and Immunity (LHI)

Nanocarriers for cell-specific targeting in the lung and development of an in vivo validated invitro screening platform of drug uptake and release

Dissertation
zum Erwerb des Doctor of Philosophy (Ph.D.) an der Medizinischen Fakultät der Ludwig-Maximilians-Universität München

vorgelegt von
Mehwish Ishaque

aus
Islamabad / Pakistan

Jahr
2025

Mit Genehmigung der Medizinischen Fakultät der
Ludwig-Maximilians-Universität München

Erstes Gutachten:	Prof. Dr. Silke Meiners
Zweites Gutachten:	Dr. Tobias Stöger
Drittes Gutachten:	Prof. Dr. Bianca Schaub
Viertes Gutachten:	Prof. Dr. Amanda Tufman

Dekan: Prof. Dr. med. Thomas Gudermann

Tag der mündlichen Prüfung: 08.05.2025

Table of content

Table of content **3**

Abstract (English): **5**

List of tables **11**

List of abbreviations **12**

1. Introduction **15**

1.1 Nanomedicine 15
1.1.1 Advantages of nanomedicine 15
1.2 General overview of nanoparticles 16
1.3 The Respiratory system 17
1.3.1 Anatomy of the Respiratory System 17
1.4 Deposition of Particles in the Lungs 21
1.5 Clearance mechanism 23
1.6 Cellular uptake pathways of nanoparticles: 25
1.7 Nanoparticles-based systems for pulmonary applications: 27
1.7.1 Solid lipid nanoparticles (SLN): 27
1.7.2 Polymeric nanoparticles 29
1.7.3 Liposomes 30
1.8 Effects of size and surface modification of nanoparticles mediated targeted delivery of cells: 31
1.9 Toxicity endpoints after pulmonary delivery 33
1.10 *In vitro* models of nanoparticle delivery 34
1.11 Key Objectives of the study 37

2. Material and Methods **38**

2.1 Materials 38
2.1.1 Nanoparticles: 38
2.1.2 Mice: 38
2.1.3 Commercially available kits and reagents: 39
2.1.4 Equipment and General Consumables 39
2.1.5 Softwares: 41
2.1.6 Chemicals: 41
2.2 Methods 42
2.2.1 Nanoparticle Characterization: 42
2.2.2 Cell cultures 43
2.2.3 Exposure of monocultures and co-cultures to particles: 43
2.2.4 Particle Uptake Analysis 46
2.2.5 Cytotoxicity Testing 47
2.2.6 In vivo Experiments: 48

2.2.7 Statistical Analysis: 50
2.2.8 Experimental design of the project 51

3. Results 53

3.1 The uptake and toxicity of different sizes and surface-modified Polystyrene (PS) latex beads by different alveolar cell types in submerged and Air-liquid interface exposure systems 53
3.1.1 Particle Characterization 54
3.1.2 PS Particle Uptake 57
3.1.3 Quantification of particle uptake based on the number of cells that have taken up particles. 75
3.1.4 Effects of Surface-modified PS Particles Exposure on Cell viability and cytotoxicity: 77
3.1.5 Summary: Correlation between PS Positive cells and toxicity: 84
3.2 The uptake of PLGA particles by alveolar macrophages and epithelial cells depends on the exposure scenario 90
3.2.1 Particle characterization 91
3.2.2 PLGA particle uptake: 92
3.2.3 Effects of PLGA particle exposure on Cell viability and cytotoxicity: 105
3.2.4 Cellular uptake of PLGA particles in an intratracheally instilled mouse model: 107

4. Discussion 114

4.1 The uptake and toxicity of different sizes and surface-modified PS latex beads by different alveolar cell types in submerged and Air-liquid interface exposure systems 114
4.2 The uptake of PLGA particles by alveolar macrophages and epithelial cells depends on the exposure scenario: Validation of this co-culture setup's uptake pattern of nanoparticles *in vivo* by intratracheal instillation of nanoparticles in mice. 121

References 128

Acknowledgments 136

Affidavit 137

Confirmation of congruency 138

Curriculum vitae ..... Error! Bookmark not defined.

List of publications ..... Error! Bookmark not defined.

Abstract (English):

Over the past few decades, there has been a remarkable increase in the utilization of nanomaterials/particles in various industries, including textiles, information technology, food, electronics, and medical sciences. Nanoparticle-mediated drug delivery is an emerging therapeutic approach for various respiratory diseases. Several forms of nano-carriers, such as polymeric, liposomes, carbon, gold, micelles, and biological particles, are used for targeted drug delivery. The nanocarrier must be stable, biocompatible, and biodegradable for successful drug delivery to targeted cells. The alveolar epithelium has a large surface area and is a significant drug interaction and absorption target. Nanocarrier-mediated drug delivery has the advantage of delivering a high concentration of drugs to the targeted cells, such as alveolar epithelial cell types (AT I and AT II) and alveolar macrophages.

Most studies have investigated the cellular interaction of particles through animal models, which can be expensive and time-consuming. To avoid animal models, in vitro exposure methods provide an efficient way to study these interactions and their effects on the cellular level. This study used conventional submerged and air-liquid interface (ALI) exposure systems to observe the targeted delivery of particles to the alveolar cells. The thesis is divided into two studies with different objectives.

The first section of this study aimed to investigate the cell-specific uptake of different-sized and anionic or cationic fluorescent-labeled polystyrene latex particles (PS) as carrier surrogates and their toxicological side effects in different in vitro exposure systems. The study used alveolar epithelial cells and macrophages in conventional submerged and air-liquid interface (ALI) culture setups. Submerged exposures are more accessible to perform, but ALI exposures are more physiologically realistic and potentially more biologically meaningful.

Amine-surface modified (PS NH2) (0.1 and 1 µm), carboxyl-surface modified (PS COOH) (0.03, 0.5, and 1 µm), and sulfate-surface modified (PS SO4) (0.1 and 0.5 nm) polystyrene latex beads (PS) were studied. The LA-4 (epithelial, type II-

like mouse lung adenoma cells) and MH-S (immortalized mouse alveolar macrophages) murine cell lines were exposed to polystyrene latex beads for 24 hours at 37°C in both ALI and submerged conditions, and the uptake was quantified using mean fluorescence intensity per cell assessed by flow cytometry. Cells were also evaluated for cell viability (WST assay) and cytotoxicity (LDH assay) after 24 hours of exposure.

The study found that in submerged conditions, epithelial cells most effectively took up larger COOH-PS and NH2-PS particles (1 µm). At the same time, macrophages internalized 1 µm carboxyl-PS particles the best, and sulfate-surface modified PS particles showed a minor uptake for all cell types. However, regardless of surface modifications, all cell lines showed stronger uptake signals at the air-liquid interface, especially for 1 µm particles. The study also found that toxicity results differed between submerged and air-liquid interface culture conditions, with more toxicity observed in air-liquid interface conditions for all particles. The amine-surface modification, especially at 0.1 µm, was identified as the most toxic modification for all cell types, particularly for macrophages. These results suggest cell-targeting studies using nano-carriers should be conducted in an air-liquid interface miming the respiratory surface.

To determine their cell-specific uptake, the study's second section investigated the uptake of differently sized fluorescently labeled biodegradable PLGA particles in various models (in vitro and in vivo). I chose to use PLGA particles instead of PS particles because PS particles cannot provide controlled release of encapsulated drugs or exhibit biocompatible properties and are non-biodegradable, non-bioabsorbable, and non-biocompatible. Therefore, their use is limited in biomedical applications that involve interaction with biological systems. However, PS particles are widely used in basic research due to their low cost, ease of preparation, and uniform size. Nevertheless, for biomedical purposes, alternative materials like biodegradable polymers (e.g., PLGA) or natural polymers (e.g., chitosan, alginate) are more appropriate because they provide excellent biocompatibility and controlled drug release capabilities. The study exposed monocultures and co-cultures of alveolar epithelial and alveolar macrophage cell lines to different-sized PLGA particles under conventional submerged or air-liquid interface

conditions and compared the uptake efficacy with that observed in the lungs of mice. The study investigated 0.1 µm, 0.5 µm, and 1 µm PLGA particles. I studied the effects of PLGA particles on mouse lung cells in vitro and in vivo. I used LA-4 and MH-S cell lines in monocultures and co-cultures and exposed them to PLGA particles for 24 hours under submerged and ALI conditions. I also exposed C57BL/6J mice to PLGA particles (sizes: 0.1 and 1 µm) via intratracheal instillation and analyzed them after 24 hours. We used confocal microscopy and flow cytometry to monitor and quantify particle uptake. Our results showed that particle uptake varied based on particle size and cell type and was influenced by culture conditions. In a submerged state, epithelial cells exhibited the highest uptake of the largest particles (1.0 µm), whereas macrophages were equally effective at taking up particles of 0.5 µm and 1.0 µm. However, under ALI conditions, there was a significantly high uptake of all particle sizes (0.1 µm, 0.5 µm, and 1 µm) by LA-4 cells in both monoculture and co-culture scenarios and also a significantly higher uptake of smaller particles of 0.1 and, 0.5 µm size as compared to 1 µm particles by MH-S cells. When 0.1 and 1 µm particles were delivered to mouse lungs, AT2 cells showed the most significant uptake for 0.1 µm particles, followed by 1 µm particles. In comparison, alveolar macrophages showed the most considerable uptake of 1 µm particles, followed by 0.1 µm particles. The absence of toxicity of these particles was observed in both in vitro and in vivo experimental settings. In conclusion, our study suggests that the correlation between particle uptake in the ALI co-culture system and in vivo epithelial cells varies depending on the cell type and particle size. While the results were similar for smaller particles, a different pattern of particle uptake was observed in BAL macrophages and AT2 cells for larger particles. Therefore, more research is needed to understand the underlying factors contributing to these discrepancies, including cell type and dose, to improve the accuracy of in vitro models for predicting in vivo particle uptake.

List of Figures

Figure 1-1 Respiratory tract: cell types and morphology. [11] 22

Figure 1-2 Schematic diagram showing the size-dependent deposition of particles in the lungs.[12] 23

Figure 1-3 Entry of NPs into the cell using different endocytotic pathways. a Macropinocytosis and phagocytosis. b Clathrin-mediated endocytosis, clathrin-caveolin independent endocytosis, and caveolae-mediated endocytosis [41] 27

Figure 1-4 Different ways of culture: Cell grown at the bottom of a well and exposed to NPs suspended in medium (a). In the culture at an air-liquid interface, cells are grown on membranes and supplied with nutrients from the basal side. In this culture, respiratory cells secrete pulmonary surfactant (blue line). Cells are exposed to NPs applied as aerosols (b). AC: alveolar cell. 36

Figure 2-1 Graphical representation of the experimental design of the project. 52

Figure 3-1 Characterization of PS Particles: Relative mean fluorescent intensities of the particles measured by plate reader. 55

Figure 3-2 The histogram generated from flow cytometry distinguishes the number of particles absorbed per cell. The mean fluorescent intensity measured in the PE channel indicates the cells' uptake of the particles. 57

Figure 3-3 Analysis of cellular uptake kinetics of 0.03µm, 0.5µm, and 1µm carboxyl, 0.1µm, and 1µm amine, and 0.1µm and 0.5µm sulfate-modified polystyrene (PS) particles alveolar epithelial and macrophages cells by flow cytometry after 4 and 24 hours. Mean fluorescent intensities show a. uptake of particles by MLE 12 cells. b. uptake of particles by A549 cells, c. uptake of particles by LA-4 cells, and d. uptake of particles by MH-S cells submerged in monoculture conditions. 60

Figure 3-4 Analysis of cellular uptake of 0.03 µm, 0.5 µm, and 1 µm carboxyl-modified polystyrene (PS) particles; 0.1 µm and 1 µm amine-modified PS particles; and 0.1 µm and 0.5 µm sulfate-modified PS particles in alveolar epithelial and macrophage cells by flow cytometry after 24 hours. The mean fluorescent intensities in positively gated histograms indicate a. uptake of particles by MLE-12 cells, b. uptake of

particles by A549 cells, c. uptake of particles by LA-4 cells, and d. uptake of particles by MH-S cells under submerged conditions in monoculture. 67

Figure 3-5 Analysis of cellular uptake of 0.03µm, 0.5µm, and 1µm carboxyl, 0.1µm, and 1µm amine, and 0.1µm, and 0.5µm sulfate-modified polystyrene (PS) particles alveolar epithelial and macrophages cells by flow cytometry after 24 hours in ALI conditions. The mean fluorescent intensities in positively gated histograms indicate a. uptake of particles by MLE 12 cells. b. uptake of particles by A549 cells, c. uptake of particles by LA-4 cells, and d. uptake of particles by MH-S cells under Air-liquid interface (ALI) conditions in monoculture.....74

Figure 3-6 Heat maps to show the cellular uptake of 0.03µm, 0.5µm, and 1µm COOH, 0.1µm, and 1µm NH2, and 0.1µm and 0.5µm SO4 (PS) particles by alveolar epithelial and macrophages cells by flow cytometry after 24 h. **a.** Percentages of PS-positive cells in submerged conditions and **b.** in ALI conditions 77

Figure 3-7 Effects of PS particles of all sizes on cell viability and cytotoxicity in submerged conditions. **a.** WST conversion into formazan, **b.** LDH release from cells compared to positive controls. Data were analyzed by 1-way ANOVA, the groups compared to the control group.....81

Figure 3-8 Kinetics of MHS cell death after exposure to 50µg/ml of amine-modified particles. 82

Figure 3-9 Effects of PS particles of all sizes on cell viability and cytotoxicity in ALI conditions. a. WST conversion into formazan, b. LDH release from cells compared to positive controls. Data were analyzed by 1-way ANOVA, the groups compared to the control group. 84

Figure 3-10 Summary: Correlation between PS-positive cells and toxicity. a) Submerged conditions, b) ALI conditions. (n=3).....90

Figure 3-11 Analysis of cellular uptake of 0.1 µm, 0.5 µm, and 1 µm PLGA nanoparticles in monocultures of LA-4 and MH-S cells by flow cytometry after 24 hours of incubation. Positively gated histograms showing mean fluorescent intensities indicate **a.** uptake of particles by LA-4 and MH-S cells in submerged monoculture conditions, and **b.** uptake of particles by LA-4 and MH-S cells under air-liquid interface (ALI) conditions in monocultures. Data were analyzed by multiple comparisons in 2-way ANOVA, and the groups were compared.....96

Figure 3-12 Analysis of cellular uptake of 0.1 µm, 0.5 µm, and 1 µm PLGA nanoparticles in co-cultures of LA-4 and MH-S cells by flow cytometry after 24 hours of incubation. Positively gated dot-plots showing mean fluorescent intensities indicate **a.** uptake of particles by LA-4 and MH-S cells in submerged coculture conditions, and **b.** uptake of particles by LA-4 and MH-S cells under air-liquid interface (ALI) conditions in

cocultures. Data were analyzed by multiple comparisons in 2-way ANOVA, and the groups were compared. 98

Figure 3-13 Analysis of cellular uptake of 0.1 µm, 0.5 µm, and 1 µm PLGA nanoparticles in monocultures of LA-4 and MH-S cells by confocal microscopy after 24 hours of incubation. Fluorescent images depict the uptake of particles by LA-4 and MH-S cells under submerged and ALICE-CLOUD monoculture conditions. Stainings: Dapi nuclear staining (Blue), PLGA particles (Green), and F actin staining (red). 102

Figure 3-14 Analysis of cellular uptake of 0.1 µm, 0.5 µm, and 1 µm PLGA nanoparticles in co-cultures of LA-4 and MH-S cells by confocal microscopy after 24 hours of incubation. Fluorescent images depict the uptake of particles by LA-4 and MH-S cells under both submerged and ALICE-CLOUD co-culture conditions. In the images, flat oval nuclei representing LA-4 cells are indicated by yellow arrows, while round dark blue nuclei representing MH-S cells are indicated by green arrows. Staining details: DAPI nuclear staining (blue), PLGA particles (green), and F-actin staining (red). 105

Figure 3-15 Effects of PLGA particles of different sizes on cell viability and cytotoxicity. **a.** WST assay showing viability, and **b**. LDH release from cells (cytotoxicity) compared to positive controls. Data were analyzed using one-way ANOVA, with comparisons to the control group. 107

Figure 3-16 Cellular compositions in bronchoalveolar lavage (BAL) fluid 24 hours after intratracheal instillation of 50 µg of 0.1 µm and 1 µm PLGA particles. Data were analyzed using one-way ANOVA, with comparisons made against the control group. 109

Figure 3-17 Histological images of mice lungs (20x) showing PLGA particles after 24 hours of intratracheal instillation of 50 µg of 0.1 µm and 1 µm PLGA particles. 110

Figure 3-18 Analysis of cellular uptake of 0.1 µm, 0.5 µm, and 1 µm PLGA nanoparticles in mice (C57BL/6J) alveolar epithelial type 2 (AT2) cells and alveolar macrophages by flow cytometry and fluorescence microscopy after 24 hours of intratracheal instillation. Mean fluorescent intensities indicate **a.** uptake of particles by BAL macrophages and **b.** uptake of particles by EpCAM-positive AT2 cells. Data were analyzed by one-way ANOVA, with comparisons made between the groups. **c.** Fluorescence microscopy (20x) images show the uptake of particles in BAL macrophages, with DAPI nuclear staining (blue) and F-actin staining (red). 113

List of tables

Table 1 **Characterization of PS Particles**. DLS Values of Average diameter with standard deviations of PS particles 54

Table 2 **Characterization of PLGA Particles**. DLS Values of Average diameter of PLGA particles, Standard deviations and mean fluorescent intensities of the particles....92

List of abbreviations

7AAD	7-amino actinomycin
AC	Alveolar cells
ALI	Air liquid interface
ALICE	Air Liquid Interface Cell Exposure
ARDS	acute respiratory distress syndrome
AT I	Alveolar epithelial cells type 1
AT II	Alveolar epithelial cells type 2
ATP	Adenosine Triphosphate
Au	Silver
BAL	bronchoalveolar lavages
CEES	2-chloroethyl ethyl sulphide
CO2	Carbon dioxide
DHA	Docosahexaenoic acid
DLS	Dynamic Light Scattering
DMEM	Dulbecco's Modified Eagle Medium
DPBS	Dulbecco's phosphate-buffered saline
DPI	Dry powder inhalers
DSPE	poly (ethylene oxide)-block-do stearoyl phosphatidylethanolamine
EDTA	ethylenediaminetetraacetic acid
ELISA	enzyme-linked immunoassay
FACS	fluorescence-activated cell sorting
FCS	Fatal Calf Serum
FDA	Food and Drug Administration
FITC	Fluorescein isothiocyanate
H&E	Haematoxylin and eosin
HBA	hydroxy benzyl alcohol
HCL	Hydrochloric acid

IL 8	Interleukin 8
IVC	individually ventilated cages
LA 4	epithelial, type II-like mouse lung adenoma cells)
LDH	lactate dehydrogenase
M1	alveolar macrophages type 1
M2	alveolar macrophages type 2
MDI	Meter dose inhalers
MFI	Mean fluorescent intensity
MHS	mouse alveolar macrophages
MTT	3-(4,5-dimethylthiazol-2-yl)-2,5-diphenyl-2H-tetrazolium bromide
NaCl	Sodium chloride
NP	Nanoparticle
PBS buffer	Phosphate Buffer Saline
PCL	poly(ε-caprolactone)
PE	Phycoerythrin
PEG	Polyethylene glycol
PLA	Polylactic acid
PLGA	poly (lactic-co-glycolic acid)
pmAECs	primary mouse alveolar cells
PS	Polystyrene particles
PS COOH	Carboxyl-modified polystyrene particles
PS NH2	Amine-modified polystyrene particles
PS SO4	Sulfate-modified polystyrene particles
QDs	Quantum dots
SLF	simulated lung fluid
SLM	Solid lipid microparticles
SLN	Solid lipid nanoparticles
TNF	Tumour necrosis factor

Transparent PET membrane	Polyester
WST 1	Water-soluble Tetrazolium salt
XTT	(2,3-bis-(2-methoxy-4-nitro-5-sulfophenyl)-2 H -tetrazolium-5-carboxanilide)

1. Introduction

1.1 Nanomedicine

Nanoscale technology development represents a remarkable achievement in disease diagnosis, treatment, and prevention. Nanotechnology is based on manipulating atoms and molecules to create nanoscale structures, such as nanoparticles. This technology has been applied across various industries, including food, agriculture, animal, microelectronics, natural chemistry, and health industries, explicitly focusing on medicine known as nanomedicine. The utilization of nanomaterials to diagnose, monitor, prevent, control, and treat diseases is known as nanomedicine. [1,3].

Because of their small size, nanoparticles can cross barriers within the body and interact with biomolecules, making them useful for drug delivery. However, before nanomedicine can assist patients, it must be evaluated for toxicity and undergo clinical trials. Nanomedicine has the potential to provide improved and cost-effective medical care, making medicines and therapies widely accessible and affordable [2]. The present obstacle and constraint faced in the field of nanomedicine pertain to the correlation between the toxicological implications of nanoscale materials and their ecological consequences [4].

1.1.1 Advantages of nanomedicine

Utilizing nanoparticles for medical assessments in vitro and in vivo can significantly enhance these procedures' efficiency and effectiveness. This is achieved through the interaction of the nanoparticles with organic particles or structures, allowing for the creation of nanocarriers for drug delivery, new treatments, and in-vivo imaging.

One key advantage of using nanoparticles in these clinical applications is their size. Due to their small size, nanoparticles are more accessible to move within the body and have faster response times to biochemical changes, making them more delicate and efficient than traditional drug delivery methods. This allows for the targeted delivery of medications to specific body cells, improving the overall outcome of the treatment [3, 5].

However, regulating drug delivery using nanoparticle carriers is a complex process that depends on several factors. These include proper confinement of the drug, efficient transportation to the desired body region, and successful delivery into the body. Ensuring these factors are appropriately addressed is crucial for successfully implementing nanotechnology in the medical field [5].

1.2 General overview of nanoparticles

Recently, there has been growing interest in drug delivery systems using nanoparticles, particles ranging from 1 to 1,000 nm in size. Utilizing these nanoparticles in drug delivery offers several benefits over traditional drug delivery systems, such as higher stability, targeted specificity, and the ability to deliver hydrophilic and hydrophobic drugs. The unique physical and chemical properties of nanoparticles, such as size, surface properties, shape, composition, molecular weight, purity, stability, and solubility, play a crucial role in determining their behavior within the body. It is essential to thoroughly characterize nanomaterials to ensure their quality and safety and to support the development of nanomedicine rationally [6]. Nanoparticles have gained significant attention as effective carriers for administering various drugs through different routes. One of the most well-researched systems is Solid Lipid Nanoparticles (SLN), which are aqueous suspensions at the nanoscale created from a mixture of phospholipids and triglycerides. In addition to SLN, biodegradable polymeric nanoparticles have also been recognized for their potential in providing sustained drug release [7, 8].

Nanoparticle-based drug delivery systems offer new opportunities for improving drug efficacy. By manipulating the physical properties of the particles, such as enhancing drug solubility, improving encapsulation effectiveness, and modifying the surface to alter drug release profiles, these systems aim to achieve optimal therapeutic outcomes. For diagnostic and therapeutic purposes, nanoparticles can be delivered to the body through various routes such as inhalation, oral, parenteral, or dermal. While the use of nanoparticles for drug delivery holds great potential, it is essential to note that it can also lead to adverse effects and toxicity. The lungs, one of the most vulnerable organs that can be affected by the interaction of nanoparticles, have been widely studied regarding toxic effects, mainly

inorganic particles such as titanium dioxide, silica, carbon nanotubes, and silver [9,10]. These particles have been reported to cause toxicological effects following lung exposure. However, due to its large surface area and efficient absorption rate, the pulmonary route is viewed as a noninvasive method for delivering drugs using nanocarriers. These attributes offer many advantages over conventional oral administration, making it possible to deliver drugs precisely while reducing the risk of adverse effects [13].

Therefore, it is crucial to understand the anatomy and function of the lungs to comprehend how a drug formulation is taken up and cleared.

1.3 The Respiratory system

The human respiratory system is a biological system that plays a crucial role in exchanging gases between the body and the environment. It comprises various organs, including the nose, pharynx, larynx, trachea, bronchi, bronchioles, lungs, and muscles responsible for breathing.

The respiratory system's primary function is to facilitate gaseous exchange, which takes place in the capillaries surrounding the alveoli. It is responsible for delivering oxygen to the body's tissues and for removing carbon dioxide waste from the body. By doing so, the respiratory system helps to maintain a balance of gases necessary for optimal body function. [13].

1.3.1 Anatomy of the Respiratory System

The human respiratory tract boasts a significant surface area of 150 square meters, making it an ideal location for absorption, gas exchange, and circulation. The lungs are widely considered to be the best route for non-invasive drug targeting, as drugs can be delivered directly to the alveolar region. This form of local drug delivery holds great promise in treating respiratory diseases and reduces the risk of systemic toxicity. [15].

Drug delivery through the pulmonary route is more advantageous than oral delivery, as the lung has a dense vasculature and a lower concentration of drug-metabolizing enzymes. For instance, drug-targeted delivery to immune cells in the pulmonary compartment via nanoparticles can minimize side effects. Nanoparticles can deliver drugs to the entire lung surface or specific cell populations in the lungs. [15].

A thorough understanding of the anatomy of the lungs is crucial for understanding the interaction between nanoparticles and immune cells.

The respiratory system comprises two main components: the conducting and respiratory portions.

The conducting portion is responsible for bringing air from the exterior to the site of respiration. This region includes:

1. The thoracic region: This area encompasses the anterior nose, nasal passages, pharynx, larynx, and mouth.

2. The bronchial region: This area encompasses the trachea and bronchi.

The respiratory portion, on the other hand, is responsible for the exchange of gases and the oxygenation of blood. This region includes:

1. The bronchiolar region consists of bronchioles and terminal bronchioles.

2. The alveolar region: This area consists of respiratory bronchioles, alveolar ducts, and sacs, as well as the alveoli, interstitial tissues, and respiratory bronchioles. [14][15]

The conduction region of the lung begins at the trachea and ends at the terminal bronchioles. The trachea splits into main bronchi, which are then divided into secondary and tertiary branches of bronchi. The bronchioles then originate from the tertiary bronchi and lead to terminal bronchioles. The respiratory portion of the lung begins from this point. [15,16]

The respiratory tree starts from the bronchioles and is made up of five types of cells:

1. Ciliated Cells: These are the most common cells in the respiratory tract and play a key role in removing debris and larger particles through the mucociliary clearance mechanism [15,17].

2. Goblet Cells: These cells contain mucin granules and shrink in size as they move toward the bronchioles, eventually being replaced by Clara cells.

3. Basal Cells are the attachment layer for ciliated and goblet cells [15,18].

4. Brush Cells: Flask-like cells throughout the respiratory tract monitor air quality by connecting to unmyelinated nerve endings [15,19].

5. Neuroendocrine Cells: Also called Kulchitsky cells, they secrete serotonin, calcitonin, and gastrin-releasing factors and are a small portion of the mucosal epithelium [15,20].

Submucosal glands secrete substances into ducts and empty onto the bronchial mucosa. Smooth muscles regulate airflow.

Afterward, alveolar ducts and alveolar sacs (grape bunch-like) originate from every respiratory bronchiole. Alveolar sacs are the respiratory tree's end, and help exchange gas. [15].

1.3.1.1 Type I Pneumocytes (Alveolar lining cells)

Type I pneumocytes, or squamous cells, are alveolar cells characterized by their flattened shape and small, densely packed nuclei. These cells line the surface of the alveoli and, due to their unique structure, are well-equipped to facilitate the exchange of gases between the cells and the capillary endothelial cells. The cytoplasm of Type I pneumocytes contains a range of organelles, including the Golgi complex, endoplasmic reticulum, and mitochondria, which are arranged around the nucleus. A significant portion of the cytoplasm is free of organelles, allowing for efficient gas exchange. The luminal surface of the alveoli is lined with

numerous pinocytotic vesicles, and the adjacent cells are connected by tight junctions, which help to regulate fluid drainage into the alveolar lumen [15].

1.3.1.2 Type II Pneumocytes (Great alveolar and septal cells)

Type II pneumocytes are a distinct type of cell found in the lung's alveoli, accounting for approximately 5% of the alveolar surface area. They are characterized by their cuboidal shape and are situated at the alveolar septal junctions, connecting to type I pneumocytes through desmosomes and occluding junctions. Compared to type I pneumocytes, type II pneumocytes are larger and have a plump appearance due to the presence of multilamellar bodies.

One critical function of type II pneumocytes is to secrete surfactant, a substance that reduces surface tension in the alveoli. This helps prevent the collapse of the alveoli during exhalation, ensuring stability in the respiratory system. Additionally, type II pneumocytes are progenitor cells that can differentiate into type I and type II pneumocytes through mitotic activity.

The cytoplasm of type II pneumocytes is rich in organelles, including the endoplasmic reticulum, Golgi apparatus, free ribosomes, mitochondria, lysosomes, and multivesicular bodies. Approximately 25% of the cytoplasm comprises lamellar bodies containing phospholipids, such as dipalmitoyl phosphatidylcholine. These lamellar bodies are released into the alveolar space through exocytosis and mixed with other secretory products to form the surfactant. This reduction in surface tension increases pulmonary compliance, making it easier for the lungs to expand and contract.

It's important to note that the surfactant produced by type II pneumocytes is not a static substance but is constantly being turned over and eliminated through mechanisms such as pinocytosis by type II pneumocytes, macrophages, and type I pneumocytes. [15].

1.3.1.3 Alveolar macrophages (Dust cells)

The alveolar macrophages form a formidable defense mechanism within the lungs and play a key role in removing environmental stressors, including inhaled particulate matter, dust, and bacteria, through phagocytosis. [15].

These macrophages can be classified into two distinct types: resident alveolar macrophages, which exhibit an M1 phenotype and are generated through mitotic division, and blood monocyte-derived macrophages, which exhibit an M2 phenotype. Both types of macrophages possess an abundance of secondary lysosomes and lipid droplets, allowing for the efficient removal of the stressors. [15].

Moreover, the resident alveolar macrophages are constantly replenished, with millions of these cells migrating to the bronchi daily. The phagocytosed macrophages are collected within mucus and expelled from the body via ciliary activity and sputum. Additionally, a proportion of the alveolar macrophages may be transported via the lymphatic circulation to the hilar lymph nodes. [15].

However, the ability of the alveolar macrophages to phagocytize environmental dust can have adverse consequences in certain cases. For instance, in the occupational lung disease known as silicosis, inhaled silica is phagocytized by the alveolar macrophages, which then transform the silica into silicic acid. This transformation leads to the proliferation of fibroblasts and collagen, resulting in fibrosis. In some instances, such as with asbestos, the phagocytosis of dust may even drive the development of malignancy within the pleura, resulting in mesothelioma. [15].

1.4 Deposition of Particles in the Lungs

The deposition of particles in various regions of the lungs is dependent upon the size of the particles. The mechanism of drug deposition is classified into three distinct categories based on particle size: impaction, sedimentation, and diffusion [23]. When impaction occurs, aerosol particles travel high speeds through the oropharynx and upper respiratory passages. Due to centrifugal force, the particles collide with the respiratory wall and are deposited in the oropharynx regions.

This process is usually seen in dry powder inhalers (DPI) and metered dose inhalers (MDI) that contain particles larger than 5 µm. Gravitational forces play a significant role in the process of particle sedimentation. Particles ranging in size from one to 5 µm, and with enough mass, tend to settle in the smaller airways and bronchioles at a slow pace, given enough time. The breathing pattern also has an impact on sedimentation. When breathing is slow, particles have a longer.

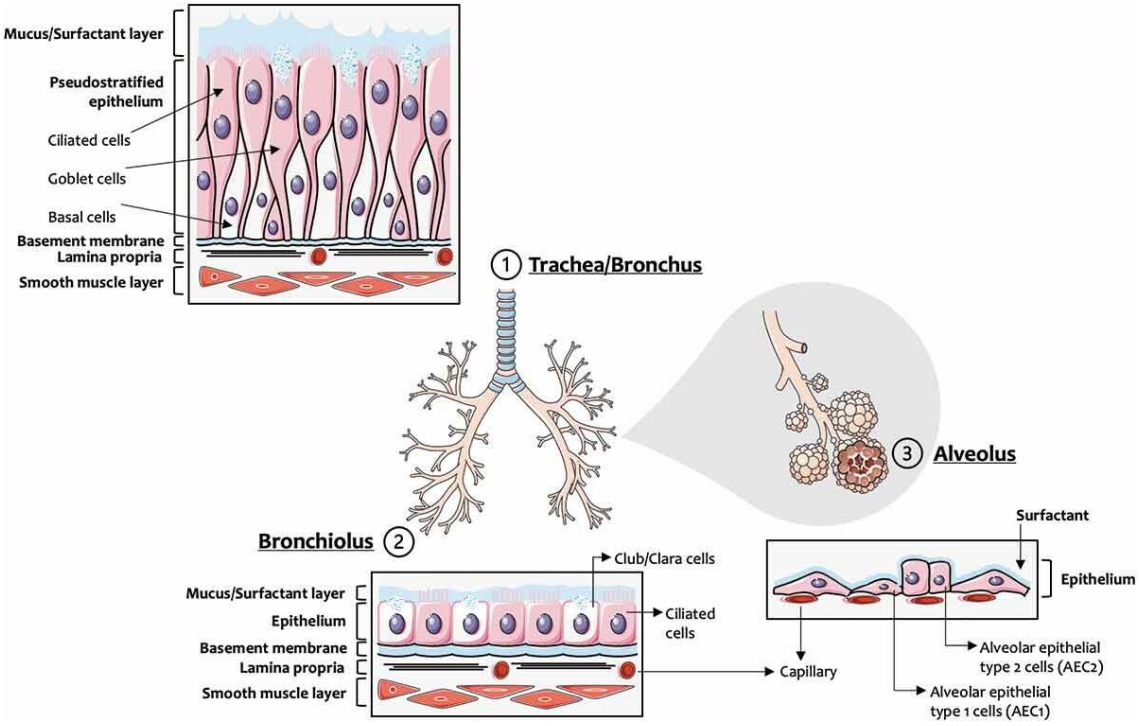

Figure 1-1 Respiratory tract: cell types and morphology. [11]

period to deposit, hence allowing for effective sedimentation. However, the deeper regions of the lungs are influenced by Brownian motion. The aqueous lung surfactant's surrounding molecules cause the particles to move randomly through Brownian motion. For diffusion, it is necessary to dissolve the particles/drugs in the alveolar fluid upon contact with the lung surfactant. The diffusion process is also affected by the concentration gradient. The particles smaller than 0.5-1 µm are deposited in the alveolar region, whereas most smaller particles are exhaled (Figure 1-2). The preferred method for depositing particles in nanoparticulate systems is sedimentation. When released from an aerosol, these systems

form aggregates in the micrometer range that are thought to have enough mass to settle in the bronchiolar region and remain there for an extended period, resulting in the desired outcome. Factors like particle size, shape, surface Characteristics, and other variables, such as mechanisms and parameters, also play a crucial role in particle deposition phenomena. [24].

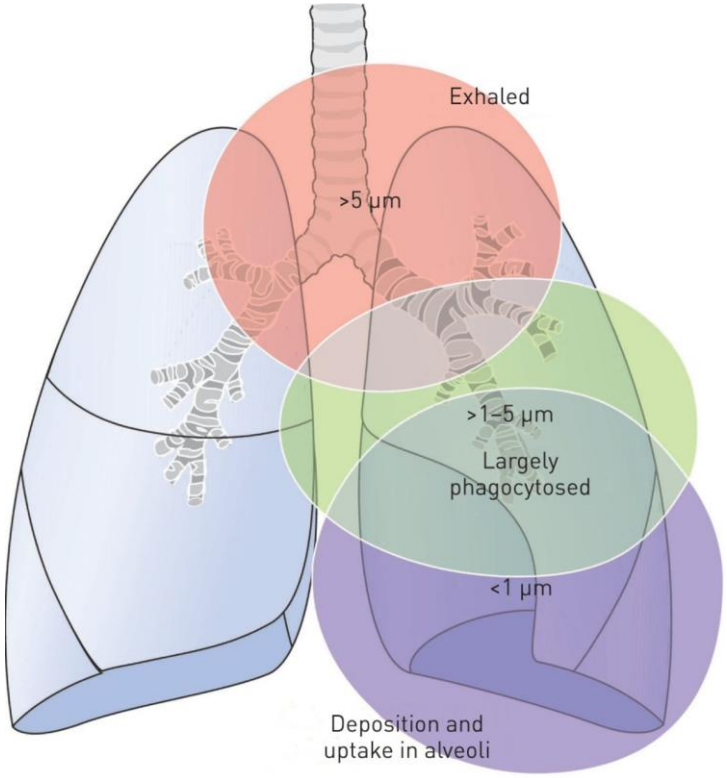

Figure 1-2 Schematic diagram showing the size-dependent deposition of particles in the lungs.[12]

1.5 Clearance mechanism

The upper respiratory tract, which encompasses the trachea and extends to the tertiary bronchi, is lined with a copious mucosal layer. This layer is a barrier that effectively captures and removes potential irritants, thereby protecting the lower airways. The mucociliary clearance process facilitates the removal of foreign particles before they can penetrate the deeper regions of the lung [21]. Lay et al. investigated the clearance and retention of radiolabelled human serum albumin and sulfur colloid particles, which are insoluble and measure 220nm in size, after depositing them into the bronchi of dogs. The mucociliary system was used to

evaluate the clearance of the particles. The study discovered that the system cleared both particles at different rates, with albumin being cleared more slowly than a sulfur colloid. These findings suggest that albumin, which is water-soluble, has a greater tendency to remain in contact with the airway epithelium compared to the insoluble Sulphur colloid particles [54]. A study by Hanes et al. discovered that Polyethylene glycol (PEG) coatings can enhance the diffusion rate through mucus for polystyrene particles larger than 500nm. PEG coating makes the particles more hydrophilic and neutral, reducing their hydrophobic interactions with mucus. [52].

The lungs have several mechanisms that contribute to the distribution and absorption of drugs, including active transport, diffusion, paracellular, transcellular, and receptor-mediated endocytosis. Researchers have found that nanocarriers made of lipids use receptor-mediated and pinocytosis pathways for endocytosis, while nanocarriers made of sugars and proteins use paracellular, transcellular, and endocytosis pathways. Studies also suggest that smaller peptides tend to follow the paracellular pathway. In contrast, larger proteins use the transcytosis pathway, with albumin being an example of a receptor-mediated transcytosis protein. As a result, larger molecules are absorbed by the respiratory region through transcytosis and endocytosis. [56].

It is widely believed that the transport mechanism in the deeper regions of the lungs, specifically the alveolar region, is more complicated. The alveolar lining, composed of a diverse array of proteins and lipids, functions as a barrier that impedes the transport of molecules. In conjunction with the tight junctions of the epithelial cells, the alveolar lining constitutes the primary barrier for transporting particles/drugs. [22]. The vital role of transporter proteins in the active absorption or passive diffusion of the particles/drugs depends on their nature and chemical structure. Additionally, the clearance of molecules by alveolar macrophages is crucial when examining drug transport mechanisms. Molecules that successfully traverse the barrier are either taken up by the cells and further absorbed into the systemic circulation or phagocytized by the alveolar macrophages. [23, 24].

1.6 Cellular uptake pathways of nanoparticles:

The plasma membrane employs different methods for exchanging substances, which can be categorized into two main types: passive transport and active Transport. Passive transport refers to the movement of substances from regions of higher concentration to areas of lower concentration without energy use. In contrast, active transport involves the movement of substances against their concentration gradient with the help of ATP energy. [38, 39] Hydrophobic biomolecules that have difficulty passing through the plasma membrane are taken up through a type of active transport called endocytosis. Endocytosis is divided into two subtypes: phagocytosis and pinocytosis.

Phagocytosis is a specialized cellular process in which specific cells, such as monocytes, macrophages, and neutrophils, engulf and compartmentalize debris and large substances with a size greater than 250nm [40]. Once engulfed, the phagocytes form membrane-bound vesicles, known as phagosomes, to contain the material. These phagosomes fuse with lysosomes, where lysosomal enzymes break down and digest the engulfed substances [41].

Pinocytosis is the process by which smaller particles or substances (a few nanometres to hundreds of nanometres) are engulfed. This involves the plasma membrane forming an invagination to take in tiny droplets of extracellular fluid that contain dissolved substances. The ingested substances are enclosed within small vesicles known as pinosomes, fusing with lysosomes and breaking down through hydrolysis. Pinocytosis encompasses different types, such as clathrin-mediated endocytosis, caveolae-mediated endocytosis, clathrin and caveolae-independent endocytosis, and macropinocytosis [41].

During **clathrin-mediated endocytosis**, the receptors on the plasma membrane bind with ligands present in the extracellular fluid, forming a ligand-receptor complex. This complex then migrates to a region of the plasma membrane abundant in clathrin, ultimately resulting in its internalization via the formation of clathrin-coated vesicles. Upon entry into the cell, the clathrin coating is shed from the vesicles before they merge with early endosomes. The cargo contained within these endosomes will ultimately reach the lysosomes, triggering the lysosomal

pathway [41]. The cell internalizes each type of NP through a preferential uptake pathway. An instance of this is the internalization of NPs containing materials such as poly(lactic-co-glycolic acid), D, L-polylactide, and poly(ethylene glycol-co-lactide), as well as silica (SiO2)-based nanomaterials, which occurs through clathrin-mediated endocytosis [42]. The cells uptake Coumarin-based solid-lipid nanoparticles through a non-energy-requiring pathway because their structure resembles cell membranes [43].

Caveolae-mediated endocytosis is a cellular entry route that involves flask-shaped membrane invaginations called caveolae. These structures are composed of membrane protein caveolin-1 and are typically 50 to 80 nm in size. Caveolae are in various cell types and regulate membrane proteins, lipids, and fatty acids. Once caveolae detach from the plasma membrane, they fuse with a compartment called caveosomes, which exist at a neutral pH and can protect the contents from lysosomal degradation. Pathogens, including viruses and bacteria, can use this entry route to prevent degradation. This pathway is also used in nanomedicine since cargo internalized by caveolin-dependent mechanisms does not end up in the lysosome [41].

In cells that lack clathrin and caveolin, endocytosis can occur through a different pathway, which is not dependent on these proteins. This pathway is used by various substances, such as growth hormones, extracellular fluid, GPI-linked proteins, and interleukin-2, to enter the cells. For example, folic acid can enter cells through this clathrin- and caveolae-independent pathway, and it is conjugated to nanoparticles and polymers used in drug delivery systems and as imaging agents [41, 44].

Macropinocytosis is when cells engulf large amounts of extracellular fluid by forming a large vesicle known as a macropinosome. This mechanism can take in apoptotic and necrotic cells, bacteria, and viruses and facilitate antigen presentation [41]. Additionally, micron-sized particles that most other pathways cannot take up can be internalized through macropinocytosis. This process can occur in most types of cells, except for brain microvessel endothelial cells [41,109].

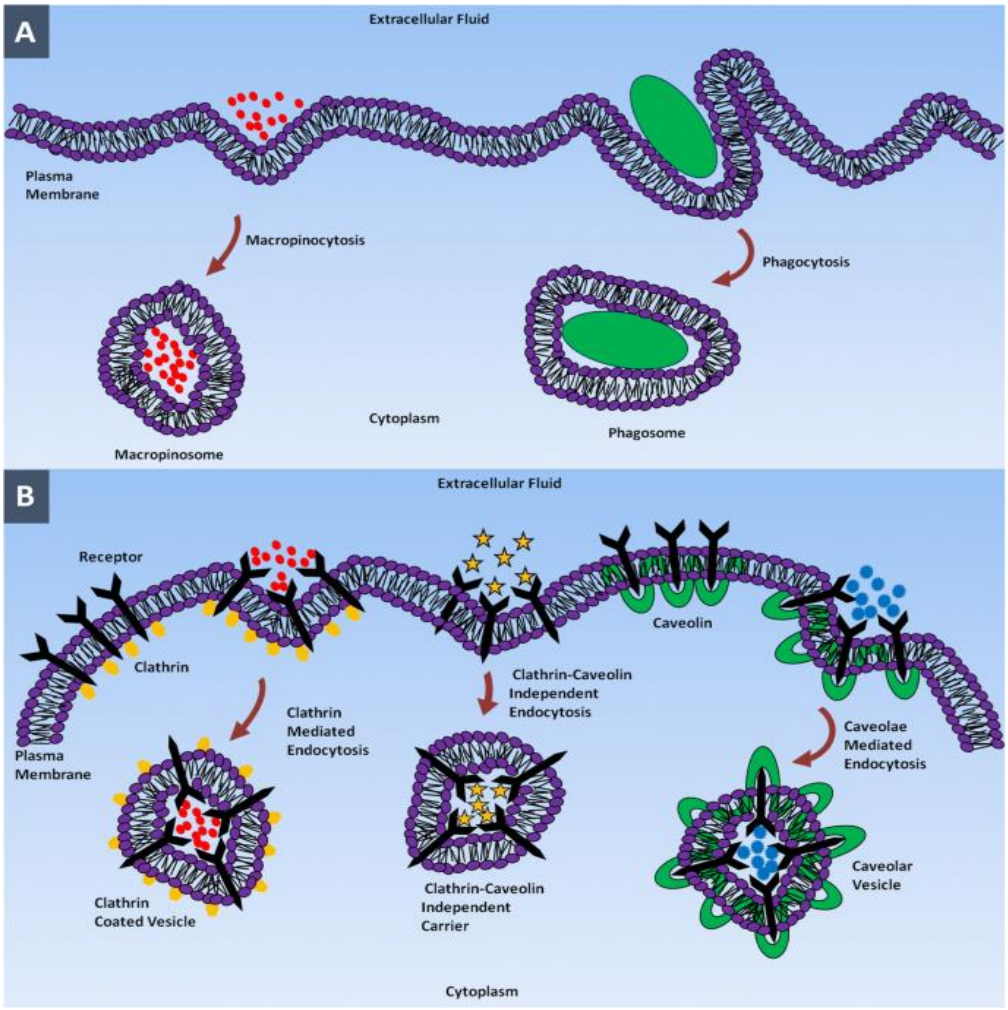

Figure 1-3 Entry of NPs into the cell using different endocytotic pathways. a Macropinocytosis and phagocytosis. b Clathrin-mediated endocytosis, clathrin-caveolin independent endocytosis, and caveolae-mediated endocytosis [41]

1.7 Nanoparticles-based systems for pulmonary applications:

1.7.1 Solid lipid nanoparticles (SLN):

Solid lipid nanoparticles (SLN) have been extensively researched as a potential method for delivering drugs to the lungs. These nanoparticles are small suspensions made from physiological lipids, including triglycerides and phospholipids. Because these formulations use natural components, they are less toxic and more suitable for pulmonary drug delivery.

Nassimi and colleagues utilized solid lipid nanoparticles (SLN) containing a combination of phospholipids and triglycerides in a 30:70 ratio to investigate their potential for pulmonary applications. They evaluated the toxicity of these SLNs using a range of methods, including in vitro, ex vivo, and in vivo models, and analyzed cytokine activation. Their research indicated that nebulizing SLN in mice did not activate pro-inflammatory cytokines such as TNF-α and chemokine-KC [25].

A further investigation was carried out to explore the possible application of solid lipid microparticles (SLM) loaded with quercetin for treating asthma, owing to the anti-inflammatory and antioxidant features of quercetin. Based on in vitro experiments, the researchers noted that the particles maintained their stability post-nebulization and were predominantly deposited in the lower regions of the lungs [26].

In a study conducted by Wang et al., SLN (solid lipid nanoparticles) loaded with curcumin were created using stearic acid and lecithin. The purpose was to treat asthma potentially. The SLN was produced using the solvent injection and was stable with sizes between 190-200 nm. The study involved testing the SLN on mice with ovalbumin-induced asthma, and it was observed that the cytokine levels decreased in the group treated with curcumin-loaded SLN compared to the untreated group [27]. The research investigated different drugs for treating lung infections and manufacturing a drug called SLN with amikacin, an antibiotic. Cholesterol was used as a lipid to make the drug using a high-pressure homogenization method [28].

Another study by Mussi et al. focused on the anti-cancer effects of doxorubicin SLN. A polyunsaturated fatty acid, docosahexaenoic acid (DHA), was used to improve drug encapsulation in the lipid melt. DHA significantly enhanced the drug encapsulation efficacy, and triethanolamine was also used to increase the solubility of doxorubicin in the lipid melt. Using solubility enhancers can improve the effectiveness of the formulation by increasing drug uptake and maximizing the cytotoxicity of doxorubicin [29].

1.7.2 Polymeric nanoparticles

Polymers are becoming increasingly important for delivering drugs to the lungs. Many different types of polymers have been studied for this purpose. Polymers offer several benefits, such as modified surface properties, high drug encapsulation, protection of the drug from degradation, prolonged drug delivery, and long shelf life. The most commonly used polymers for therapeutic purposes are poly(lactic acid) (PLA), poly(lactic-co-glycolic acid) (PLGA), poly(ε-caprolactone) (PCL), alginate, chitosan, and gelatine, which have been modified chemically and on their surface to make them biodegradable [30]. Polymeric particles loaded with paclitaxel, an anti-cancer compound, have been used in multiple studies. In a recent study, researchers combined polyethene glycol (PEG5000) and polymer poly (ethylene oxide)-block-do stearoyl phosphatidylethanolamine (DSPE) polymers to produce paclitaxel-loaded polymeric micelles. These micelles were then tested in vivo using intratracheal and intravenous administration routes and compared with the commercially available Taxol compound. The study found that intratracheal administration had better drug absorption than intravenous administration, and maximum drug localization occurred in the lung tissue. Additionally, polymeric paclitaxel had superior drug release profiles to taxol [31].

A study was conducted to improve the effectiveness of paclitaxel by combining it with an amphiphilic block copolymer made of poly-glycolide-ε-caprolactone with PEG and tocopheryl succinate. The goal was to increase the drug's encapsulation efficiency and cellular uptake. The copolymer-paclitaxel was labeled with coumarin-6 to track its uptake in an in vitro A549 cell model. The study also included a comparison of the cytotoxicity of the copolymer-paclitaxel with a commercial taxol compound and free paclitaxel. The results showed that the copolymer-paclitaxel had higher cytotoxicity than the other two compounds [35]. Researchers have explored the use of cancer-fighting agents and investigated the potential of antioxidants in polymeric nanoparticles. In a study by Yoo et al., a new anti-inflammatory compound named hydroxy benzyl alcohol (HBA) was incorporated into PLGA-based polymeric nanoparticles known as HPOX. These nanoparticles were administered to mice with asthma induced by ovalbumin via

the intratracheal route. The researchers observed a reduction in the inflammation. The response was demonstrated by lower levels of pro-inflammatory cytokines in the ovalbumin-treated group. These results indicate that the HPOX polymeric nanoparticles, which contain the novel anti-inflammatory compound, could be a promising treatment option for airway inflammation and asthma [37].

Also, another study shows that PLGA and polyethylene amine (PEI) together could be used instead of viral vectors for pulmonary delivery of pDNA [32]Shindi et al. showed that PLGA and PLA particle composites could be used for in vitro RNAi delivery. [33].

Previous studies on particle uptake by Tetley et al. compared the uptake of unmodified carboxyl and amine-modified polystyrene particles. They found that the uptake of surface-modified particles by alveolar epithelial cells was much greater than that of unmodified particles of the same size. They suggested that this may be due to glycoproteins, glycolipids, and receptors in the cell membrane that could provide electrostatic interaction sites for carboxyl and amine groups [34]. The effects of polystyrene particles have been extensively studied in many investigations. For example, Stock et al. found that the human epithelial cell line CaCo-2 showed a toxic response after interaction with 1 µm PS particles [36]. However, few studies have investigated the effects of different sizes and surface modifications of PS particles. Therefore, in this study, we investigate the uptake and cytotoxic effects of PS particles with various sizes and surface modifications by alveolar epithelial cells and alveolar macrophages.

1.7.3 Liposomes

Liposomes made primarily from phospholipids found in the lungs, are a popular method for drug delivery, especially for pulmonary applications. They are created using lung surfactants, phospholipids, and cholesterol. Liposomes can release drugs over an extended period, resulting in maximum drug effectiveness. In the 1990s, the first liposomal product, purified bovine surfactant (Alveofact®), was introduced to treat acute respiratory distress syndrome (ARDS) in infants via pulmonary instillation. Later, amphotericin B-loaded liposomes (Ambisome®) were

developed for parenteral, rather than pulmonary, use [45]. Liu et al. conducted a study where they created ciprofloxacin-loaded liposomes using phospholipids and cholesterol through the film method. These liposomes had an average size of 350 nm and a high encapsulation efficacy of up to 93%. The study included an in vitro drug release test with simulated lung fluid and saline solution, where a higher release of ciprofloxacin-liposomes was observed in simulated lung fluid (SLF). Additionally, in vivo experiments with rats showed that ciprofloxacin-liposomes had higher drug-targeting efficiency than the ciprofloxacin solution [49].

Hoesel and colleagues conducted a study that used the film method to create phospholipid-based liposomes using antioxidants such as n-acetylcysteine, vitamin E, and glutathione. They observed a reduction in pro-inflammatory cytokine levels in the bronchoalveolar lavage fluid of rats that were injured with mustard gas derivative 2-chloroethyl ethyl sulfide (CEES) in an *in vivo* study. These antioxidant nanoparticles can be delivered to the lungs through nebulization or instillation and may be beneficial in treating lung injuries related to hypoxia and oxidative stress [53].

1.8 Effects of size and surface modification of nanoparticles mediated targeted delivery of cells:

Despite the method of internalization, the interactions between cells and nanoparticles are influenced by their physical and chemical characteristics, such as their size, shape, surface charge, and surface chemistry.

The uptake of various nanoparticles by different cell lines depends on the nanoparticles' size. Hökstra et al. conducted an experiment using fluorescent latex beads of various sizes ranging from 50 to 1000 nm to study the impact of nanoparticle (NP) size on the entry mechanism in nonphagocytic B16 cells. They discovered that NPs smaller than 200 nm were internalized through clathrin-coated pits, while larger particles exhibited a shift towards caveolae-mediated internalization. In particular, the predominant entry pathway for 500-nm particles was caveolae-mediated internalization [55].

Nienhaus and colleagues thoroughly investigated how different-sized nanoparticles (ranging from 3.3 to 100 nanometers) were taken up by live HeLa cells. They discovered that nanoparticles such as QDs and Au nanoclusters with a diameter of fewer than 10 nanometers tended to accumulate on the plasma membrane before eventually entering the cell [57][58]. On the other hand, larger polystyrene nanoparticles (100 nanometres) were immediately internalized without any noticeable prior accumulation on the plasma membrane [59]. Lunov et al. discovered that human macrophages and monocytic THP-1 cells internalize 100-nm carboxy and amino-functionalized polystyrene nanoparticles (PS-COOH and PS-NH2) through different mechanisms. The type of nanoparticle, cell type, and experimental conditions influenced the internalization mechanism. They observed that only PS-NH2 NPs triggered NLRP3 inflammasome activation and the human macrophages' release of proinflammatory interleukin 1β (IL-1β) [60].

The shape of nanoparticles, in addition to their size, plays a critical role in cellular uptake. For example, a study conducted by Chithrani et al. found that HeLa cells take up spherical AuNPs more efficiently than rod-shaped AnNPs [46]. However, Gratton et al. reported contradictory results, demonstrating that HeLa cells take up rod-shaped hydrogel particles more readily than spheres, cylinders, and cubes [47]. In a separate investigation, researchers explored the uptake of disc-shaped and rod-shaped polystyrene particles by Caco-2 cells, revealing that these particles are taken up more effectively than spherical nanoparticles. Consequently, they concluded that nanoparticle-mediated drug delivery could be improved by considering the shape of the nanoparticles [48].

To improve the effectiveness of drug delivery, scientists are altering the surface and dimensions of nanoparticles to avoid being cleared by the body too quickly, traveling through barriers, and staying longer at the desired location. They are achieving this by incorporating different compounds to modify the surface of the nanoparticles based on various conditions [61].

Nanoparticles that look like brushes have been created using short chains of poly(ethylene glycol) (PEG) to decrease the likelihood of phagocytosis. These

PEGylated nanocarriers were also observed to easily and quickly penetrate the mucus layer in individuals with chronic obstructive lung diseases [62].

Also, to improve the drug uptake, bioavailability, and therapeutic efficacy in non-obstructive lung diseases like allergies and lung cancer, chitosan can be used to modify the surface of nanoparticles. This modification can enhance mucoadhesion and circulation, allowing the nanoparticles to stay at the targeted site for a longer period. This is a desirable property for drug delivery [63].

Li and colleagues examined how positive and negative polystyrene particles interact with the cellular membrane. Their findings revealed that cationic polystyrene particles strongly interact with the membrane's phosphate groups, which ultimately leads to increased surface tension and pore formation. This was demonstrated in their study results [50].

In a separate study, Huhn and colleagues observed that fibroblast cells had higher uptake of cationic AuNPs compared to their anionic counterparts. Furthermore, their cytotoxicity investigation suggested that positively charged particles exhibit higher toxicity than negatively charged particles [51].

1.9 Toxicity endpoints after pulmonary delivery

In the context of pulmonary nanoparticle-mediated drug delivery, a critical aspect is the assessment of parameters of cytotoxicity. Nanotoxicology can be evaluated via various endpoints, such as mitochondrial function, membrane integrity, oxidative stress, and inflammatory response.

Multiple techniques exist to evaluate cellular integrity based on metabolic activity, including using colored stains to identify damaged cells, such as MTT, XTT, and WST 1 assays [65]. These assays utilize NADPH-dependent oxide reductase enzymes to reduce tetrazolium dye, forming formazan crystals in viable cells. Consequently, the intensity of the colored solution generated by these assays correlates with cellular metabolic activity. An alternative approach to assess cellular toxicity is the lactate dehydrogenase (LDH) assay [66].

Several assays are available for detecting two distinct modes of cell death: apoptosis, a programmed cell death, and necrosis, an accidental cell death. Caspase 3, an activated protease in apoptotic cells, can be detected to quantify the number of apoptotic cells [67][68][71]. Apoptotic cells can be discriminated from necrotic and intact cells by annexin V coupled with FITC green fluorescent combined with red fluorescence propidium iodide. Apoptosis can also be monitored by membrane blebbing. Cell death can also occur due to undesirable oxidation, a phenomenon called oxidative stress in cells. This oxidative stress is primarily triggered by free radicals such as nitric oxide, reactive oxygen species, reactive nitrogen species, hydrogen peroxide, iron ions, hydroxyl radicals, and others that facilitate Haber-Weiss and Fenton reactions [69]. When pollutants, ultraviolet radiation, smoke, or nanoparticles enter the body, the balance between oxidants and antioxidants is disrupted, forming reactive oxygen species. Numerous studies have demonstrated that the lungs are the primary site of oxidative stress reactions. [70].

In vivo experiments often employ the quantification of polymorphonuclear leukocytes (PMNs) recruited into the lungs to characterize toxicity. To do so, bronchoalveolar lavage (BAL) cells are identified and counted using a haematocytometer. In contrast, fluid from the same lavage is stained with Romanowsky reagent to quantify the number of PMNs. In nanoparticle-mediated drug delivery, these toxicity endpoints must be considered, as many of these particles have been shown to induce toxicity in previous research. For instance, titanium oxide has been found to elicit DNA damage, oxidative stress, and inflammatory response. [72] [73]. Similarly, several environmental nanoparticles, such as metal hydroxides, silica, gold, or silver, have been demonstrated to induce toxicity, inflammation, and oxidation when introduced into the lungs. [74]. Nevertheless, certain particles, such as PLGA, have already been approved for drug delivery, including in the lungs, owing to their biodegradability and biocompatibility. [75].

1.10 *In vitro* models of nanoparticle delivery

The most employed lung epithelial cell lines for investigating nanoparticle interactions in vitro are A549, Calu 3, H441, and 16HBE14o. It has been noted that

all of these cell lines, except for A549, establish tight junctions. Notably, the translocation of nanoparticles is reportedly reduced in cell models lacking tight junctions compared to those that possess them [76] [77]. In co-culture models, lung epithelial cells are the foundation, with various other cell lines incorporated into the basic model. For instance, the addition of endothelial cells to epithelial cells creates the alveolar-capillary barrier [78]. Alveolar macrophages can also be incorporated into this model. Furthermore, the model may be modified by including dendritic cells, macrophages, and type 2 alveolar cells. Alternatively, fibroblasts may be added to the basic epithelial cell model instead of endothelial cells [79] [80].

In addition to variations in cell types, *in vitro* models can be made more predictive by improving the experimental setup, and one way to achieve this is through aerosolized drug delivery. However, most current in vitro technologies for aerosol-cell delivery have limitations in terms of delivery rate, which exceeds the clinically acceptable range. The Air Liquid Interface Cell Exposure (ALICE) technology is an exception that allows for dose-controlled, aerosolized drug delivery to lung cell culture models. [84].

Hence, *in vitro* lung models can differ based on the nanoparticle exposure system employed, such as a submerged system or a system utilizing an air-liquid interface for culturing. While the former system is technically less complex, it is limited by the potential for alterations in nanoparticle properties resulting from interactions with the culture medium, which can have consequential impacts on cellular uptake. [81] [82]. In contrast, several air-liquid interface models have been developed to offer a more realistic representation of inhalation exposure.

There is a difference between ALI-cultured human bronchial epithelial cells and submerged cultured cells in terms of responding to exposure to environmental nanoparticles. Research has shown that the ALI culture exhibited a lower level of inflammation in response to air pollution particles than the submerged culture. This is because the submerged culture and the particles created hypoxic conditions that led to inflammation. On the other hand, the ALI culture had increased access to oxygen, preventing hypoxic conditions. [83].

Additionally, the ALI culture demonstrates a quicker drug onset, as shown in a study conducted by Lenz et al. (2009), where a direct comparison of both cell culture modes indicated that the ALI culture resulted in more rapid absorption of the proteasome inhibitor Bortezomib. [84].

Exposure of particles by ALI cultures has a further advantage in dosimetry since they ensure a direct calculation of the dose delivered to the cells, which is not possible with submerged cell models. [85]The primary benefit of utilizing ALI culture conditions is that they mimic the in vivo conditions of the lungs. [86] [87].

This study conducted a comparative analysis of in vitro exposure systems, specifically the Submerged and Air-Liquid Interface (ALI) methods, and in vivo exposure was conducted to investigate particle exposure to alveolar cells. The analysis used polymeric nanoparticles, specifically polystyrene latex beads and Poly(lactide-co-glycolide) (PLGA) particles. The choice of PLGA particles was motivated by their biodegradability, biocompatibility, and approval by the Food and Drug Administration (FDA). This investigation aimed to augment the existing knowledge on particle exposure to alveolar cells.

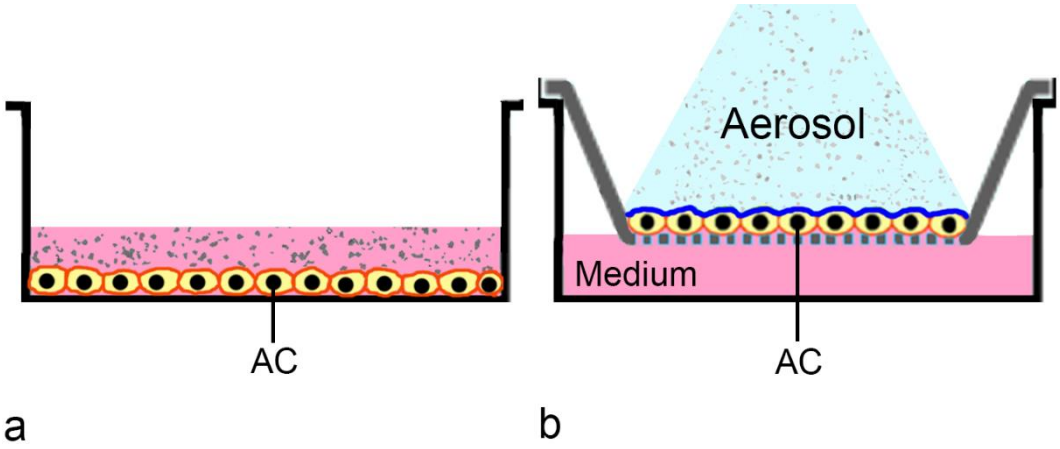

Figure 1-4 Different ways of culture: Cell grown at the bottom of a well and exposed to NPs suspended in medium (a). In the culture at an air-liquid interface, cells are grown on membranes and supplied with nutrients from the basal side. In this culture, respiratory cells secrete pulmonary surfactant (blue line). Cells are exposed to NPs applied as aerosols (b). AC: alveolar cell.

1.11 Key Objectives of the study

This study is divided into two sections and uses two types of nanoparticles: surface-modified polystyrene particles (PS) and polylactic glycolic acid (PLGA) particles.

1: The uptake and toxicity of different sizes and surface-modified PS latex beads by different alveolar cell types in submerged and Air-liquid interface exposure systems

2: The uptake of PLGA particles by alveolar macrophages and epithelial cells depends on the exposure scenario: Validation of this co-culture setup's uptake pattern of nanoparticles *in vivo* by intratracheal instillation of nanoparticles in mice.

2. Material and Methods

2.1 Materials

2.1.1 Nanoparticles:

Fluorescently labeled Polystyrene microspheres were procured from Sigma Aldrich at a concentration of 2.5mg/ml in stock. These microspheres, which were used in the study, were of three distinct sizes and surface modifications: Carboxylate (0.03µm, 0.5µm, 1µm), Amine (0.1µm, 1µm), and Sulphate (0.1µm, 0.5µm). The particles were characterized by their respective fluorescence emissions, which were determined as follows: Carboxylate (0.03µm (470/505), 0.5µm (529/540), 1µm (470/505)), Amine (0.1µm (481/644), 1µm (520/540)) and Sulphate (0.1µm (520/540), 0.5µm (520/540)).

In addition, fluorescently labeled Poly Lactic-co-Glycolic acid (PLGA) beads of varying sizes (100nm, 500nm, 1µm) were obtained from Phosphorex (Hopkinton, MS 01748) at a concentration of 10mg/ml in stock. These PLGA beads were prepared using (D, L-lactate-co-glycolide) with an L/G ratio of 50/50 and a molecular weight of 30,000.

2.1.2 Mice:

Ten-week-old mice with wildtype C57BL/6J genetic makeup were acquired from Charles River Laboratories in Sulzfeld, Germany. All in vivo experiments were conducted using these mice. The mice were bred under specific pathogen-free conditions, kept in individually ventilated cages (IVC), and maintained at a constant temperature and humidity with a 12-hour light cycle, following institutional, state, and federal guidelines of Helmholtz Zentrum Muenchen. All animal experiments were conducted in conformity with the FELASA Guidelines and Recommendations, the German animal welfare law, and approved by the institutional animal welfare committee (‘committee for animal experiments and animal facility’ of the Helmholtz Zentrum München) as well as by the District Government of Upper Bavaria.

2.1.3 Commercially available kits and reagents:

Kits and chemicals name	Company
Cytotoxicity Detection Kit (LDH)	Sigma
Cell proliferating Reagent (WST-1)	Roche
Giemsa and May Grünwald solutions kit	Sigma-Aldrich
Alexa fluor 594 Phalloidin	Thermofischer Scientific
VybrantDiD cell labeling solution	Thermofischer Scientific
Prolong gold antifade mountant with DAPI.	Thermofischer Scientific

2.1.4 Equipment and General Consumables

Equipment name	Company
ALICE chamber (commercial)	Vitrocell
ALICE chamber (Prototype)	Lab: Institute of lung health and immunity at Helmholtz Center Munich
Autoclave machine	Systec
BD FACSCantoTM II Flow Cytometer	BD Biosciences, San Jose, CA, USA
Brightfield microscope	Olympus
Centrifuge: Eppendorf 5415D	Eppendorf, Hamburg, Germany
Centrifuge: Sigma 3K18	Sigma, Osterode am Harz, Germany
cytospin3 cytocentrifuge	Shandon, PA
Cell culture T75, T150 flasks	Greiner Bio-One
Cell culture Incubator	Thermo Fisher Scientific
Cell culture workflow- HERA Safe KS	Thermo Fisher Scientific
Chemical workflow hood	Köttermann

Confocal microscope	Zeiss
Cover slips 24 x 50mm	Menzel-Gläser
Cytospin centrifuge	Shandon, PA
Easypet automatic pipette	Eppendorf
Falcon tubes (15 mL, 50mL)	Corning science
Fluorescence microscope	Olympus
Gloves	Nitril NextGen
Ice machine	Buchner Labortechnik
Multipipette	Eppendrof
Pipetman (2µl, 10µl, 20µl, 200µl, 1ml)	Eppendorf
QCM	Scientific instruments GmbH
Sonication water bath	Bandelin
Syringe	Braun
Tecan Reader NanoQuant infinite M200 Pro	Tecan Group
Tips (2µl, 10µl, 20µl, 200µl, 1ml)	Starlab
Vortexer	Scientific Industries, Karlsruhe, Germany
Water bath for cell culture	Lauda, Koenigshofen, Germany
0.5 ml, 1.5ml and 2ml tubes	Eppendorf
6-well transwell insert plate	Corning
96 healthy plates for WST-1 and LDH assay	Greiner Bio-one

Product	Company
CellSens Dimension, version 5	Olympus Corp.
GraphPad Prism 6	GraphPad
Magellan Software	Tecan Group
Zen 2010-Digital imaging for light microscopy software	Sigma-Aldrich

2.1.5 Software:

2.1.6 Chemicals:

Dulbecco's Modified Eagle Medium (DMEM), Dulbecco's Phosphate Buffered saline (DPBS), Fetal Bovine Serum (FBS), Fetal Calf Serum (FCS), RPMI Media 1640 and penicillin and streptomycin antibiotics were purchased from BioChrome (Berlin, Germany) and Invitrogen (Karlsruhe, Germany)

Name	Concentration	Chemicals
PBS buffer (10X)	137 mM 2.7 mM 10 mM 2 mM	NaCl KCl Na2HPO4 KH2PO4
RPMI-1640 medium	1X 10% 1% 2 mM	RPMI-1640 medium Fetal bovine serum penicillin/streptomycin glutamine

Dulbecco's Modified Eagle Medium (DMEM)	1X 10% 1% 2 mM 50 µM	Dulbecco's Modified Eagle Medium Fetal bovine serum penicillin/streptomycin glutamine ß-mercaptoethanol (for macrophage culture)
HAM-12 medium	1X 15% 1% 2 mM 1%	HAM-12 medium FBS Penicillin/streptomycin Glutamine Non-essential amino acids
FACS Buffer	1X 1%	PBS BSA
NaCl 0.9%		NaCl Distilled water

2.2 Methods

2.2.1 Nanoparticle Characterization:

The particles were suspended in distilled water in a ratio of 1:20, followed by sonication in a sonication bath for 2 minutes before their hydrodynamic diameter was assessed using Dynamic Light Scattering (DLS) with a Malvern Zeta Sizer Nano Instrument. In addition, the mean fluorescent intensity of each particle size was measured using a plate reader based on their mass and excitation/emission.

2.2.2 Cell cultures

The MH-S cell line, which is a murine alveolar macrophage cell line immortalized by SV40 (RRID: CVCL_ 3855), along with the MLE 12 cell line, derived from FVB/N-Tg (SFTPC-Tag)5.1 Jaw SV40 transgenic mice (RRID: CVCL_ 3751), and the LA-4 cell line, derived from lung adenoma (RRID: CVCL_ 3535), were procured from the American Type Culture Collection (ATCC) in Manassas, USA. In addition, the A549 cell line, a human epithelial cell line, was also obtained from ATCC.

The MH-S cell line was cultured in DMEM medium supplemented with 10% FBS (Bio-chrome), 0.05mm B-mercaptoethanol, and 1% penicillin/streptomycin (Life Technologies).

The LA-4 cell line was cultured in Ham's media supplemented with 15% FBS (Bio-chrom), 1% non-essential amino acids (NEAs), and 1% penicillin/streptomycin (Life technologies).

A549 cells were cultured in RPMI 1640 medium supplemented with 10% FBS (Bio-chrome), 1% L-glutamine, and 1% penicillin/streptomycin (Life Technologies), while MLE 12 cells were maintained in RPMI 1640 medium supplemented with 10% FBS (Bio-chrome) and 1% penicillin/streptomycin (Life Technologies). All cells were maintained at 37°C in a 5% CO2 humidified atmosphere.

Upon confluence, cells were washed with 10ml PBS, and 5ml pre-warmed Trypsin EDTA was added to the flask to cover the cells. The cells were then incubated for 5 minutes at 37°C to facilitate detachment from the flask. To stop the reaction of Trypsin EDTA, fresh medium was added, and the cells were collected in a 50ml falcon tube and centrifuged at 1200 rpm for 5 minutes. The supernatant was aspirated, and the cells were suspended in a 2ml fresh medium. Cell counting was performed in a hemacytometer at a 1:20 dilution.

2.2.3 Exposure of monocultures and co-cultures to particles:

2.2.3.1 Conventional Submerged Conditions

To investigate the uptake kinetics and toxicity of PS particles in monocultures of A549 cells, MLE 12 cells, LA-4 cells, and MH-S cells, cells were seeded biweekly

at a density of 0.5 x 10^6 cells per well in 6 well plates with appropriate culture media containing serum (FBS). At two time points (4 and 24 hours), the culture medium was replaced with a fresh suspension of fluorescent polystyrene latex beads that were diluted to a dose of 50µg/ml (5.2µg/cm^2) in medium and incubated at 37°C. After 24 hours of incubation, the particle uptake and toxicity were evaluated.

In the context of examining the effects of PLGA particles on cell cultures, monocultures of MH-S and LA-4 cells were seeded biweekly into 6-well plates at a density of 0.5 x 10^6 cells per well and cultured in DMEM and HAM's media, respectively, both supplemented with fetal bovine serum (FBS). For co-culture experiments, LA-4 cells were uniformly labeled with Vybrant® DiD Cell-labeling Solution (Catalogue: V22887, Thermo Fischer) (Ex/Em: 644/665) according to the manufacturer's protocol, then seeded at a density of 60,000 cells per well in HAM's media supplemented with FBS. After 24 hours, the medium was replaced with DMEM containing 30,000 MH-S cells per well. Following 24 hours of exposure to PLGA particles, the supernatant was replaced with a fresh suspension of fluorescent particles, diluted to a concentration of 1:100 in the respective medium, and incubated at 37°C. After a further 24 hours of incubation, particle uptake was evaluated.

2.2.3.2 ALICE CLOUD (Air-liquid interface)

For PS particle exposure

In this study, we employed a cell culture model to investigate the effects of polystyrene (PS) particle exposure on various cell types, including MH-S, MLE 12, A549, and LA-4 cells. Specifically, the cells were seeded into cell culture inserts with a transparent PET membrane, which had an effective growth area of 4.2cm^2 and a pore size of 1µm (with 1.6 x 10^6 pores/cm^2) and were seeded with approximately 0.5 x 10^6 cells per insert. The inserts were then placed into BD Falcon 6-well tissue culture plates, with 2ml medium in the apical compartment and 3ml in the basal compartment.

After four days of growth under submerged conditions at 37°C, the cells formed a confluent monolayer. The medium in the apical compartment was then removed to transfer the cells to an air-liquid interface, and the cells were incubated for another 24 hours at 37°C. Next, the medium in the basal compartment was replaced with a 2ml serum-free culture medium, and the cells were placed into the exposure chamber of the ALICE system for exposure to PS particles. The dilution was 1:10, and the dose was 50µg (0.35 µg/cm^2).

After exposure to PS particles, the inserts were removed from the chamber and placed back into the cell culture plates. The cells were then incubated for an additional 24 hours at 37°C to investigate the kinetics of particle uptake.

For PLGA particle exposure

Monoculture experiments were conducted using 0.5 x 10^6 LA-4 and MH-S cells, seeded into cell culture inserts featuring a transparent PET membrane with a 4.2cm^2 effective growth area, 1µm pore size, and 1.6 x 10^6 pores/cm^2. These inserts were subsequently placed in BD FalconTM 6 wells tissue culture plates, with 2ml of medium added to the apical compartment and 3ml to the basal compartment. Following two days of growth under submerged conditions at 37°C, a confluent monolayer was formed, and the cells were transferred to the air-liquid interface by incubating them for an additional 24 hours at 37°C after removing the medium from the apical compartment.

In co-culture experiments, LA-4 cells were labeled with vybrant Did (Ex/Em: 644/665) and cultured using 60,000 cells in cell culture inserts. The inserts were then placed in BD FalconTM 6 wells tissue culture plates, with 2ml of Hams medium added to the apical compartment and 3ml to the basal compartment. Following two days of growth under submerged conditions at 37°C, the cells formed a confluent monolayer and were subsequently replaced with DMEM-containing MH-S cells on the inserts. After 24 hours, the cells were transferred to the air-liquid interface by removing the medium from the apical compartment and incubating them for an additional 24 hours at 37°C.

In both monoculture and co-culture conditions, the medium in the lower compartment was replaced with 2ml of serum-free culture medium, and the cells were placed in the ALICE system's exposure chamber for exposure to PLGA particles (Dilution 1:5; dose: 2.7µg/cm^2). Subsequently, the inserts were removed from the chamber and placed back into cell culture plates, where they were incubated for 24 hours at 37°C to investigate the kinetics of particle uptake.

2.2.4 Particle Uptake Analysis

2.2.4.1 Flow Cytometry

Following 24 hours of treatment with PS and PLGA in monoculture and PLGA in co-culture under submerged and air-liquid interface (ALI) conditions, the supernatant was removed from the submerged conditions plate wells, and the plates were rinsed twice with phosphate-buffered saline (PBS). The cells were then harvested by trypsinization and collected in a fluorescence-activated cell sorting (FACS) tube. The tube was centrifuged for 20 minutes at 400 relative centrifugal force (RCF) and 4°C, and the resulting pellet was washed with PBS and quenched with 0.4% Trypan blue. The pellet was washed twice with PBS and centrifuged for 5 minutes, then resuspended in 500 µL of FACS buffer. The uptake of particles was evaluated using flow cytometry (BD FACSCanto II, BD Biosciences) in both cell monocultures and co-cultures. The mean fluorescent intensities (MFI) of PS particles were analyzed in the phycoerythrin (PE) channel, while the MFI of PLGA particles was analyzed in the fluorescein isothiocyanate (FITC) channel. In co-cultures, LA-4 cells were stained with Vybrant DID and gated in the 7-amino actinomycin D (7AAD) channel to differentiate them from unstained MH-S cells. The values were expressed as the ratio of the MFI of each sample to the MFI of non-treated cells and were adjusted based on the fluorescence factor of each particle. Three Independent experiments were conducted (N=3).

2.2.4.2 Confocal microscopy

Following a 24-hour treatment of particles under both monoculture and co-culture conditions, the supernatant was discarded in the case of submerged conditions and subsequently washed with phosphate-buffered saline (PBS). Each well was then subjected to fixation with 3% Paraformaldehyde (PFA) in a volume of 800 mL for 15 minutes, followed by two rounds of washing. Subsequently, cells were subjected to staining using 200 µL of Phalloidin stain for 20 minutes at ambient temperature, post-washing. For submerged conditions, a drop of DAPI stain was placed on a glass slide and then mounted with a coverslip bearing the stained cells. In contrast, for air-liquid interface (ALI) conditions, the membrane was cut into two pieces, and a drop of DAPI was placed on the membranes. After 30 minutes, the membranes were washed with PBS and mounted on a microscopic slide using Dako Fluorescent mounting media. Cells' uptake of particles was analyzed using a laser scanning confocal microscope (LSCM).

2.2.5 Cytotoxicity Testing

2.2.5.1 Water-soluble Tetrazolium salt (WST) cell viability assay:

0.5 x 10^6 cells were seeded onto 6-well plates and allowed to adhere for 24 hours. Subsequently, the cells were treated with particles at a 10µg/cm2 concentration under **submerged conditions**.

Following a 5-day incubation period, the cells were treated with particles at a 2.7µg/cm2 concentration under **air-liquid interface (ALI) conditions**.

After a 24-hour treatment period, the supernatant was removed, and the cells were washed with phosphate-buffered saline (PBS). A media suspension containing the WST reagent (Roche) was added to the cells at a ratio of 1:20, and the cells were then incubated at 37°C for 15 minutes (for MH-S, MLE 12, and A549 cells) or 45 minutes (for LA-4 cells). After incubation, the media was collected, and 200µl was added to each well of a 96-well plate in triplicate. The absorbance of the samples was measured using a microplate (ELISA) reader at a

wavelength of 450nm (with a range of 420-480nm) with background controls measured as blank.

2.2.5.2 LDH release Test:

The experiment involved seeding 0.5 x 10^^{6} cells on 6-well plates, then treatment with particles at a concentration of 10µg/cm^{2} **under submerged conditions** after 24 hours.

After 5 days, cells were treated with particles at a 2.7µg/cm2 concentration **under air-liquid interface (ALI) conditions**.

The cytotoxicity of the treated cells was determined by measuring the concentration of the cytosolic enzyme lactate dehydrogenase (LDH) in the supernatants, using a cytotoxicity detection kit from Sigma according to the manufacturer's instructions. The LDH concentration was measured using a spectrophotometer with an ELISA reader set to a wavelength of 492nm. The maximum LDH release was induced by treating cells with 1% Triton X-100, as instructed by the manufacturer, which served as the high control. The relative LDH release was calculated as the ratio of LDH release over the total LDH in the intact cells (high control).

2.2.6 In vivo Experiments:

The present study utilized a cohort of 22 mice to investigate the uptake of nanoparticles by bronchoalveolar lavage (BAL) macrophages and alveolar type 2 (AT2) cells. Specifically, four mice were assigned as a sham control group without nanoparticle administration, serving as a reference for comparison with the particle-treated mice. Nine mice were instilled with 0.1 µm particles, with three mice undergoing BAL cytospins, three mice undergoing AT2 isolation, and three mice undergoing histology. Similarly, another group of nine mice received 1 µm particles, with the same distribution of experimental procedures as for the 0.1 µm particle group. The isolation of BAL macrophages and AT2 cells was performed for all mice in the study.

2.2.6.1 Intratracheal Instillation:

The experiment involved the intratracheal instillation of 50µg PLGA particles with 100nm and 1000nm diameters into mice, as outlined in *Stoeger et al.'s 2006* [116] protocol. Following a 24-hour exposure, the mice were anesthetized via intraperitoneal injection of ketamine and xylazine and subsequently euthanized to extract alveolar macrophages and lung alveolar type 2 cells.

2.2.6.2 Bronchoalveolar lavage (BAL) Isolation:

Following the sacrifice of mice, bronchoalveolar lavage (BAL) was performed through tracheal cannulation and lung infusion with 1 ml of calcium and magnesium-free PBS, as previously described by *Stoeger et al. (2006)* [116]. The BAL cells were separated by centrifugation at 425g for 20 minutes at room temperature. The resulting cell pellets were suspended in 1 ml of RPMI media (BioChrome, Berlin, Germany) containing 10% fetal calf serum (FCS) for enumeration of viable cells using the trypan blue exclusion method, as described by *Chen et al. (2016)*. The BAL samples were then prepared by adding FACS buffer to assess particle uptake by BAL macrophages using flow cytometry in the FITC channel. BAL cytospins were also prepared on glass slides, as previously described by *Chen et al. (2016)*, and stained with DAPI and phalloidin to visualize nuclei and actin, respectively, for analysis of particle uptake by cells using fluorescence microscopy, as previously described by *S.H. Van Rijt et al. (2016)*. Briefly, the fixed cells were treated with 70% methanol for 10 minutes and then washed and blocked with Roti-Immunoblock (Carl Roth, Berlin, Germany) for 1 hour at room temperature. Phalloidin staining was performed by incubating the BAL cytospins with a mixture of phalloidin and DAPI for 30 minutes at room temperature. The stained cells were mounted using a mounting medium (DAKO, USA), and fluorescence microscopy analyzed particle uptake.

2.2.6.3 Alveolar epithelial type 2 cells Isolation:

In this study, primary mouse alveolar cells (pmAECs) were obtained from 8–10-week-old female C57BL/6J mice via a previously described method *(Chen et al., 2016)* following a 24-hour exposure to 50µg of PLGA particles via intratracheal

instillation. The isolation process involved perfusing the lungs with ice-cold phosphate-buffered saline, followed by intratracheal instillation of cold dispase and low-melting agarose. Single-cell suspensions were obtained after digestion and magnetic depletion using CD45 and CD31 microbeads to obtain a CD45-/CD31--cell population. The pmAECs were then positively selected using microbeads specific for epithelial cell adhesion molecule (EpCAM). The uptake of particles by AT2 cells was analyzed via flow cytometry using the FITC channel after adding FACS buffer to the samples.

2.2.6.4 Histology:

Following intratracheal instillation of PLGA particles of 0.1µm and 1µm size, three mice were selected from each group of particle treatment. They were euthanized 24 hours post-treatment to perform histological analysis. Haematoxylin and eosin (H&E) staining, as outlined by S.H. Van Rijt et al. in 2016, was performed on the alveolar epithelial tissue to examine its architecture. The lungs were fixed in 4% (w/v) paraformaldehyde and embedded in paraffin before being sliced and stained. The staining protocol involved washing the tissue slices twice in xylene for five minutes, followed by immersion in 100% ethanol (EtOH) once, and 90%, 80%, and 70% EtOH each for one minute. After washing the tissue in distilled water for one minute, Mayer's Hemalum solution was used to stain the nuclei for five minutes. The slides were washed briefly with water and 0.1 HCL-ETOH and washed again in running tap water for ten minutes. Eosin at a concentration of 0.5% was used to stain the plasma for eight minutes, and the slides were dehydrated using ethanol and xylene solutions repeatedly. Finally, the dried slides were mounted in entellan and observed under Bright Field microscopy.

2.2.7 Statistical Analysis:

The statistical analysis was executed through Microsoft Excel 365 and GraphPad Prism 8.0 software (GraphPad Software, Inc., La Jolla, CA 92037, USA). The presentation of data is in the form of mean ± SEM, and the experiments were conducted independently in triplicate. To evaluate the significance of differences between the experimental and control groups, the analysis of variance (ANOVA)

was employed. Significance Levels were set at *, $p < 0.05$; **, $p < 0.01$; and ***, $p < 0.001$.

2.2.8 Experimental design of the project

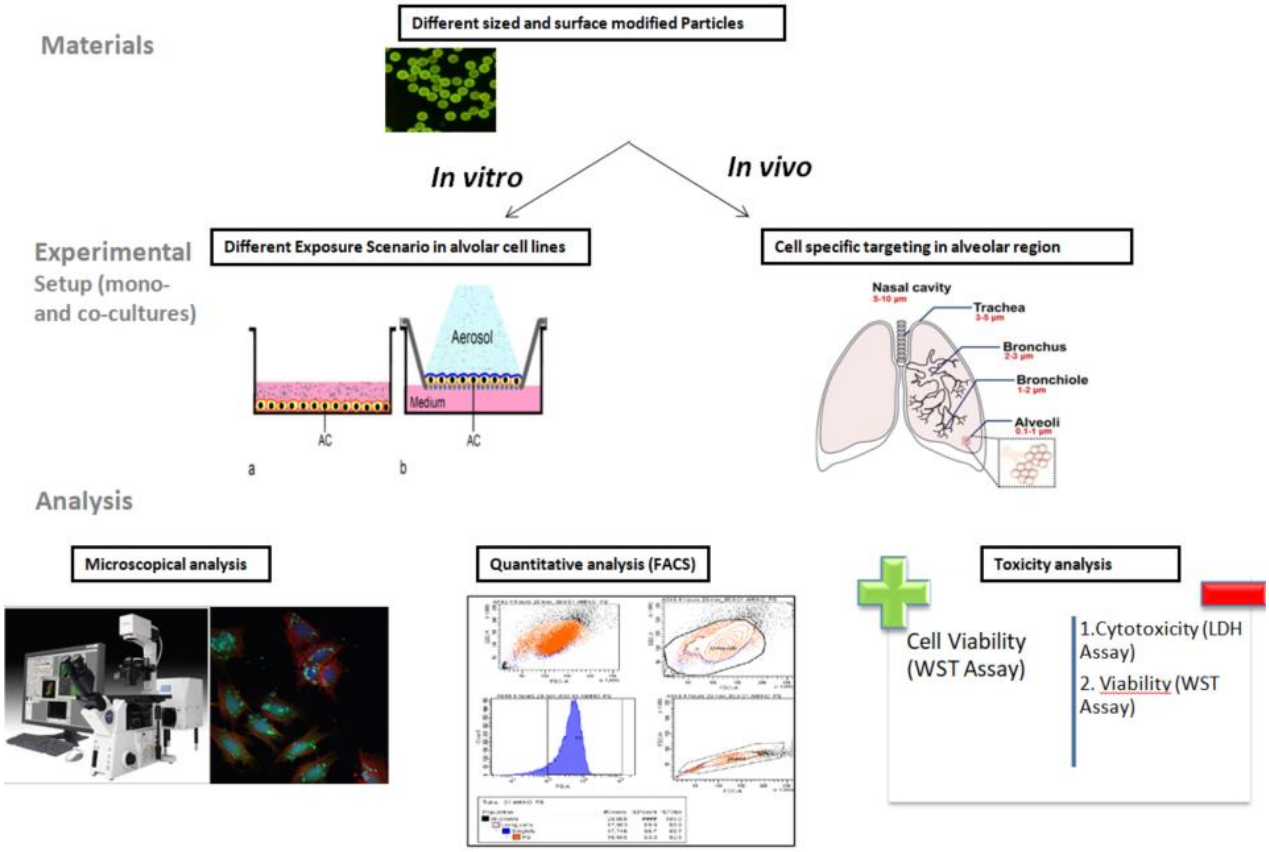

Figure 2-1 Graphical representation of the experimental design of the project.

3. Results

3.1 The uptake and toxicity of different sizes and surface-modified Polystyrene (PS) latex beads by different alveolar cell types in submerged and Air-liquid interface exposure systems

The purpose of the PS study was to investigate the uptake of fluorescently labeled poly-styrene particles with different surface modifications (carboxyl-, amine-, and sulfate-modified) and sizes (0.03 µm, 0.1 µm, 0.5 µm, and 1 µm) by alveolar epithelial cell lines (A549 cells, MLE-12 cells, LA-4 cells), and alveolar macrophage cell line (MH-S cells). Specifically, the study aimed to examine the impact of particle size and surface modification on uptake by alveolar epithelial cells and compare the uptake and toxicity of PS particles in two exposure systems: submerged and air-liquid interface.

3.1.1 Particle Characterization

This study confirmed particle size confirmation using Dynamic Light Scattering (DLS) with a sample size of N=3. The results of the DLS analysis indicate that the hydrodynamic radius of the particles was 35.6nm/±8 for 30nm particles, 422.8nm/±113.7 for 500nm particles, and 911.8nm/±235.5 for 1000nm carboxyl-modified particles. The peak size for 100nm particles was 125.2nm/±50; for 1000nm amine-modified particles, it was 1011nm/±253.8. For 100nm particles cataloged as sulfate-modified, the peak size was 121.8nm/±29.17, and for 500nm particles, it was 446.6nm/±121.9 with low polydispersity indexes. Based on these results, it is evident that the particle samples did not have a broad size distribution and were suitable for analysis using the DLS technique. All measurements were conducted in dH2O because the particle stocks were diluted in water, as outlined in Table 1.

PS particles green	DLS Hydrodynamic radius (nm)	Standard deviation
30nm Carboxyl-modified	35.62	± 8
500nm Carboxyl-modified	422.8	± 113.7
1000nm Carboxyl-modified	911.8	±235.5
100nm Amine-modified	125.2	±50
1000nm Amine-modified	1011	±253.8
100nm Sulfate-modified	121.8	±29.17
500nm Sulfate-modified	446.7	±121.9

Table 1 **Characterization of PS Particles**. The average diameter and standard deviations of PS particles.

To address variations in mean fluorescent intensity (MFI) due to particle size, MFI measurements for each of the seven particle types were normalized to particle mass using a plate reader. The MFI signal of 0.5 µm sulfate particles was used as the reference standard, with all other particle types normalized relative to this reference. Specifically, 0.03 µm carboxyl (COOH) and 0.1 µm sulfate particles exhibited MFI signals half that of the 0.5 µm sulfate particles, while 1 µm amine (NH2) particles exhibited twice the MFI signal of the 0.5 µm sulfate particles. The 0.5 µm and 1 µm COOH particles, as well as the 0.1 µm NH2 particles, showed the same signal as the 0.5 µm sulfate-modified particles. These differences are due to variations in particle size, as larger particles can incorporate more dye than smaller particles (as depicted in Figure 3.1). To correct for particle uptake in *in-vitro* cellular experiments, the MFI signal of the test sample was subtracted from that of the control and normalized to the particle mass to their MFI.

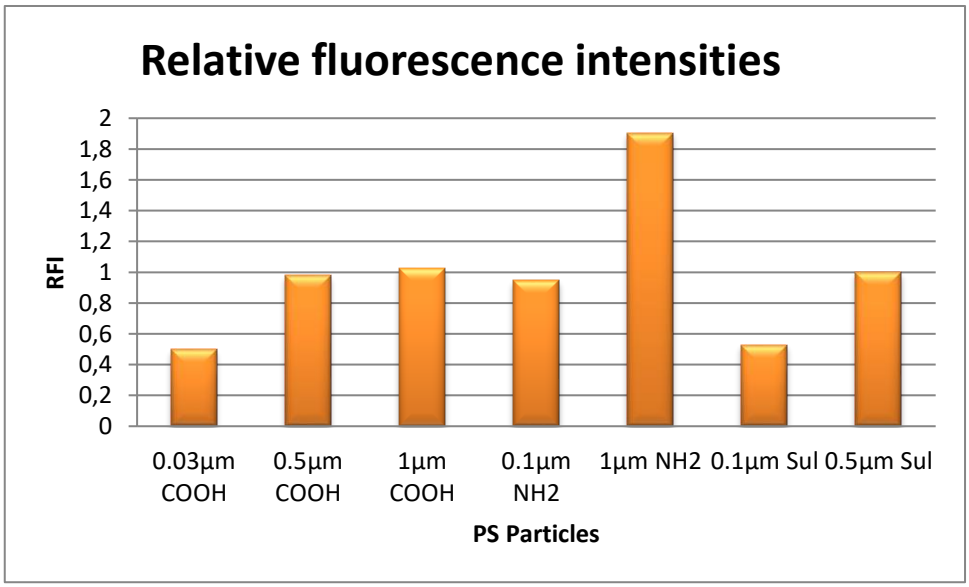

Figure 3-1 Characterization of PS Particles: Relative mean fluorescent intensities of the particles measured by plate reader.

In the present investigation, flow cytometry was used to evaluate the mean fluorescent intensity of intracellular particles in cell lines under investigation, representative of the alveolar epithelium.

Gating Strategy:

Before analyzing fluorescence-activated cell sorting (FACS) experiments involving particles, a background fluorescence correction was performed to account for cells not exposed to particles. In principle, internalized particles may be differentiated from extracellular particles using pH-sensitive fluorophores in flow cytometry. In our study, the choice of phycoerythrin (PE) as the fluorescent dye was guided by its compatibility with the wavelength of polystyrene (PS) particles used in our experiments. This strategic selection facilitated precise detection and quantification of PS particle uptake within cellular systems through gating strategies. By utilizing gating techniques based on the fluorescence emitted by PE, we could effectively distinguish between internalized and external particles. This approach, leveraging the fluorescence emitted by PE in FACS analysis, provided valuable insights into the dynamics of cellular uptake of PS particles, thereby significantly contributing to the experimental outcomes and enhancing our understanding of particle-cell interactions.

The term "uptake" refers to the number of particles absorbed by cells, which is illustrated by each peak in the positively gated histogram (positively gated denotes the heightened intensity per cell, as illustrated in Fig 2.1 “Quantitative analysis FACS”). For instance, the histograms enable the differentiation of the number of particles absorbed per cell, as each individual internalized particle contributes to an incremental rise in fluorescence, transitioning from <200 (cells without particles) to 1,200 (1 particle), 2,300 (2 particles), and 3,700 (3 particles). Consequently, an elevated mean fluorescent intensity signifies a larger population of particles within the cell group. These experiments depend on the signal emitted by internalized particles, translated into the quantity of internalized particles through multiplication by a scaling factor. Utilizing the mean fluorescence intensity per particle as a scaling factor streamlines the conversion of fluorescence

intensity from internalized fluorescent particles into the corresponding particle count in flow cytometry (Fig 3-2).

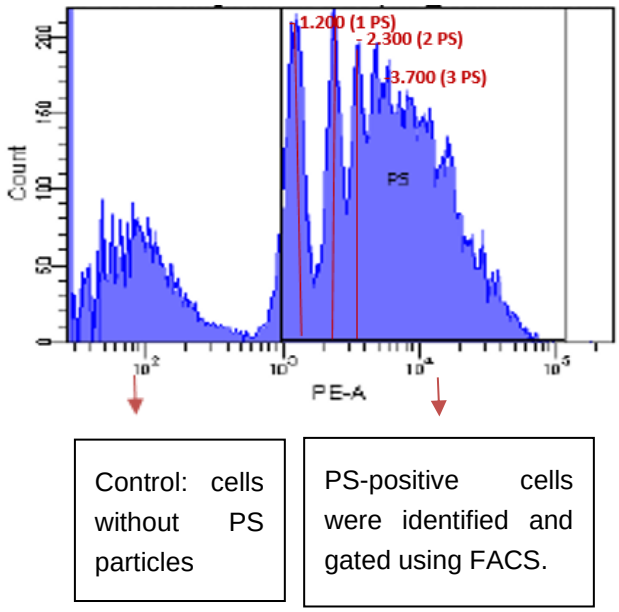

Figure 3-2 The histogram generated from flow cytometry distinguishes the number of particles absorbed per cell. The mean fluorescent intensity measured in the PE channel indicates the cells' uptake of the particles.

3.1.2 PS Particle Uptake

3.1.2.1 Comparison of PS particle uptake at two-time points:

Initially, a specific time point was determined for conducting additional experiments on particle uptake. Subsequently, two-time points, namely 4 hours and 24 hours, were chosen to evaluate particle uptake concerning mean fluorescence intensity (MFI) using fluorescence-activated cell sorting (FACS) analysis. To account for particle uptake in cellular experiments conducted in vitro, the control's Mean Fluorescence Intensity (MFI) was subtracted from the test sample as a **correction measure**.

PS particle uptake by MLE 12, A549, and LA 4 cell lines:

This study shows no significant difference in particle uptake between the carboxyl and sulfate-modified polystyrene particles in MLE 12 and A549 cells at both time

points. However, amine-modified particles showed significantly better uptake after 24 hours in these cell lines. In LA-4 cells, a significant difference was observed between the two time points for 1µm carboxyl modified particles and both sizes of amine-modified particles, as also seen in MLE 12 and A549 cell lines. These findings suggest that exposure of alveolar epithelial cell lines to particles for 24 hours enhances particle uptake (Fig 3-3).

PS particle uptake by MH-S cell line:

The FACS particle uptake data revealed that except for 1µm amine-modified particles, there were no significant differences in particle uptake by alveolar macrophages (MH-S cell line) at both 4-hour and 24-hour time points. Notably, the 1µm amine-modified particles exhibited higher uptake after 24 hours than after 4 hours (Fig 3d). These findings suggest that a longer exposure time enhances particle uptake, as evidenced by the higher mean fluorescent intensities observed after 24 hours. Therefore, I selected the 24-hour time point for further uptake experiments in submerged and ALI exposure scenarios (Fig 3-3).

The following factors can explain the variation in MFI:

- Particle size: Larger particles can absorb more dye and exhibit higher fluorescence intensity than smaller particles.
- Uptake of particle numbers by cells: The cells with more particles display stronger fluorescence intensity.

a.

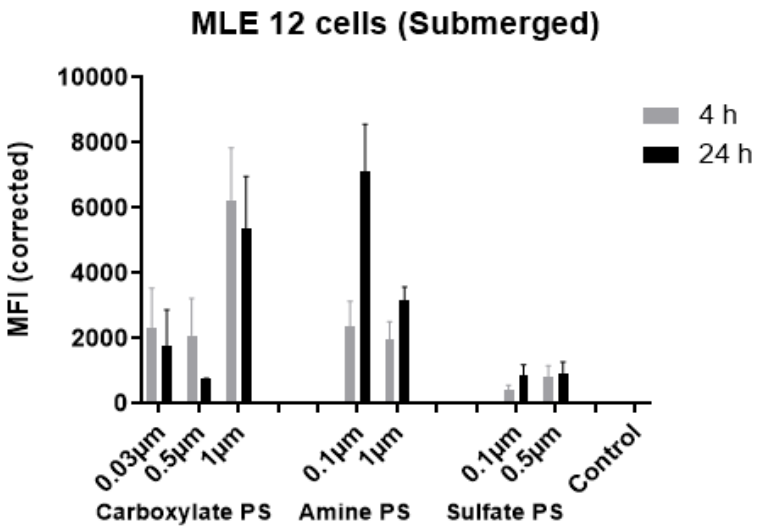
MLE 12 cells (Submerged)
MFI (corrected)
10000
8000
6000
4000
2000
0
4 h
24 h
0.03µm
0.5µm
1µm
0.1µm
1µm
0.1µm
0.5µm
Control
Carboxylate PS
Amine PS
Sulfate PS

b.

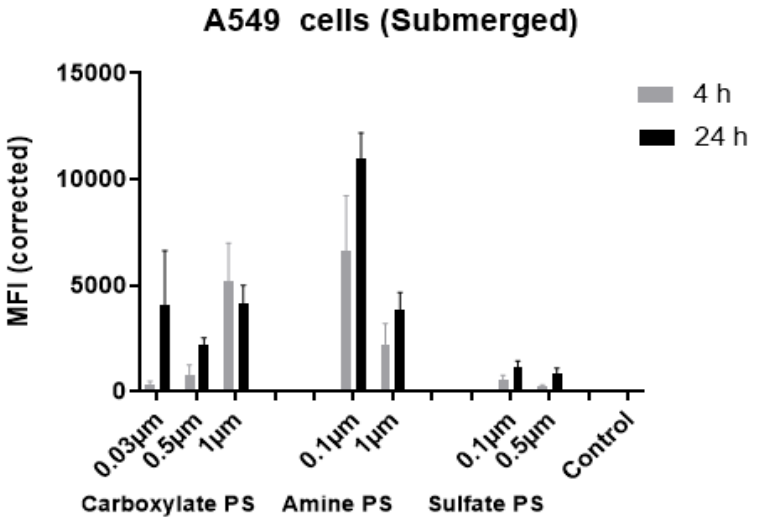
A549 cells (Submerged)
MFI (corrected)
15000
10000
5000
0
4 h
24 h
0.03µm
0.5µm
1µm
0.1µm
1µm
0.1µm
0.5µm
Control
Carboxylate PS
Amine PS
Sulfate PS

c.

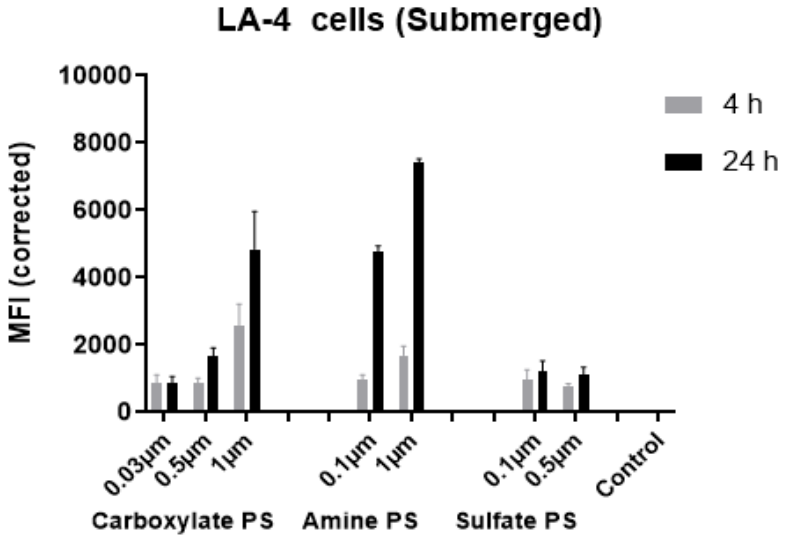

d.

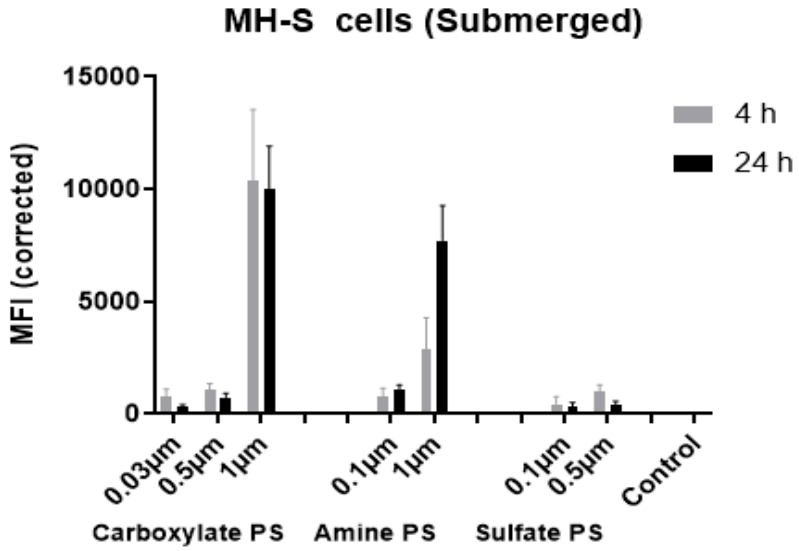

Figure 3-3 Analysis of cellular uptake kinetics of 0.03µm, 0.5µm, and 1µm carboxyl, 0.1µm, and 1µm amine, and 0.1µm and 0.5µm sulfate-modified polystyrene (PS) particles alveolar epithelial and macrophages cells by flow cytometry after 4 and 24 hours. Mean fluorescent intensities show a. uptake of particles by MLE 12 cells. b. uptake of particles by A549 cells, c. uptake of particles by LA-4 cells, and d. uptake of particles by MH-S cells submerged in monoculture conditions.

3.1.2.2 Measurement of particle uptake under submerged conditions using MFI:

Additional experiments were conducted to evaluate particle uptake using fluorescence-activated cell sorting (FACS) analysis, with a specific exposure time of 24 hours. To correct for particle uptake, the control's Mean Fluorescence Intensity (MFI) was subtracted from that of the test sample.

PS particle uptake by MLE 12, A549, and LA 4 cell lines:

- The results of this study demonstrate that MLE 12 cells exhibit a significant uptake of 1 µm carboxyl-modified particles when compared to both 0.03 µm and 0.5 µm carboxyl-modified particles ($P \leq 0.05$). Furthermore, 0.1 µm amine-modified particles demonstrate better uptake by MLE 12 cells than larger 1 µm amine-modified particles. In contrast, 0.1 µm and 0.5 µm sulfate particles did not exhibit significant uptake. These findings suggest that MLE 12 cells display greater uptake of larger (1 µm) carboxyl-modified particles and smaller (0.1 µm) amine-modified particles when compared to all other particles analyzed in this study (see Fig. 3.4a). The positive surface charge and smaller size of NH2 particles at 0.1 µm enhance their interaction with negatively charged cell surfaces, leading to stronger fluorescence intensity and higher cell uptake.
- The results demonstrate that A549 cells exhibit limited uptake of particles with sizes of 0.03 µm, 0.5 µm, and 1 µm, with no discernible variance in uptake between the three carboxyl-modified particles. However, there was a marked and statistically significant uptake ($P \leq 0.001$) of amine-modified particles with a size of 0.1 µm compared to their 1 µm counterparts. In contrast, sulfate-modified particles did not exhibit a significant uptake. Overall, it can be concluded that 0.1 µm amine-modified particles exhibit the highest uptake ($P \leq 0.001$) compared to all other particles (as illustrated in Fig. 3.4b).

- To investigate the uptake efficiency of different sizes and surface modifications of particles by LA-4 cells, the results demonstrated that 1 µm carboxyl and amine-modified particles exhibited significant uptake compared to 0.03 µm ($P \leq 0.001$) and 0.5 µm ($P \leq 0.01$) particles. Additionally, 1 µm amine-modified particles displayed higher uptake efficiency compared to 0.1 µm ($P \leq 0.05$) amine-modified particles, while 0.1 µm and 0.5 µm sulfate particles did not exhibit significant uptake. Overall, the findings suggest that larger particles (1 µm) with carboxyl and amine surface modifications demonstrated better uptake efficiency by LA-4 cells. In comparison, 0.1 µm amine-modified particles also exhibited significant uptake compared to 0.03 µm ($P \leq 0.001$), 0.5 µm ($P \leq 0.01$) carboxyl, and 0.1 µm ($P \leq 0.01$) and 0.5 µm ($P \leq 0.01$) sulfate-modified particles, as shown in Figure 3.4c.

PS particle uptake by MH-S cell line

- In this study, the cellular uptake of carboxyl-modified and amine-modified particles with varying sizes (0.03 µm, 0.5 µm, and 1 µm) by MH-S cells was investigated. The results demonstrated a statistically significant increase in the uptake of 1 µm particles compared to both 0.03 µm ($P \leq 0.0001$) and 0.5 µm ($P \leq 0.0001$) particles by MH-S cells. Additionally, 1 µm amine-modified particles exhibited a greater uptake than their smaller counterparts, namely 0.1 µm amine-modified particles ($P \leq 0.01$). Notably, no significant uptake was observed for 0.1 µm and 0.5 µm sulfate particles. Overall, these findings are consistent with those of previous studies and indicate that MH-S cells, like LA-4 cells, exhibit a higher ($P \leq 0.0001$) uptake of larger particles (1 µm) in both carboxyl and amine-modified particles, as compared to smaller particles (Fig 3.4d).

Hence, In ***Submerged conditions:***

1. Compared to smaller particles, epithelial cells (excluding the A549 cell line) and macrophages internalize 1µm particles more effectively in carboxyl PS.

2. Epithelial cells show the highest uptake for 0.1µm amine-PS particles, while macrophages effectively internalize 1µm PS particles.
3. Sulphate-modified particles have low uptake and are barely detectable in alveolar epithelial cells and macrophages.

a.

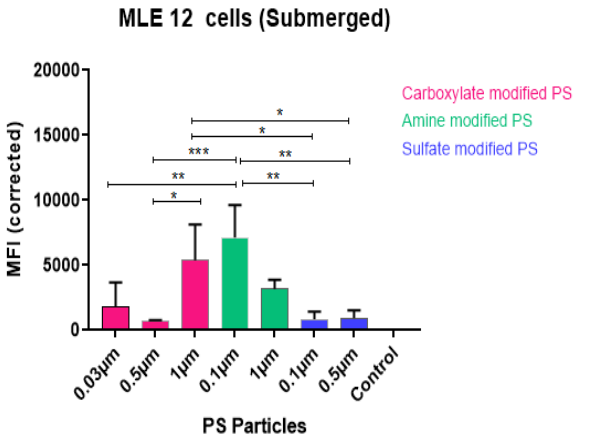

MLE 12 Control

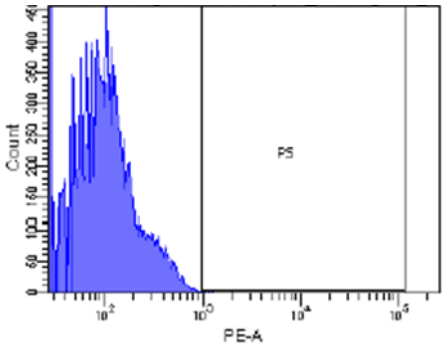

MLE 12 cells + 0.03µm COOH PS

MLE 12 cells + 0.5µm COOH PS

MLE 12 cells + 1µm COOH PS

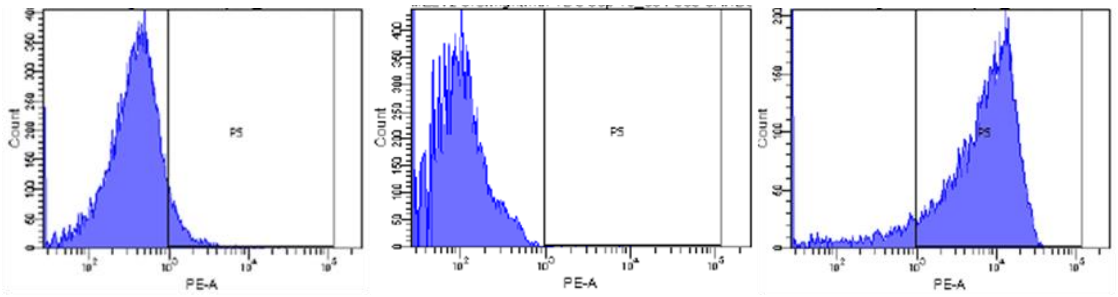

MLE 12 cells + 0.1µm NH_2 PS

MLE 12 cells + 1µm NH_2 PS

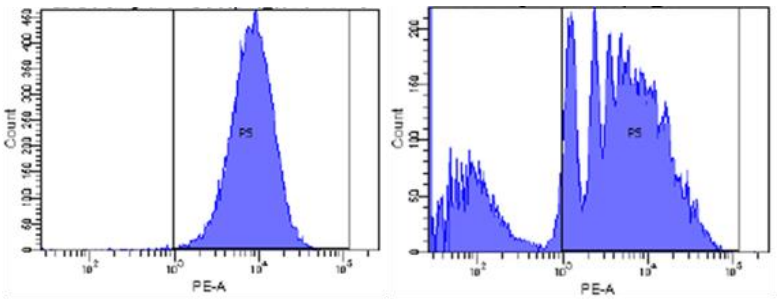

MLE 12 cells + 0.1µm SO_4 PS

MLE 12 cells + 0.5µm SO_4 PS

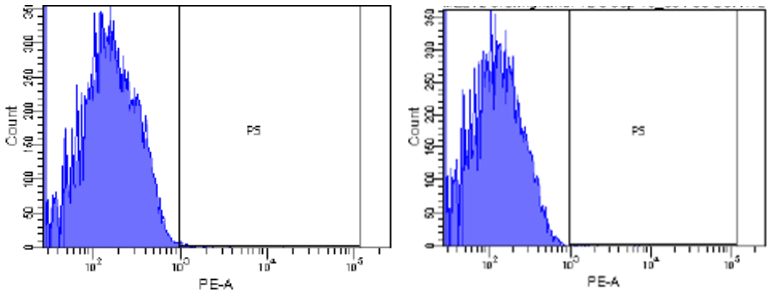

b.

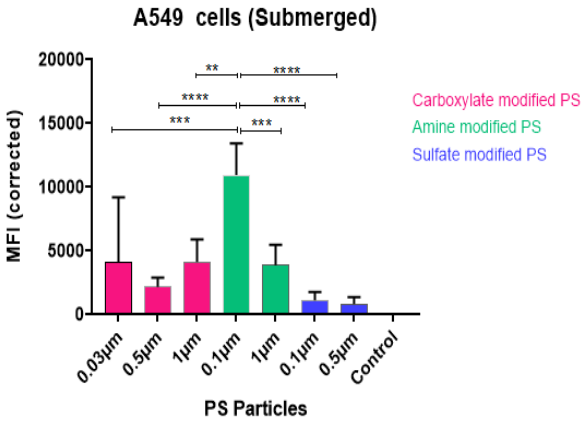

A549 Cells Control

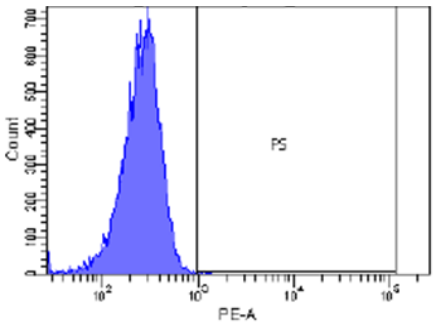

A549 cells + 0.03µm COOH PS

A549 cells + 0.5µm COOH PS

A549 cells + 1µm COOH PS

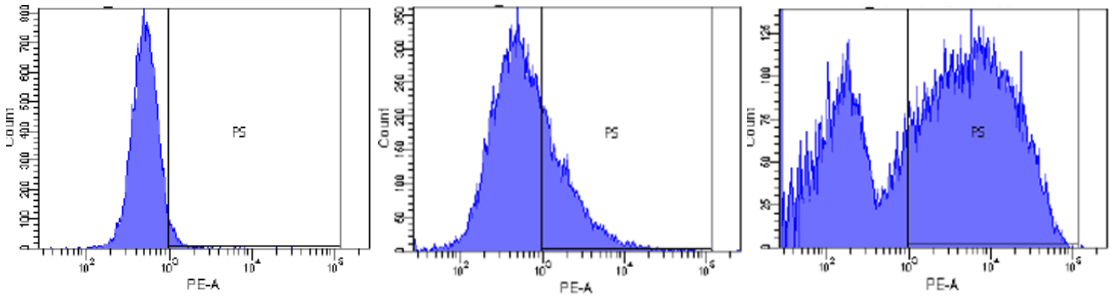

A549 cells + 0.1µm NH_2 PS

A549 cells + 1µm NH_2 PS

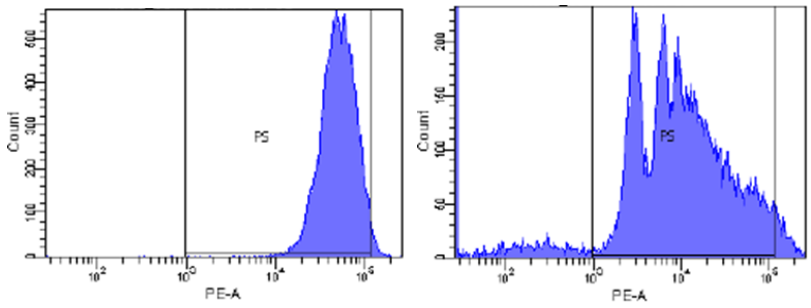

A549 cells + 0.1µm SO_4 PS

A549 cells + 0.5µm SO_4 PS

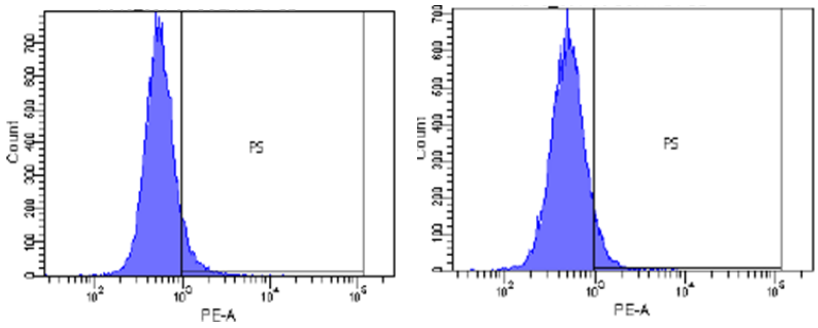

c.

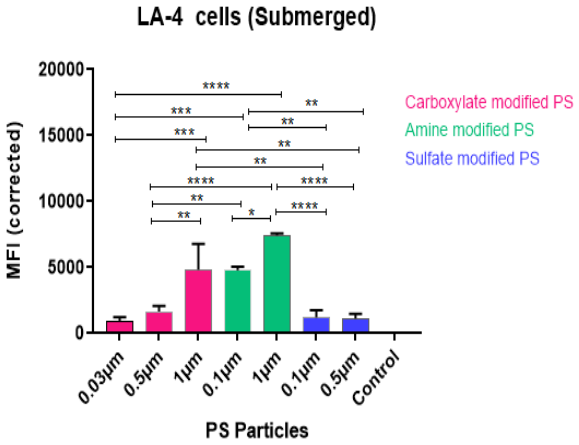

LA-4 Cells Control

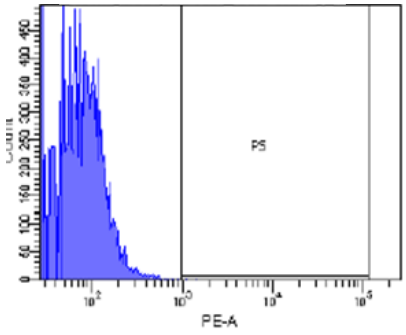

LA-4 cells + 0.03µm COOH PS

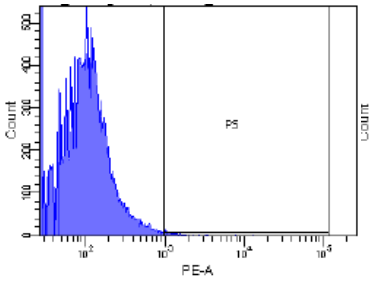

LA-4 cells + 0.5µm COOH PS

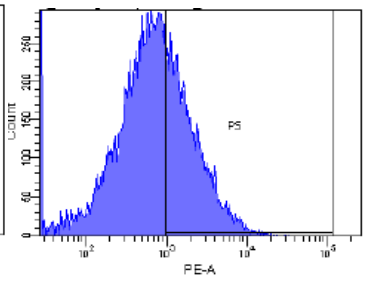

LA-4 cells + 1µm COOH PS

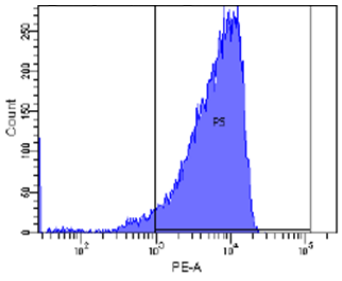

LA-4 cells + 0.1µm NH_2 PS

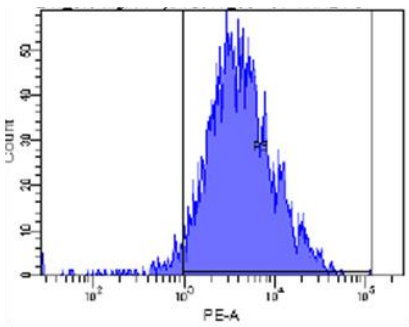

LA-4 cells + 1µm NH_2 PS

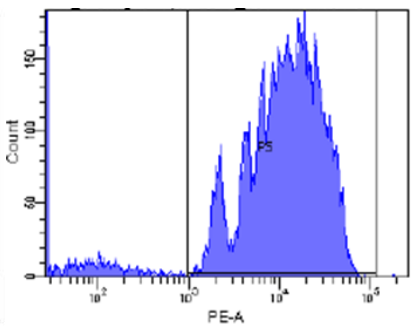

LA-4 cells + 0.1µm SO_4 PS

LA-4 cells + 0.5µm SO_4 PS

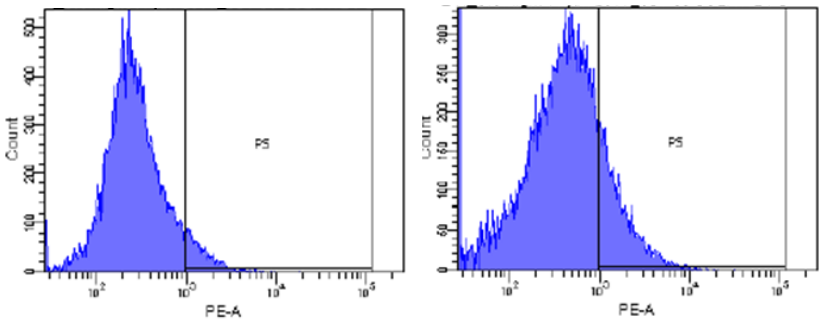

d.

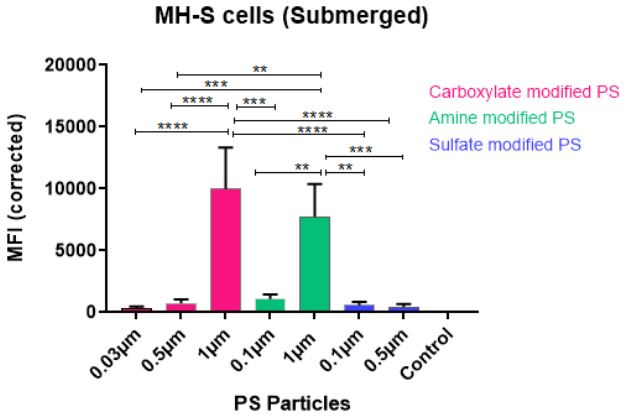

MH-S Cells Control

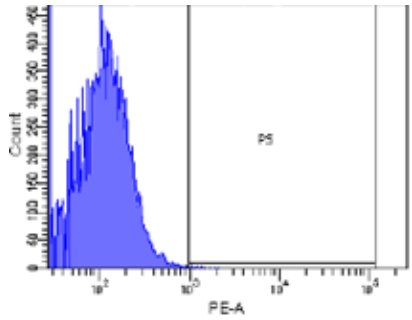

MH-S cells + 0.03µm COOH PS

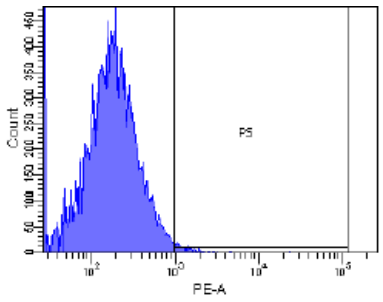

MH-S cells + 0.5µm COOH PS

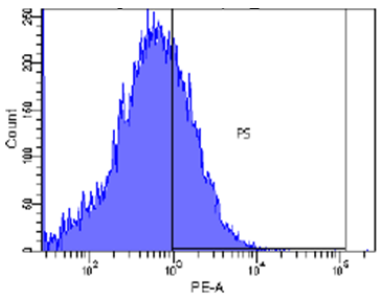

MH-S cells + 1µm COOH PS

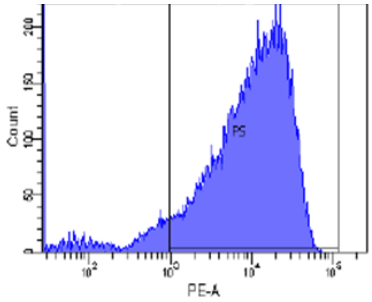

MH-S cells + 0.1µm NH_2 PS

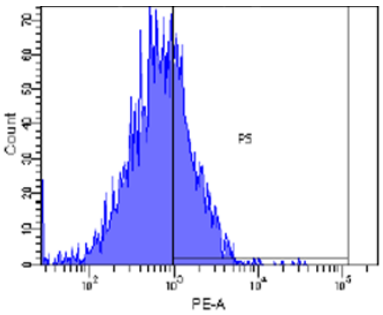

MH-S cells + 1µm NH_2 PS

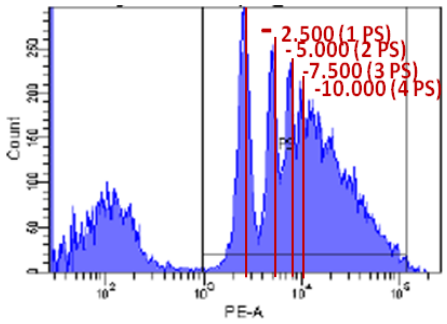

MH-S cells + 0.1µm SO_4 PS

MH-S cells + 0.5µm SO_4 PS

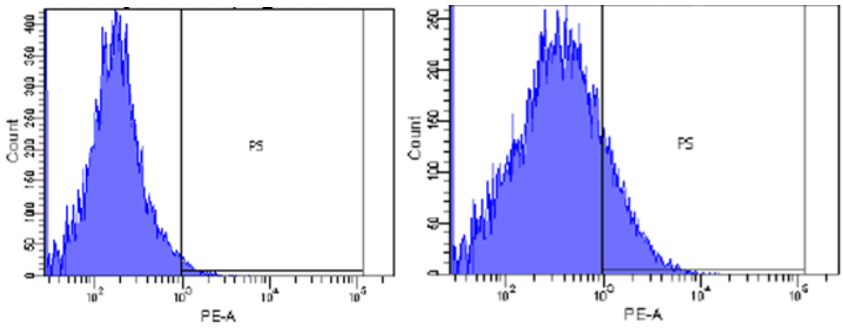

Figure 3-4 Analysis of cellular uptake of 0.03 µm, 0.5 µm, and 1 µm carboxyl-modified polystyrene (PS) particles; 0.1 µm and 1 µm amine-modified PS particles; and 0.1 µm and 0.5 µm sulfate-modified PS particles in alveolar epithelial and macrophage cells by flow cytometry after 24 hours. The mean fluorescent intensities in positively gated histograms indicate a. uptake of particles by MLE-12 cells, b. uptake of particles by A549 cells, c. uptake of particles by LA-4 cells, and d. uptake of particles by MH-S cells under submerged conditions in monoculture.

3.1.2.3 Measurement of particle uptake under ALICE CLOUD exposure conditions using MFI:

The ALICE CLOUD exposure system was employed to assess particle uptake in a more realistic setting and overcome the potential for uptake bias resulting from particle size-dependent deposition under submerged conditions. This system utilized fluorescence-activated cell sorting (FACS) analysis to evaluate particle uptake over a specified exposure period of 24 hours. To account for particle uptake, the Mean Fluorescence Intensity (MFI) of the control sample was subtracted from that of the test sample.

<u>PS particle uptake by MLE 12, A549, and LA 4 cell lines:</u>

The experimental findings indicate that MLE 12 cells exhibited noteworthy uptake of 0.5 µm ($P \leq 0.01$) and 1 µm ($P \leq 0.05$) particles in comparison to 0.03 µm carboxyl-modified particles. Notably, there were no discernible differences in the uptake of 0.1 µm amine-modified particles and 1 amine-modified particle by MLE 12 cells, as both were taken up significantly. Similarly, both 0.1 µm and 0.5 µm sulfate particles exhibited substantial uptake, but there was no noticeable difference between their uptakes. Therefore, it can be inferred

that MLE 12 cells evinced significant uptake of all particles except 0.03 µm (Fig 3.5a).

Then, the cellular uptake of particles with varying surface modifications was evaluated in A549 cells. It was observed that the uptake of 0.5 µm and 1 µm carboxyl-modified particles were negligible, with no significant difference in uptake between these two sizes. However, their uptake was greater than that of the 0.03 µm particles. In contrast, the uptake of 0.1 µm and 1 µm amine-modified particles was comparable, and both were significantly taken up by the cells. Similarly, 0.1 µm and 0.5 µm sulfate particles demonstrated substantial uptake, with no significant difference in uptake between them. Overall, 0.1 µm and 1 µm amine-modified and 0.1 µm sulfate-modified particles exhibited a significantly higher uptake ($P \leq 0.05$) compared to the smallest carboxyl-modified particles (0.03 µm), as illustrated in Figure 3.5b.

The results indicate that LA-4 cells exhibited superior uptake of 0.5 µm and 1 µm particles compared to 0.03 µm carboxyl-modified particles, with a statistically significant difference ($P \leq 0.05$). Also, LA-4 cells exhibited a greater uptake of 1 µm amine-modified particles than 0.1 µm. The cells internalized both carboxyl and amine-modified particles, while no significant difference was observed in the uptake of 0.1 µm and 0.5 µm sulfate particles. Larger carboxyl and amine-modified particles generally demonstrated higher uptake than smaller particles. Furthermore, the uptake of carboxyl and amine-modified particles was found to increase with particle size, as shown in Figure 3.5c.

PS particle uptake by MH-S cell line

The MH-S cells exhibited minimal uptake of 0.5 µm and 1 µm particles. However, no dissimilarity was observed between the two carboxyl-modified particles regarding uptake, which was superior to that of 0.03 µm uptake. The uptake of 0.1 µm and 1 µm amine-modified particles by MH-S cells was identical, with both particles being taken up considerably by the cells. Similarly, significant uptake of 0.1 µm and 0.5 µm sulfate particles was observed, but no dif-

ference in their uptake was found. Overall, the uptake of 0.1 µm amine-modified particles was significantly ($P \leq 0.05$) more significant than that of the smallest particles, 0.03 µm carboxyl-modified particles (Fig 3.5d).

In ***ALICE CLOUD conditions:***

Importance of particle modification and size:

1. Tracking 0.03 µm PS uptake presents challenges due to potential limitations arising from internalized PS mass and low exposure dose compared to submerged. Nonetheless, a minor uptake of 0.03 µm PS has been identified in LA4 alone.

2. Comparable uptake of 0.1, 0.5, and 1.0 µm PS has been observed across all cell types. The highest overall uptake is noted for 1 µm carboxy- and amine-PS in LA4 and 0.1 µm sulfated-PS in A549. MLE12, however, exhibits uptake of all particles except 0.03 µm.

Importance of cell line:

1. The mean fluorescent intensities indicate that LA4 cells exhibit greater uptake of amine- and carboxy-modified PS compared to MLE 12 and A549 cell lines.
2. PS uptake by MHS macrophages is lower overall, potentially due to PS toxicity.

a.

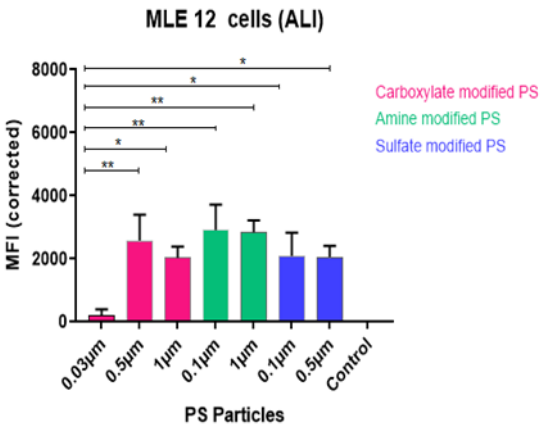

MLE 12 Control

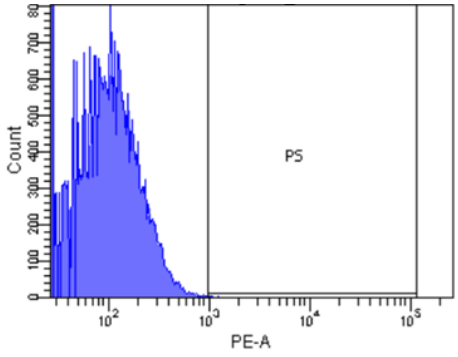

MLE 12 cells + 0.03µm COOH PS

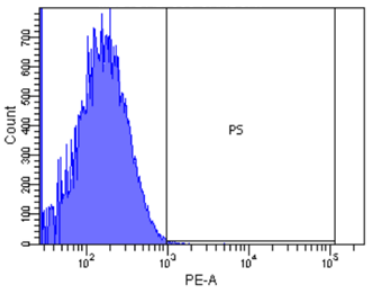

MLE 12 cells + 0.5µm COOH PS

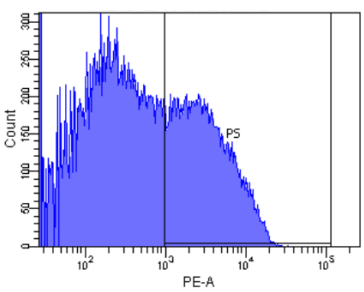

MLE 12 cells + 1µm COOH PS

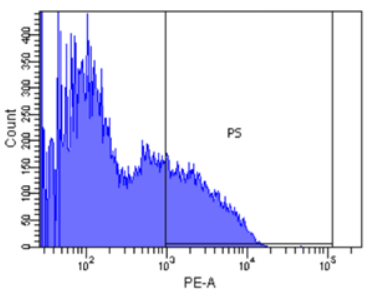

MLE 12 cells + 0.1µm NH_2 PS

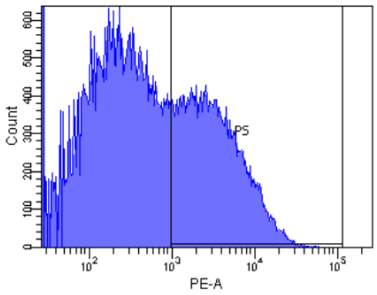

MLE 12 cells + 1µm NH_2 PS

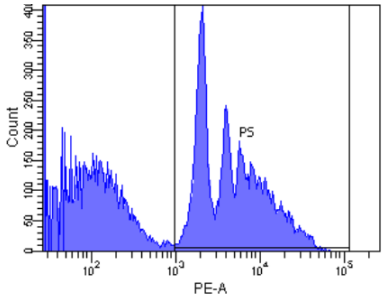

MLE 12 cells + 0.1µm SO_4 PS

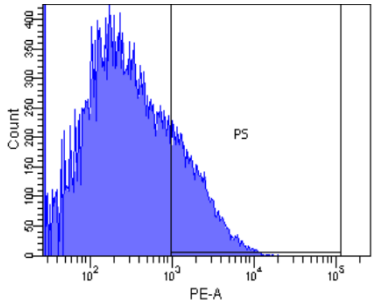

MLE 12 cells + 0.5µm SO_4 PS

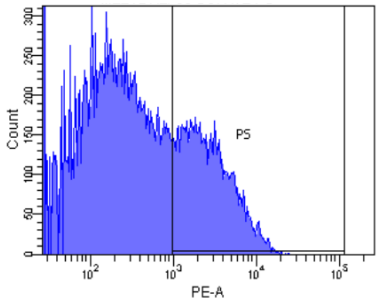

b.

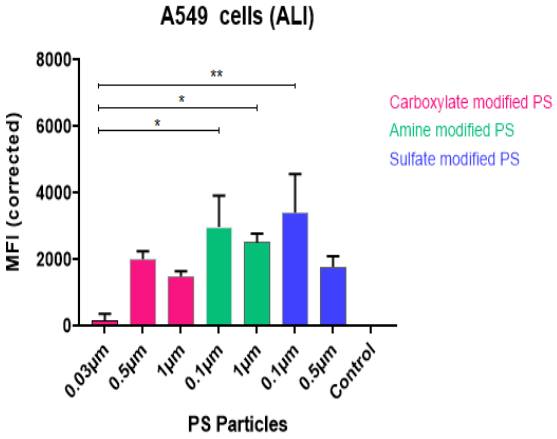

A549 Cells Control

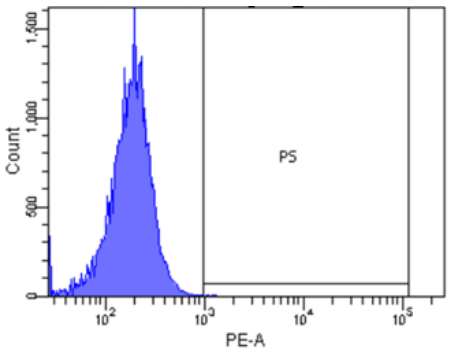

A549 cells + 0.03µm COOH PS

A549 cells + 0.5µm COOH PS

A549 cells + 1µm COOH PS

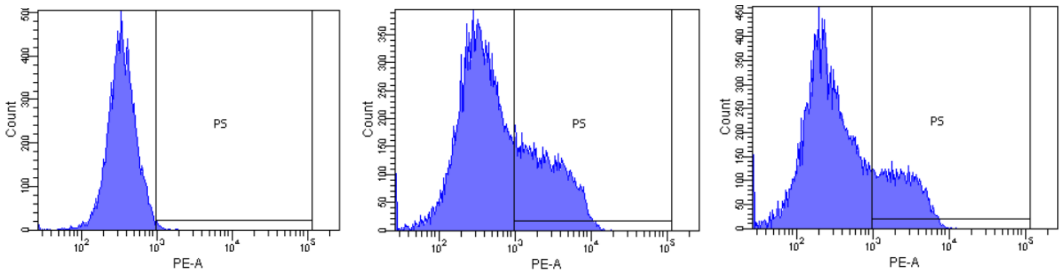

A549 cells + 0.1µm NH_2 PS

A549 cells + 1µm NH_2 PS

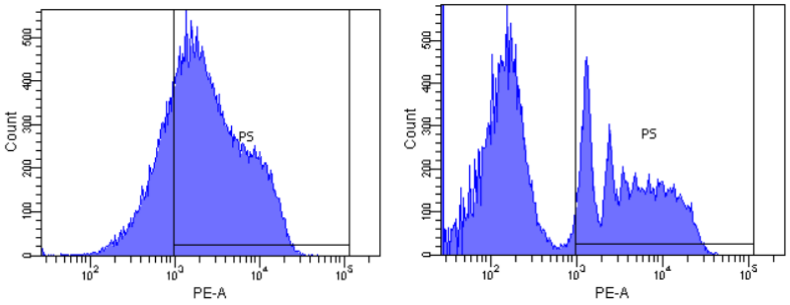

A549 cells + 0.1µm SO_4 PS

A549 cells + 0.5µm SO_4 PS

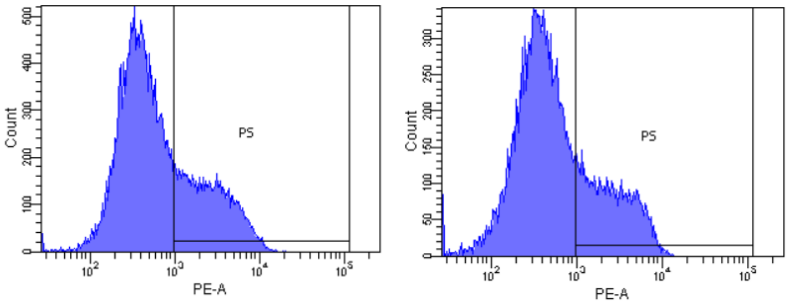

c.

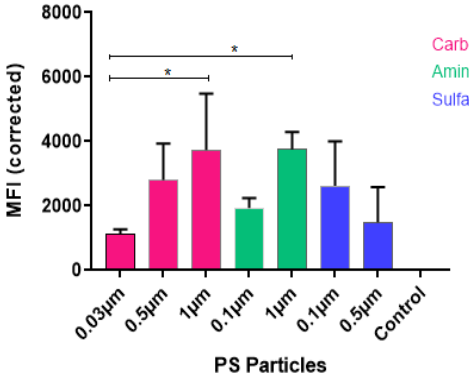

LA-4 Cells Control

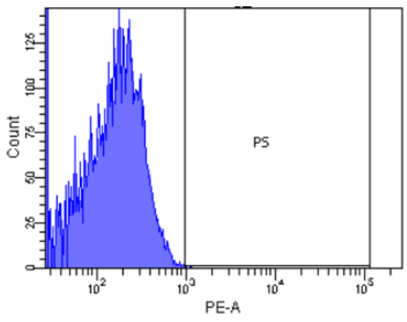

LA-4 cells + 0.03µm COOH PS

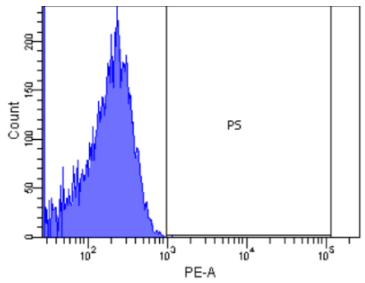

LA-4 cells + 0.5µm COOH PS

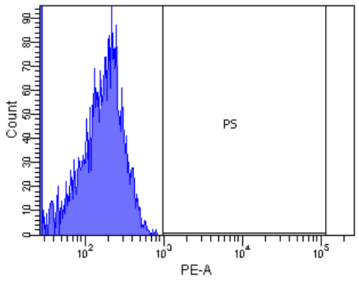

LA-4 cells + 1µm COOH PS

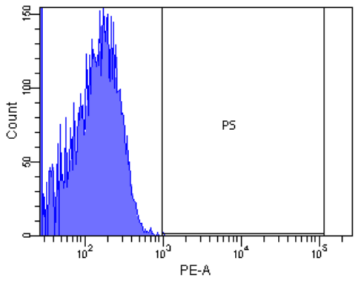

LA-4 cells + 0.1µm NH_2 PS

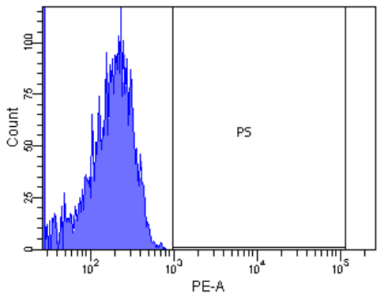

LA-4 cells + 1µm NH_2 PS

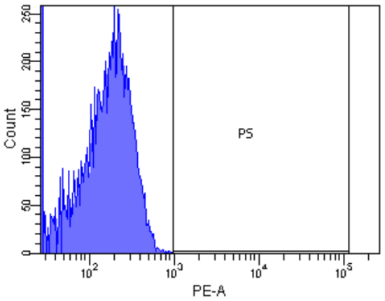

LA-4 cells + 0.1µm SO_4 PS

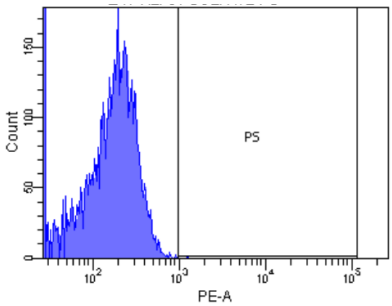

LA-4 cells + 0.5µm SO_4 PS

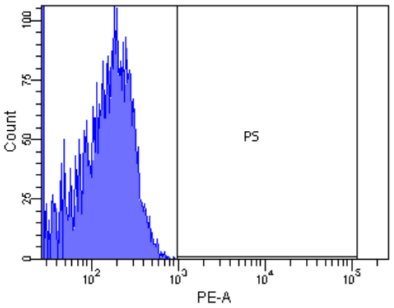

d.

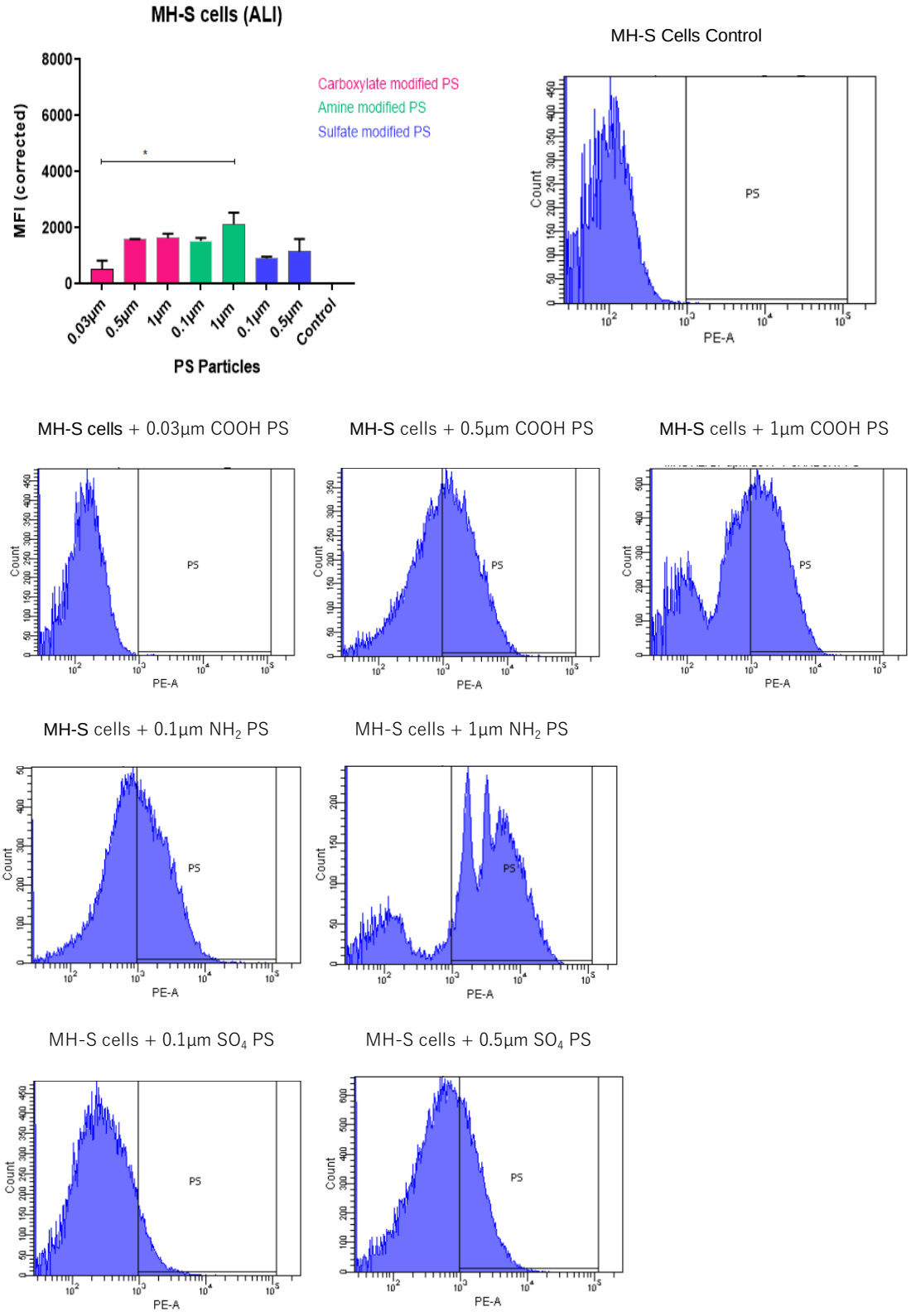

Figure 3-5 Analysis of cellular uptake of 0.03µm, 0.5µm, and 1µm carboxyl, 0.1µm, and 1µm amine, and 0.1µm, and 0.5µm sulfate-modified polystyrene (PS) particles alveolar

epithelial and macrophages cells by flow cytometry after 24 hours in ALI conditions. The mean fluorescent intensities in positively gated histograms indicate a. uptake of particles by MLE 12 cells. b. uptake of particles by A549 cells, c. uptake of particles by LA-4 cells, and d. uptake of particles by MH-S cells under Air-liquid interface (ALI) conditions in monoculture.

3.1.3 Quantification of particle uptake based on the number of cells that have taken up particles.

The interpretation of flow cytometry data is a critical aspect of our research. We have employed a rigorous analytical approach that focuses not only on the number of internalized particles but also on the number of particle-positive cells. This approach, facilitated by flow cytometry's ability to recognize distinctive fluorescence' events', allows for the identification of various populations, including free particles, cells devoid of particles, cells with adherent particles, and cells with internalized particles. Gating techniques, a common practice in such studies, are used to distinguish these populations, and the choice of gating parameters significantly influences quantitative analyses. In addition to quantifying the mean fluorescent intensities of particle uptake, we have also quantified the number of cells that tested positive for particles, further enhancing the reliability and comprehensiveness of our findings.

3.1.3.1 Measurement of particle uptake under submerged conditions using particle-positive cells

The data indicate that MLE 12 and LA 4 cells exhibit noteworthy uptake of carboxyl-modified particles of 1 µm compared to carboxyl-modified particles of 0.03 µm and 0.5 µm ($P \leq 0.05$) in terms of the percentage of particle-positive cells. Additionally, these cells' uptake of amine-modified particles of 0.1 µm was more substantial than that of larger amine-modified particles of 1 µm. In contrast, a high percentage of particle-positive A549 cells was observed for 0.5 µm carboxyl-modified, 0.1 µm, and 1 µm amine-modified particles. However, all these cells did not demonstrate significant uptake of sulfate particles of 0.1 µm and 0.5 µm. These findings suggest that these cells exhibit greater uptake of larger (1 µm) carboxyl-modified particles and smaller (0.1 µm) amine-modified particles (see Fig. 3.6a)

based on the percentages of particle-positive cells. Compared to other particles, a higher percentage of MHS cells with particles was observed for carboxyl-modified particles of 1 µm (see Fig. 3.6a).

3.1.3.2 Measurement of particle uptake under ALICE CLOUD conditions using particle-positive cells:

According to the data, MLE 12 cells show significant uptake of carboxyl-modified particles that are 0.5 µm in size, compared to particles that are 0.03 µm and 1 µm in size (with a significance level of $P \leq 0.05$), as evidenced by the percentage of particle-positive cells. Furthermore, these cells show greater uptake of amine-modified particles that are 0.1 µm in size, as opposed to larger amine-modified particles that are 1 µm. Conversely, A549 and LA4 cells demonstrate high percentages of particle-positive cells for carboxyl-modified particles that are 0.5 µm in size and amine-modified particles that are 0.1 µm and 1 µm. LA4 cells also show positive uptake of carboxyl-modified particles that are 1 µm in size. However, none of these cells showed significant uptake of sulfate particles that are 0.1 µm and 0.5 µm in size. These results suggest that these cells have a greater tendency to take up larger (0.5 µm and 1 µm) carboxyl-modified particles and smaller (0.1 µm) amine-modified particles (see Fig. 3.6b), based on the percentage of particle-positive cells. Compared to other cells, MHS cells demonstrated similar percentages of particle uptake for all types of particles (see Fig. 3.6b).

a.

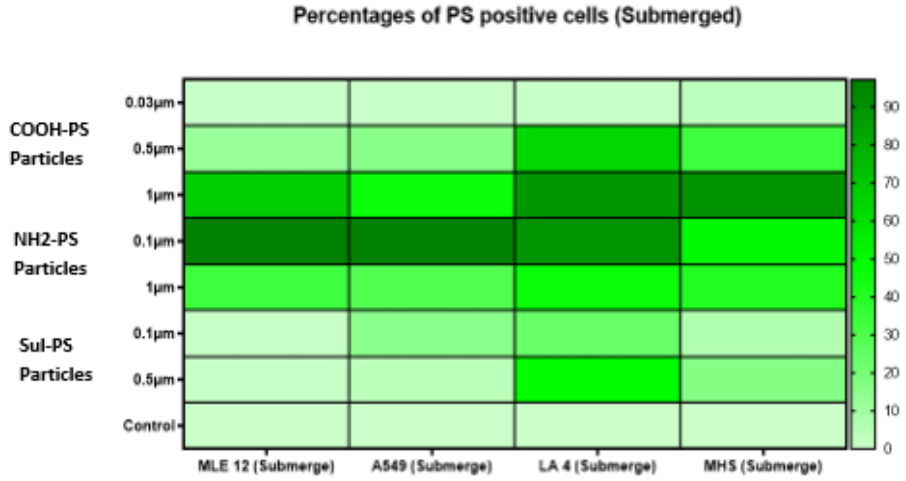

b.

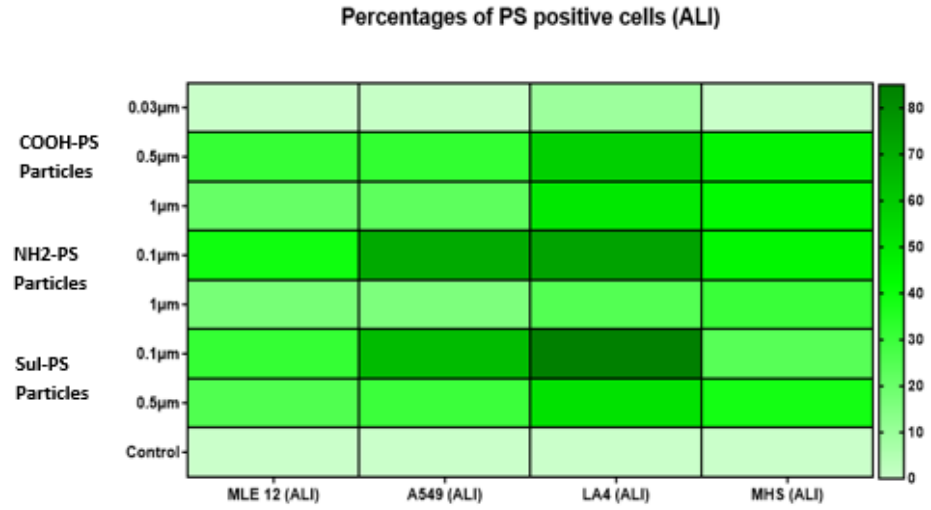

Figure 3-6 Heat maps to show the cellular uptake of 0.03µm, 0.5µm, and 1µm COOH, 0.1µm, and 1µm NH2, and 0.1µm and 0.5µm SO4 (PS) particles by alveolar epithelial and macrophages cells by flow cytometry after 24 h. **a.** Percentages of PS-positive cells in submerged conditions and **b.** in ALI conditions

3.1.4 Effects of Surface-modified PS Particles Exposure on Cell viability and cytotoxicity:

In addition to investigations about particle uptake, it is crucial to understand the impact of particles on cellular viability. The reason is that if cells become nonviable, the uptake of particles ceases, and they are consequently released. Moreo-

ver, the cellular uptake of particles can potentially result in interactions with various organelles such as the mitochondria, Golgi, nuclei, or lysosomes, which can elicit toxic effects, including damage to organelles or DNA, impairment of cell integrity, oxidative stress, and apoptosis.

Henceforth, two techniques, WST -1 and LDH assay, have been selected to evaluate the cytotoxic impacts of PS particles. The former determines cellular metabolic activity, while the latter measures the loss of intracellular LDH, which is released into the surrounding culture medium, thus indicating irreversible cell death from damage to the cell membrane.

3.1.4.1 Effects of surface-modified PS particle exposure on cell viability and cytotoxicity in submerged conditions:

The conversion of WST 1 tetrazolium salts to formazan in MLE 12 cells indicates a slight reduction in viability, although not statistically significant. However, the WST viability assay reveals a decline in viability with decreasing sizes of all three surface-modified PS particles (as shown in Figure 3.7a). Furthermore, the MLE 12 cells cultured in submerged conditions exhibit no toxicity, as evidenced by the absence of LDH levels (Figure 3.7b).

Carboxyl-modified particles did not exhibit any toxicity, except for those measuring 0.5 µm, which were found to be significant ($P \leq 0.05$) in A549 cells. Meanwhile, amine-modified particles measuring 0.1 µm showed significant ($P \leq 0.0001$) toxicity. The sulfate-modified particles measuring 0.1 µm and 0.5 µm were also found to be significantly ($P \leq 0.0001$) toxic according to the WST assay (Fig 7a). LDH levels indicated low toxicity for carboxyl-modified particles measuring 0.5 µm and 1 µm, as well as for sulfate-modified particles measuring 0.1 µm and 0.5 µm. However, this was insignificant in A549 cells under submerged conditions (Fig 3.7b).

The WST assay showed no toxicity in LA-4 cells for any of the particles tested (Fig 3.7a). Although exposure to 1 µm carboxyl particle and 0.5 µm sulfate-modified particles resulted in low levels of LDH in the cells, the toxicity was insignificant (Fig 3.7b).

The MH-S cells exhibited significant toxicity ($P \leq 0.001$) when exposed to 0.1 µm and 0.5 µm carboxyl modified particles, while 1 µm particles showed no toxicity. On the other hand, 0.1 µm and 1 µm amine-modified particles showed significant ($P \leq 0.0001$) toxicity, and only 0.1 µm sulfate-modified particles showed toxicity ($P \leq 0.01$) according to the WST assay (Fig 3.7a). Additionally, LDH levels in cells exposed to 0.1 µm and 1 µm amine-modified particles were increased. These results indicate that smaller particles are more toxic than larger ones, and amine-modified particles are toxic for both sizes of MH-S cells (Fig 3.7b) adhesive effects and the proton sponge hypothesis result in the highest toxicity levels observed in amine-PS and MHS. Due to surface effects, smaller PS particles are more toxic than larger ones at an equal mass dose. Then, I also examined the kinetics of MHS cell death at various time intervals following exposure to amine-modified particles, and the findings revealed that prolonged exposure to NH2 particles increased toxicity and reduced viability, as demonstrated in Figure 3.8.

a. b.

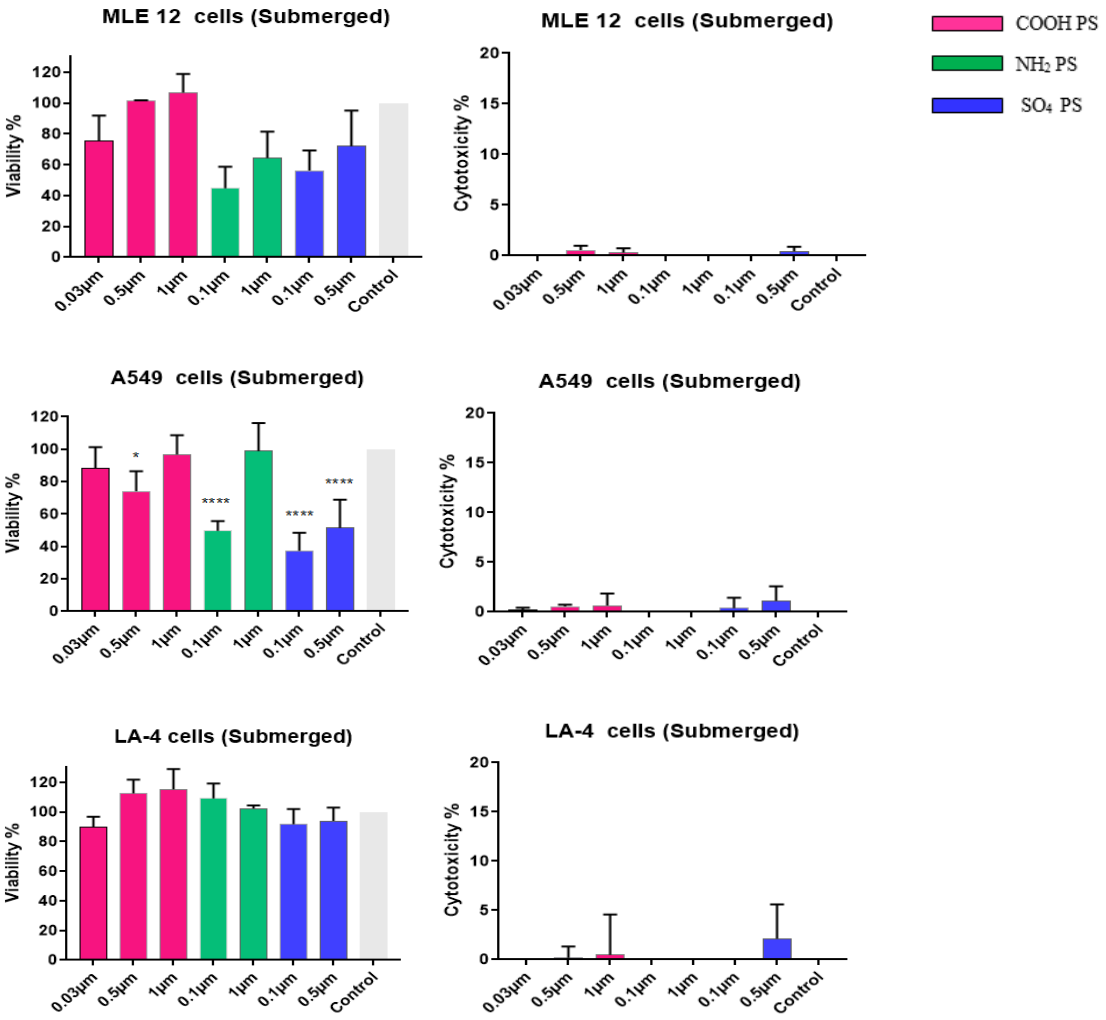
MLE 12 cells (Submerged)
Viability %
Cytotoxicity %
A549 cells (Submerged)
LA-4 cells (Submerged)
0.03µm
0.5µm
1µm
0.1µm
1µm
0.1µm
0.5µm
Control
COOH PS
NH2 PS
SO4 PS
*
****

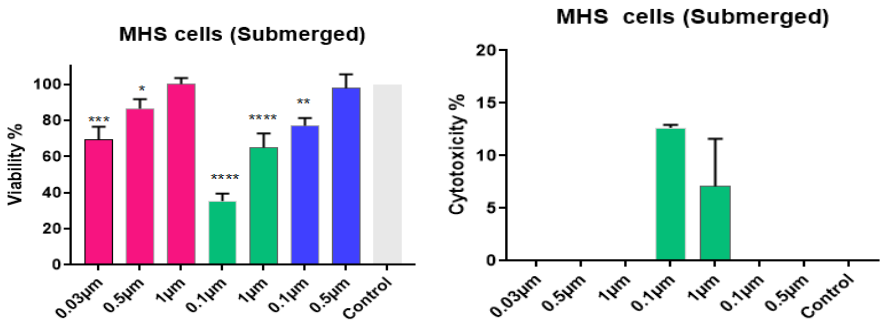

Figure 3-7 Effects of PS particles of all sizes on cell viability and cytotoxicity in submerged conditions. **a.** WST conversion into formazan, **b.** LDH release from cells compared to positive controls. Data were analyzed by 1-way ANOVA, the groups compared to the control group.

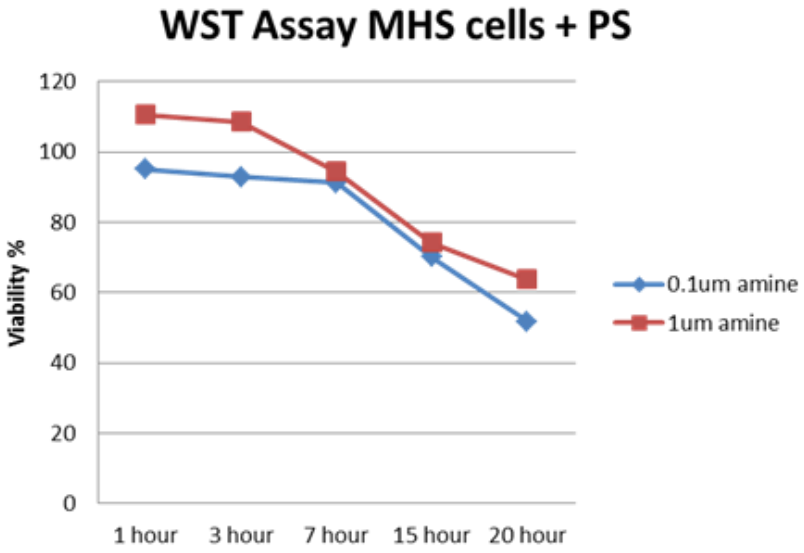

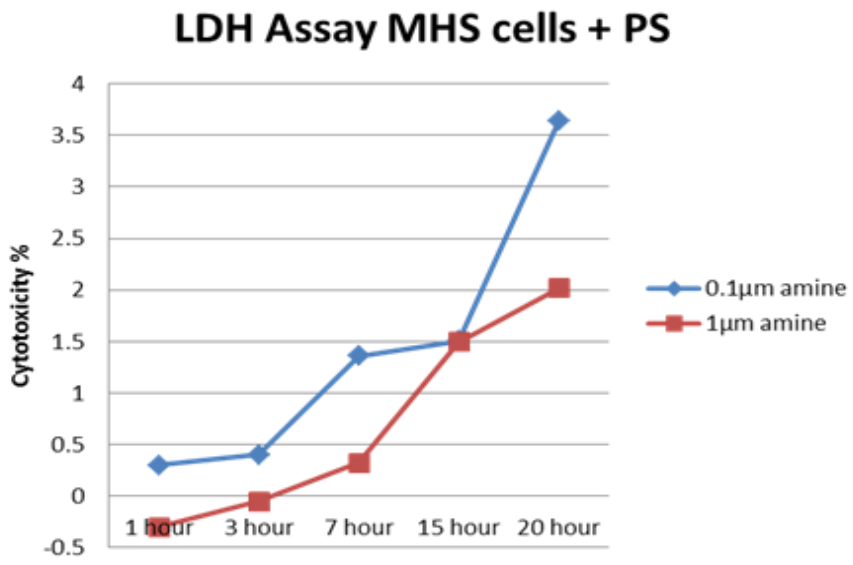

Figure 3-8 Kinetics of MHS cell death after exposure to 50µg/ml of amine-modified particles.

3.1.4.2 Effects of surface-modified PS particle exposure on cell viability and cytotoxicity in ALICE CLOUD conditions:

In the ALI exposure scenario, none of the particles showed any toxicity in MLE 12 cells as per the WST assay results in Figure 3.9a. However, exposure to carboxyl-modified particles of 0.5 µm and 1 µm and sulfate-modified particles of 0.1 µm showed some low toxicity per the LDH levels. Still, the toxicity was not significant, as shown in Figure 9b. In the A549 cells, none of the particles except the 0.03 µm carboxyl modified particles ($P \leq 0.05$) showed any toxicity in the WST assay (Fig 3.9a). However, exposure to the 0.03 µm, 0.5 µm, and 1 µm carboxyl modified particles, as well as the 1 µm amine-modified particles, resulted in significant toxicity as evidenced by the levels of LDH in the cells (Fig 3.9b). The WST assay showed no signs of toxicity in LA-4 cells for most particles, except for slight toxicity observed in the 0.03 µm carboxyl modified particles ($P \leq 0.05$) and 0.1 µm amine-modified particles ($P \leq 0.05$) (Fig 3.9a). However, the LDH levels in the cells exposed to certain particles showed significant toxicity, such as the 0.03 ($P \leq 0.001$), 0.5 µm ($P \leq 0.001$), and 1 µm ($P \leq 0.05$) carboxyl modified

particles, 0.1 µm (P ≤ 0.001), and 1 µm (P ≤ 0.01) amine-modified particles, and 0.1 µm (P ≤ 0.01) sulfate modified particles (Fig 3.9b).

The WST assay did not indicate any toxicity in MH-S cells caused by the particles, except for the 0.1 µm amine-modified particles, which showed significant toxicity (P ≤ 0.0001) (Fig 3.9a). Similarly, exposure to the 0.1 µm and 1 µm amine-modified particles resulted in low cell toxicity levels by LDH assay, although this was insignificant (Fig 3.9b). As a result, amine-PS and MHS (due to adhesive effects and the proton sponge hypothesis) showed the highest toxicity, and smaller particles were found to be more toxic than larger PS particles at an equal mass dose (due to surface effects).

a.

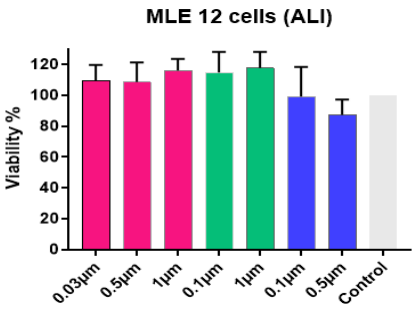

b.

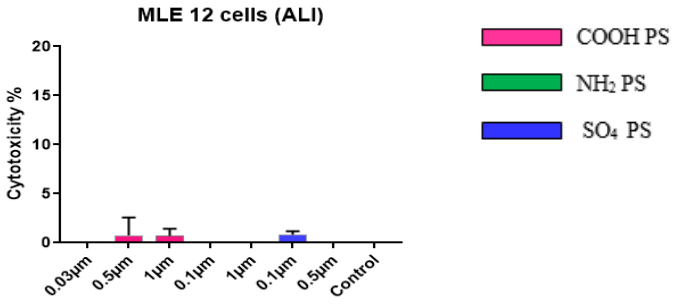

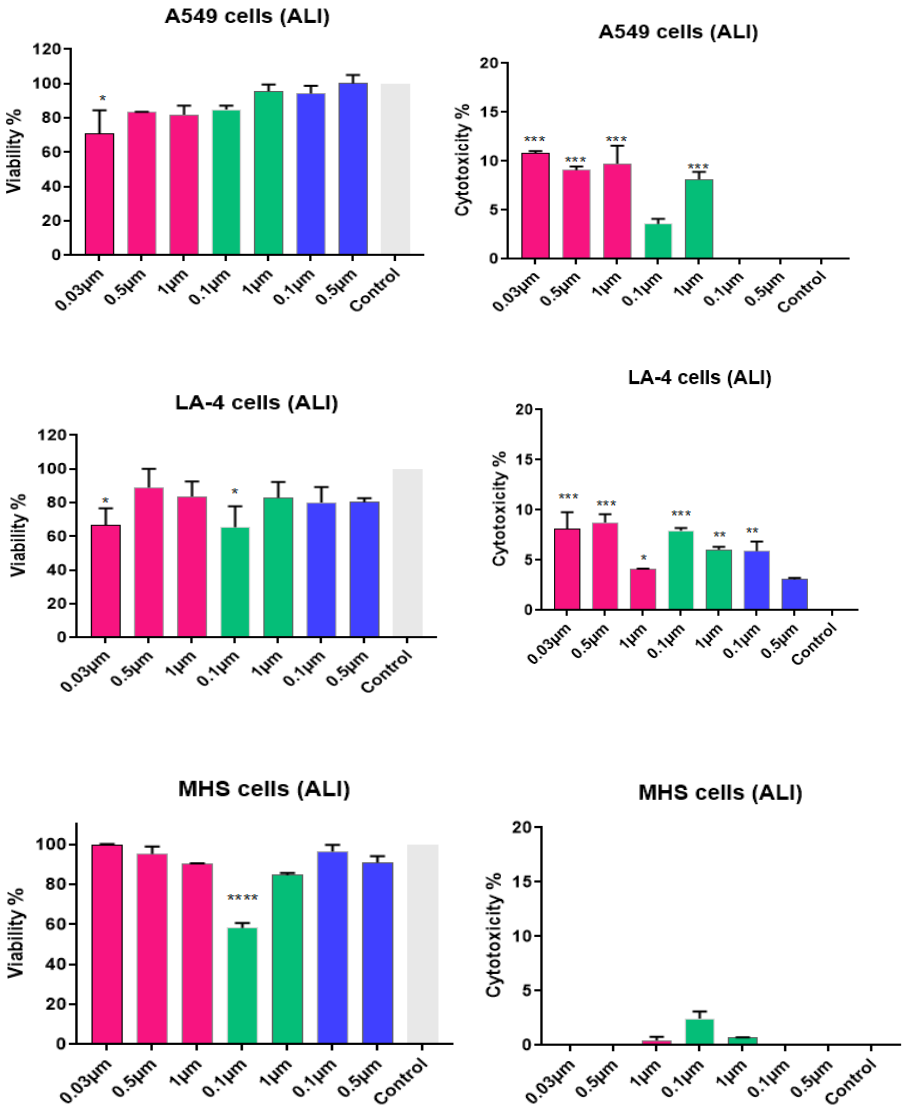

Figure 3-9 Effects of PS particles of all sizes on cell viability and cytotoxicity in ALI conditions. a. WST conversion into formazan, b. LDH release from cells compared to positive controls. Data were analyzed by 1-way ANOVA, the groups compared to the control group.

3.1.5 Summary: Correlation between PS Positive cells and toxicity:

This section utilizes the results of the above-mentioned experimental data on the percentage of positive (PS) cells and their viability. Examining the relationship between particle-positive cells and toxicity is paramount to generating a comprehensive summary and identifying the surface modifications and sizes of particles that are most toxic upon internalization by cells.

In the context of **submerged conditions**, LA4, MLE 12, A549, and MHS cells exhibit improved cellular viability when a higher percentage of cells are positive for COOH PS particles. This indicates that larger particles have a higher cellular uptake and greater viability. For A549 cells, there is an observed trend where 0.1µm SO4 results in reduced viability accompanied by an increased number of particle-positive cells. Conversely, 0.5µm SO4 leads to increased viability but with fewer particle-positive cells. Compared to their smaller counterparts, A549 cells with 1µm COOH particles exhibit higher viability and more uptake. Compared to the 1µm particles, the viability of all these cells exposed to 0.1µm NH2 PS particles is lower, while their uptake is higher (Fig.3.10a). Hence, In the context of submerged conditions, the toxicity of LA4, MLE 12, A549, and MHS cells under cytotoxicity assessment follows a size-dependent trend. Smaller particles demonstrate higher toxicity levels, particularly amine-modified ones, due to increased particle uptake. It is important to note that although dead cells cannot take up particles, those with high particle uptake can result in more significant toxicity if the intracellular dose is substantial (Fig 3.10a). PS-SO4 0.1um is the most toxic for A549 and MLE12 but not LA4. There could be several reasons why LA4 cells appear less responsive to PS-SO4 0.1µm compared to A549 and MLE12 cells. One possible explanation is that LA4 cells may have a different mechanism for internalizing and processing the particles, which could affect their toxicity response. Other cell lines may also have different sensitivity levels to various environmental stressors, including particulate matter. When assessing the correlation between particle-positive cells and viability, it is important to consider that dead cells resulting from particle uptake will not be detected as particle-positive cells. The most toxic particles would likely be those that result in low viability even at low levels of particle uptake, indicating high toxicity even at low exposure levels.

Regarding **ALI conditions**, it has been observed that LA4, MLE 12, and A549 cells demonstrate enhanced cellular viability when more cells show positivity for PS COOH. This suggests that larger particles have greater cellular uptake and result in increased viability. Conversely, MHS cells do not exhibit any toxicity due to PS COOH regardless of particle size and uptake, although their uptake does increase with larger PS particle size. The viability of LA4 cells and MHS cells

decreases while their uptake increases when exposed to 0.1µm NH2 PS particles compared to 1µm PS NH2 particles. On the other hand, A549 cells and MLE 12 cells display no toxicity when exposed to PS NH2 particles, but they exhibit a higher uptake of 0.1µm NH2 PS particles. Regardless of the extent of particle uptake, the exposure of A549 cells, LA4 cells, MLE 12, and MHS cells to SO4 PS particles did not result in any toxic effects on their integrity (Fig.3.10b). Hence, smaller particles that are taken up more readily by cells result in increased toxicity of the cells.

The phenomenon of effects for the size of carboxyl and sulfate particles observed exclusively for submerged cells and not under air-liquid interface (ALI) conditions, except for PS-NH2, in the same experimental setup can be attributed to various factors. One plausible explanation could be the differential behavior of the particles in ALI conditions compared to submerged conditions, which can be attributed to the differences in the mode of exposure of the cells to the particles. The deposition of particles on the surface of the cell monolayer in ALI conditions can lead to direct interactions with the cells. In contrast, in submerged conditions, the particles remain suspended in the culture medium and may not interact with the cells to the same extent. Therefore, the observed size effects in submerged conditions may not apply to ALI conditions. Furthermore, the particles' properties could influence their interaction with the cells. For instance, carboxyl and sulfate particles may possess properties that promote their interaction with the cell membrane or internalization into the cell in submerged conditions but not in ALI conditions. Conversely, PS-NH2 may have characteristics that enable it to interact with cells in both submerged and ALI conditions. In addition to these factors, the behavior of particles in ALI conditions can also be influenced by other factors, such as the presence of mucus and cilia, which can affect particle deposition and clearance.

So, according to this study's results, sedimentation, diffusion, and protein effects can impede particle uptake in submerged conditions but not in conditions where the air-liquid interface is present. However, exposing particles to air-liquid interface conditions resulted in heightened toxicity for all cell lines tested. These findings have significant implications for developing and designing nanoparticle-based drug delivery systems for respiratory ailments. Further studies would be

needed to fully understand the reasons for the differences in toxicity response observed between the different cell lines.

a.

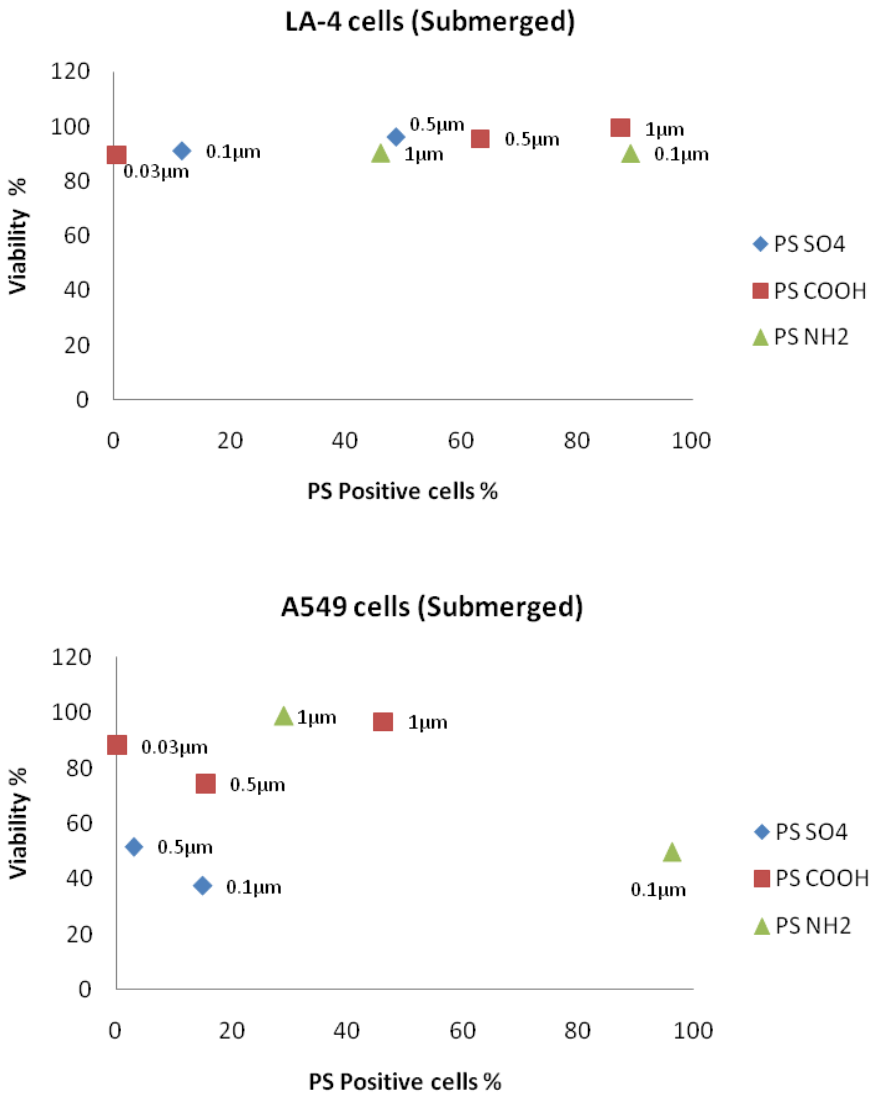

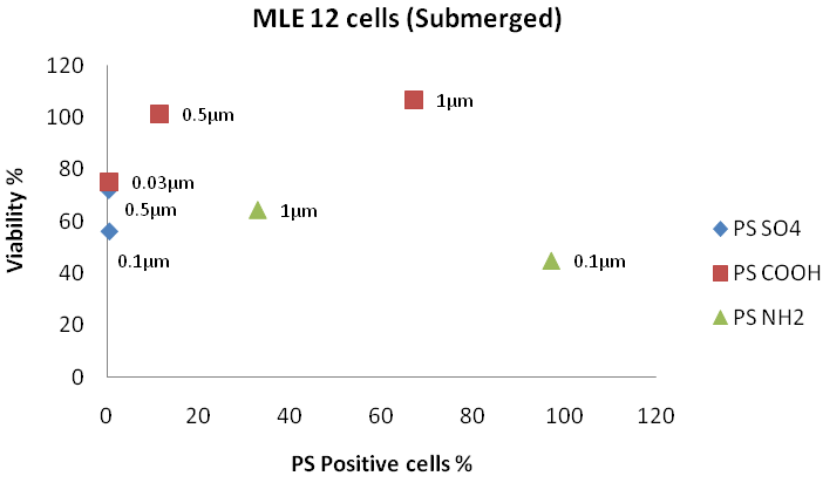
MLE 12 cells (Submerged)
Viability %
PS Positive cells %
0.5µm
1µm
0.03µm
0.5µm
1µm
0.1µm
0.1µm
PS SO4
PS COOH
PS NH2

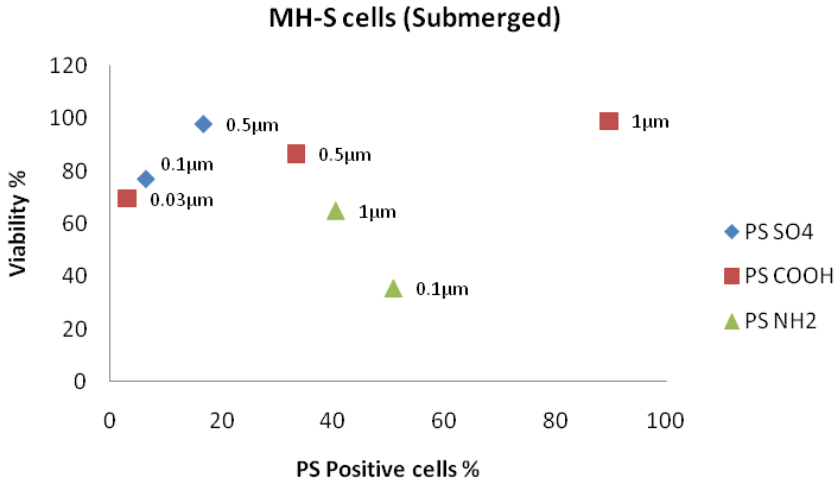
MH-S cells (Submerged)
Viability %
PS Positive cells %
0.5µm
1µm
0.1µm
0.5µm
0.03µm
1µm
0.1µm
PS SO4
PS COOH
PS NH2

b.

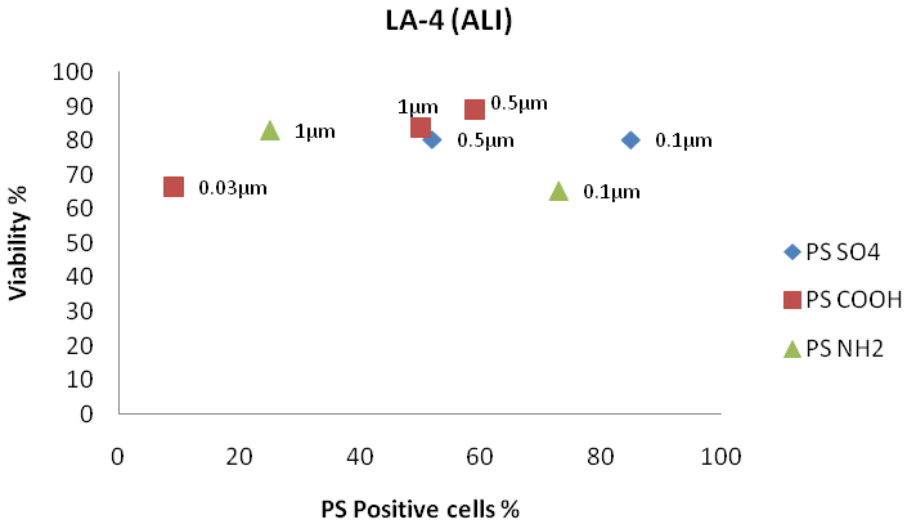
LA-4 (ALI)
Viability %
PS Positive cells %
1µm
0.5µm
1µm
0.5µm
0.1µm
0.03µm
0.1µm
PS SO4
PS COOH
PS NH2

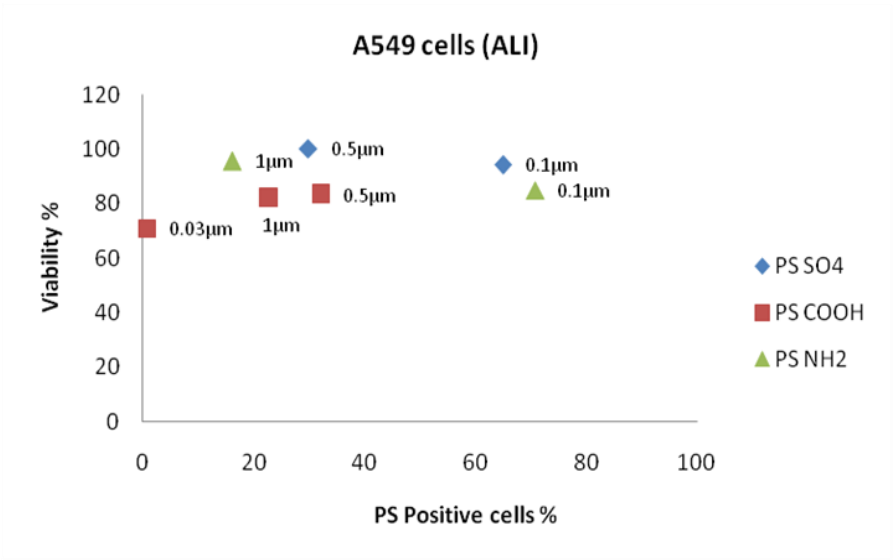
A549 cells (ALI)
Viability %
PS Positive cells %
120
100
80
60
40
20
0
0
20
40
60
80
100
1µm
0.5µm
0.1µm
0.5µm
0.1µm
0.03µm
1µm
PS SO4
PS COOH
PS NH2

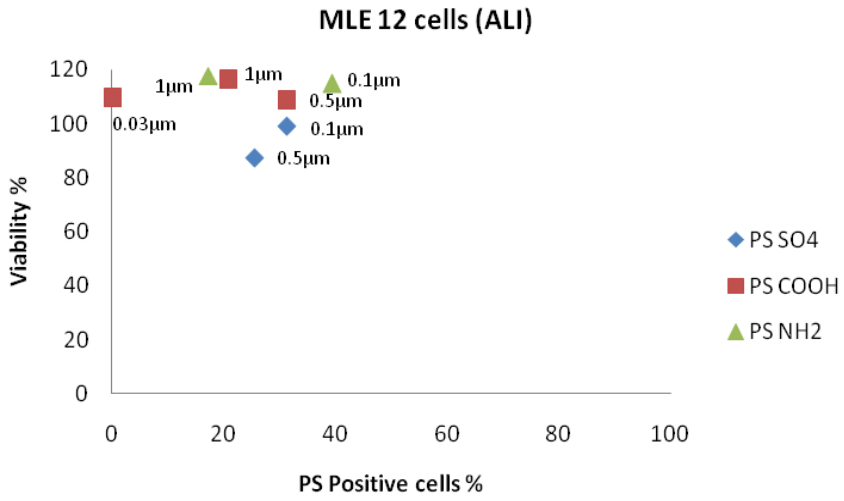
MLE 12 cells (ALI)
Viability %
PS Positive cells %
120
100
80
60
40
20
0
0
20
40
60
80
100
1µm
1µm
0.1µm
0.03µm
0.5µm
0.1µm
0.5µm
PS SO4
PS COOH
PS NH2

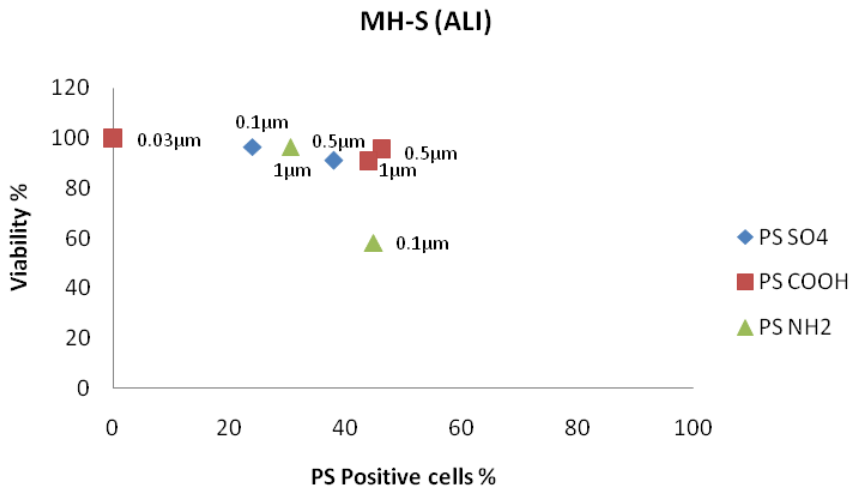

Figure 3-10 Summary: Correlation between PS-positive cells and toxicity. a) Submerged conditions, b) ALI conditions. (n=3).

3.2 The uptake of PLGA particles by alveolar macrophages and epithelial cells depends on the exposure scenario

The objective of the PLGA study was to employ a co-culture system consisting of alveolar epithelial cells and alveolar macrophages for two purposes:

- Investigating the uptake of PLGA nanoparticles delivered to the lungs and
- Validating the uptake pattern of nanoparticles in vivo using this co-culture setup by administering nanoparticles to mice through intratracheal instillation.

3.2.1 Particle characterization

Before conducting cellular experiments, a thorough investigation was conducted on three different sizes of poly (lactic-co-glycolic acid) (PLGA) particles. The use of Dynamic Light Scattering (DLS) allowed for the determination of the average hydrodynamic radius of the particles, which was found to be 103 nm, 475 nm, and 756 nm for particles categorized as 100 nm, 500 nm, and 1000 nm, respectively (as presented in Table 2). The low polydispersity indexes indicated that the particle samples had a narrow size distribution, rendering them suitable for use with the DLS technique. All measurements were performed using deionized water as the diluent for the particle stocks. The observed mean fluorescent intensities (MFIs) of the three sizes of particles studied exhibited variations, which were measured based on their mass. The 0.1 µm particles demonstrated one-third of the MFI observed for the 1 µm particles. In contrast, the 0.5 µm particles exhibited half of the MFI observed for the 1 µm particles, attributed to the particle size, whereby larger particles possess more volume to incorporate a more significant amount of dye than smaller particles (Table 2).

PLGA particles green	DLS	Standard deviation	MFI (mass and ex-em based)

	Hydrodynamic radius (nm)		
100nm	101.2	± 26	4771
500nm	482.7	± 146.9	8902
1000nm	763	± 110.9	13147

Table 1 **Characterization of PLGA Particles**. Average diameter of PLGA particles by DLS, Standard deviations and mean fluorescent intensities of the particles.

3.2.2 PLGA particle uptake:

3.2.2.1 Use of mono and co-cultures to study particle cellular uptake in different exposure scenarios:

Flow cytometry was employed with confocal laser scanning microscopy (CLSM) to explore particle uptake by various cell types within the alveolar epithelium. Fluorescently labeled PLGA particles with diameters of 0.1, 0.5, and 1 µm were incubated with cells, with 10 µg/cm2 doses for submerged conditions and 2.7 µg/cm2 for air-liquid interface (ALI) conditions. Particle uptake was analyzed via FACS in mono and co-cultures of LA-4 and MH-S cells after 24 hours of treatment with the particles.

Results showed that in submerged conditions, monocultures of LA-4 cells exhibited significant uptake of 0.5 µm and 1 µm particles, with approximately 2-fold ($p<0.01$) and 3-fold ($p<0.001$) increased uptake compared to 0.5 µm and 0.1 µm particles, respectively. This indicates that larger particles have a greater uptake pattern. In co-cultures, LA-4 cells displayed a significant uptake of 0.1 µm particles ($p<0.001$) compared to the control, but less than 0.5 µm and 1 µm particles, as shown by Q2 in dot plots. For alveolar macrophages (MH-S cells), bigger particles (i.e., 1 µm and 0.5 µm) exhibited significant ($p<0.001$) uptake in both mono-

culture (histogram) and co-cultures (Q4 in dot plots) compared to smaller particles (i.e., 0.1 µm). In monocultures, 0.5 µm particles were observed to have a higher uptake ($p<0.01$) by MH-S cells compared to 1 µm particles. Consequently, larger PLGA particles had the highest uptake in monoculture and co-cultures under submerged conditions, as shown by histograms and dot plots (Q4) (Fig. 3.11a, 3.12a).

In monoculture conditions at the air-liquid interface (ALI), we have observed that both LA-4 and MH-S cells take up particles. Still, no significant differences in particle uptake were observed. Conversely, in co-culture ALI conditions, we have observed a significant uptake of all particles by both LA-4 and MH-S cells (Q2 and Q4 in dot plots, respectively). Upon comparing the uptake patterns of the three particles, it was observed that LA-4 cells exhibited the highest uptake of 0.5µm particles ($p<0.01$) and a slightly higher uptake of 0.1µm particles than 1µm particles. In comparison, MH-S cells showed a greater uptake of 0.5µm ($p<0.05$) and 0.1µm ($p<0.05$) particles as compared to 1µm particles (Fig. 3.11b, 3.12b). Therefore, under air-liquid interface conditions, Alveolar epithelial and alveolar macrophage cell lines demonstrate the highest uptake of smaller PLGA particles.

These reliable results demonstrate a slightly higher particle uptake in LA-4 cells than in MH-S cells in co-cultures. This phenomenon may be attributed to the phagocytic capacity of macrophages, which can engorge numerous particles and consequently exhibit reduced capacity to uptake additional particles at early endpoints. Accordingly, LA-4 cells may uptake the remaining particles, as they are relatively larger and require more time to engulf particles than MH-S cells. Notably, after a 4-hour particle exposure, MH-S cells exhibited higher particle uptake than LA-4 cells (data not presented). Confocal laser scanning microscopy (CLSM) images demonstrated that most of the particles were located perinuclear or intracellularly in mono and co-culture conditions, regardless of whether cells were maintained under submerged or air-liquid interface (ALI) conditions. However, the smaller size (0.1 µm) of PLGA particles resulted in lower mean fluorescence intensity (MFI), possibly challenging their detection under a microscope. Flat, oval nuclei characterize LA-4 cells, while round, dark blue nuclei typify MH-S cells (see Fig. 3.13 and 3.14).

These significant findings underscore the importance of co-cultures of alveolar epithelial and alveolar macrophage cell lines in enhancing the uptake of larger particles (1 µm) in a submerged environment, in contrast to smaller particles (0.1 µm and 0.5 µm) as shown by dot plots. Conversely, smaller particles (0.1 µm and 0.5 µm) exhibit greater uptake compared to larger particles (1 µm) under conditions of the air-liquid interface (ALI). To determine the in vitro method that best approximates the lung, we conducted in vivo particle exposure by administering 0.1 µm and 1 µm PLGA particles via intratracheal instillation in a mouse model, specifically C57BL/6 J.

a. Submerged conditions (Monoculture):

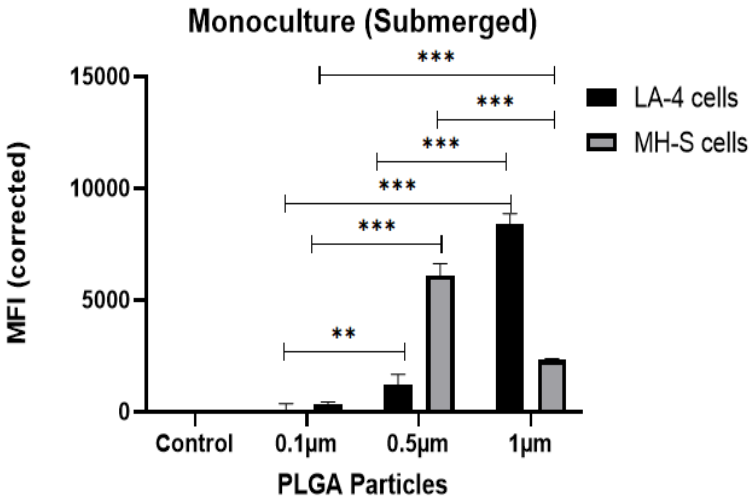

MH-S Cells

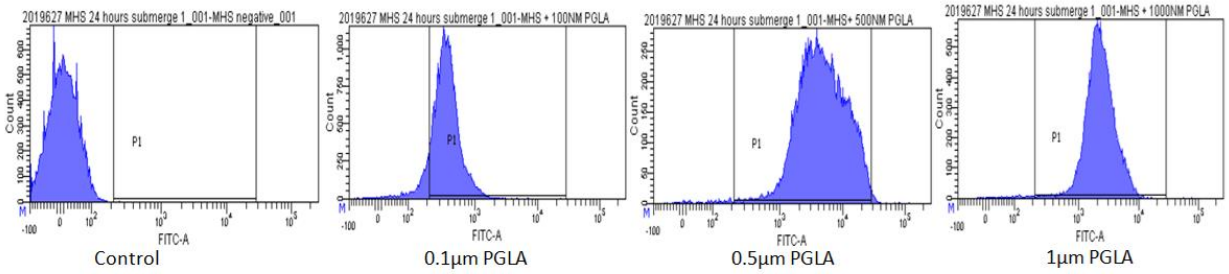

LA-4 Cells

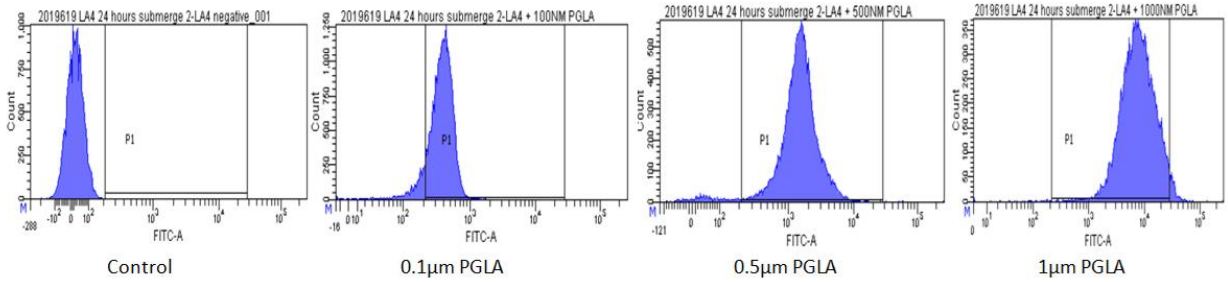

b. Air-Liquid Interface (ALI) Conditions (Monoculture):

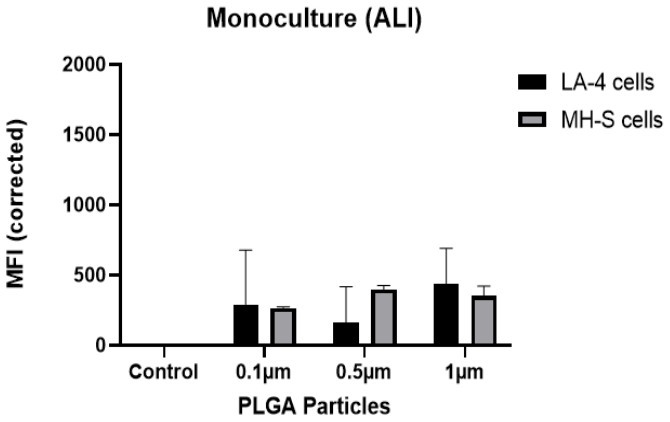

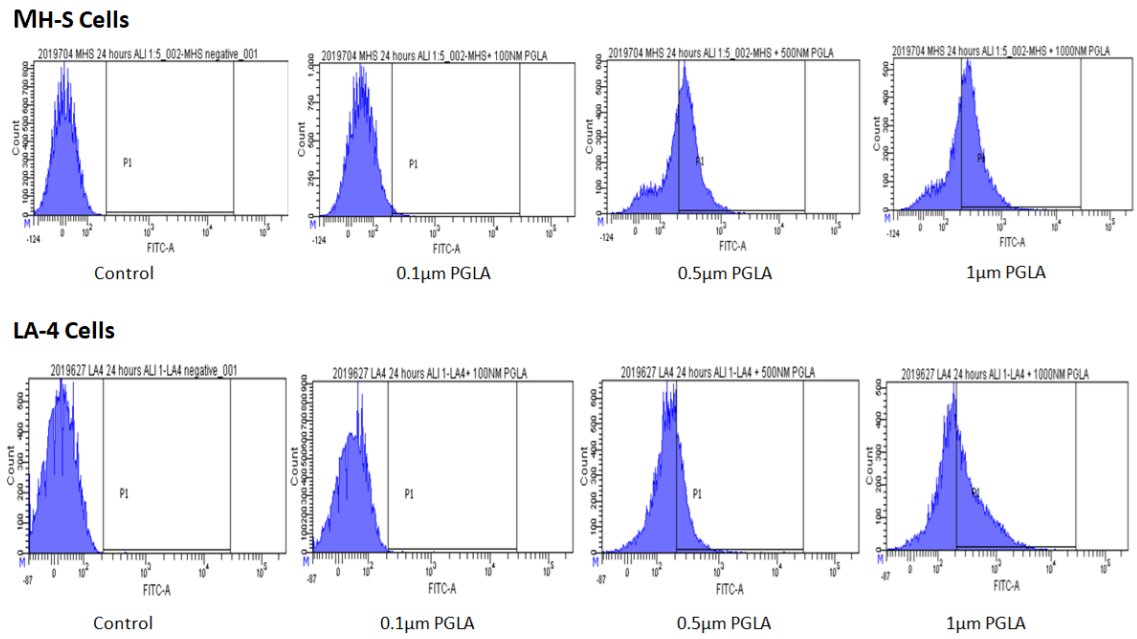

Figure 3-11 Analysis of cellular uptake of 0.1 µm, 0.5 µm, and 1 µm PLGA nanoparticles in monocultures of LA-4 and MH-S cells by flow cytometry after 24 hours of incubation. Positively gated histograms showing mean fluorescent intensities indicate **a.** uptake of particles by LA-4 and MH-S cells in submerged monoculture conditions, and **b.** uptake of particles by LA-4 and MH-S cells under air-liquid interface (ALI) conditions in monocultures. Data were analyzed by multiple comparisons in 2-way ANOVA, and the groups were compared.

a. **Submerged conditions (Co-culture):**

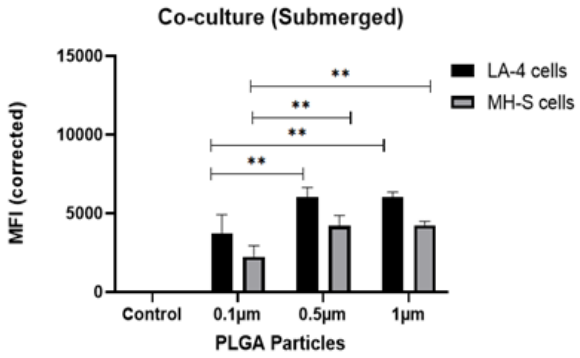

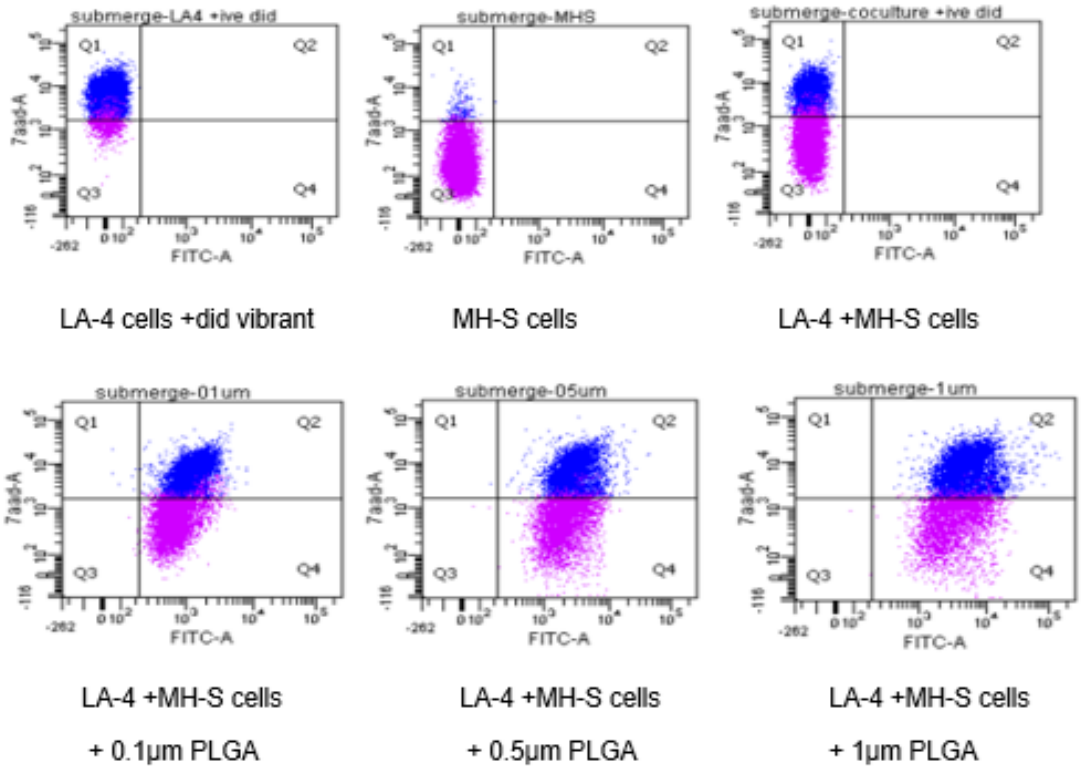

LA-4 cells +did vibrant | MH-S cells | LA-4 +MH-S cells

LA-4 +MH-S cells + 0.1µm PLGA | LA-4 +MH-S cells + 0.5µm PLGA | LA-4 +MH-S cells + 1µm PLGA

b. **Air-Liquid Interface (ALI) Conditions (Co-culture):**

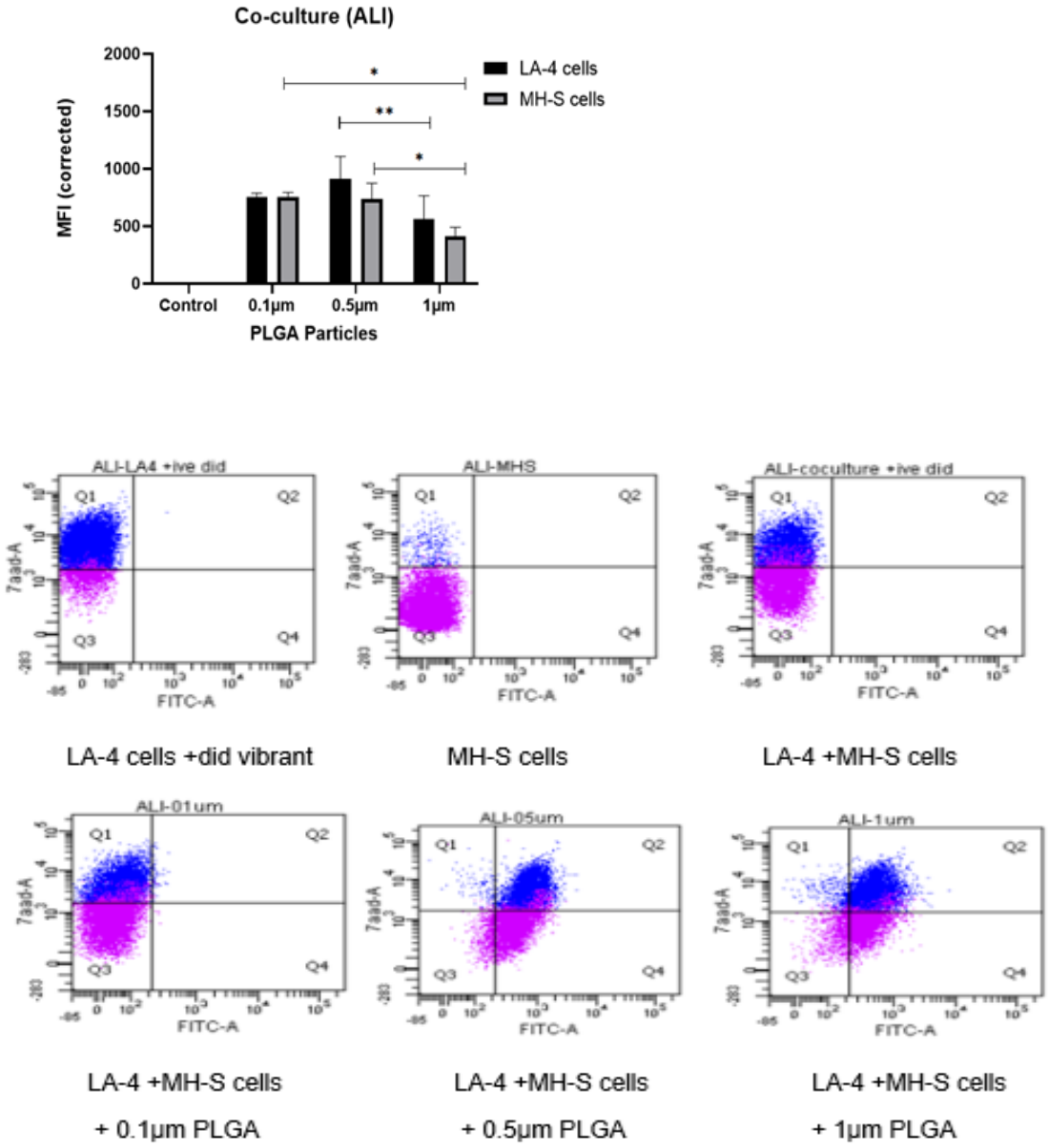

Figure 3-12 Analysis of cellular uptake of 0.1 µm, 0.5 µm, and 1 µm PLGA nanoparticles in co-cultures of LA-4 and MH-S cells by flow cytometry after 24 hours of incubation. Positively gated dot-plots showing mean fluorescent intensities indicate **a.** uptake of particles by LA-4 and MH-S cells in submerged coculture conditions, and **b.** uptake of particles by LA-4 and MH-S cells under air-liquid interface (ALI) conditions in cocultures. Data were analyzed by multiple comparisons in 2-way ANOVA, and the groups were compared.

Monoculture:

Submerged Conditions:

LA-4 cells.

Control

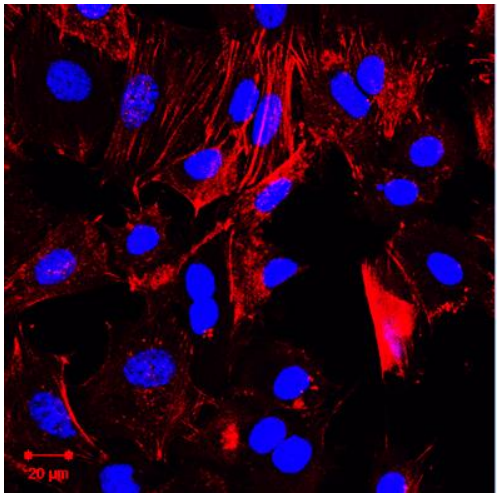

0.1µm PLGA particles

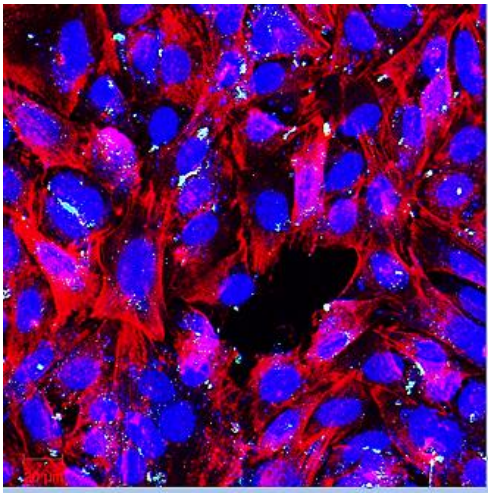

0.5µm PLGA particles

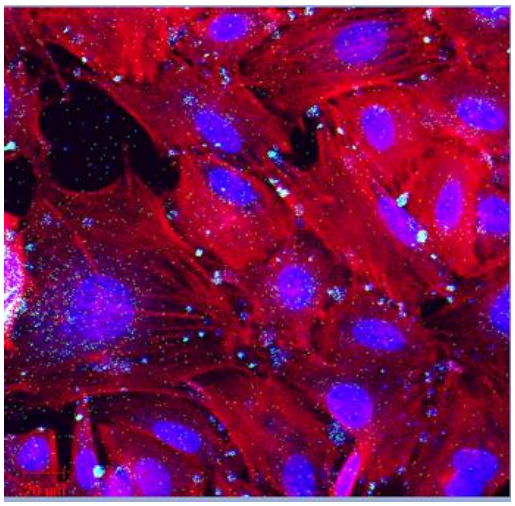

1µm PLGA particles

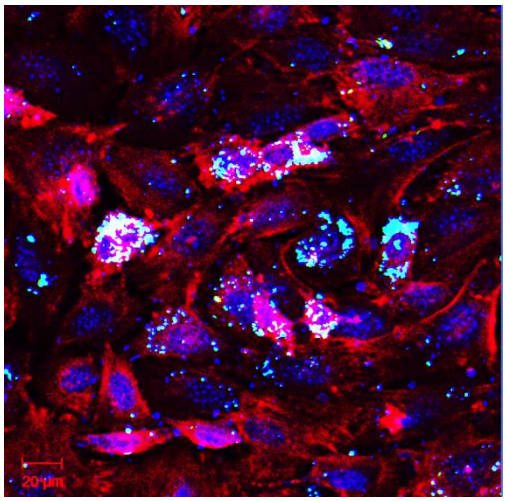

Submerged Conditions:

MH-S cells

Control

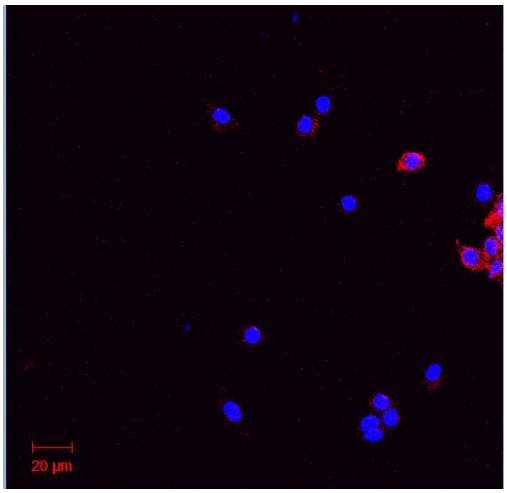

0.1µm PLGA particles

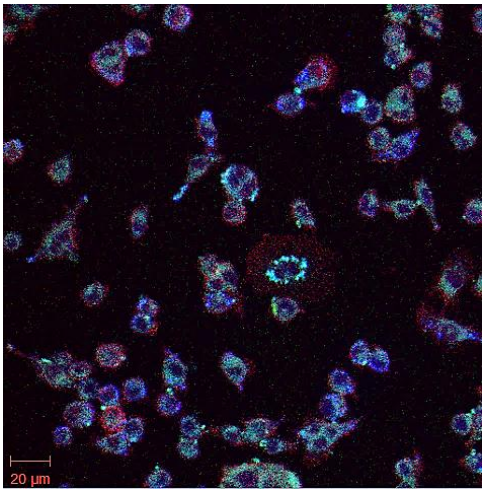

0.5µm PLGA particles

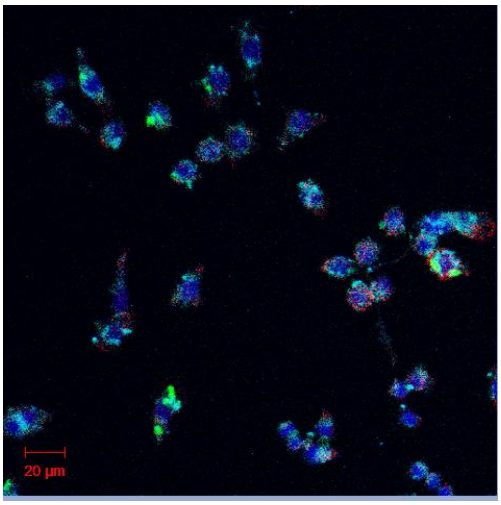

1µm PLGA particles

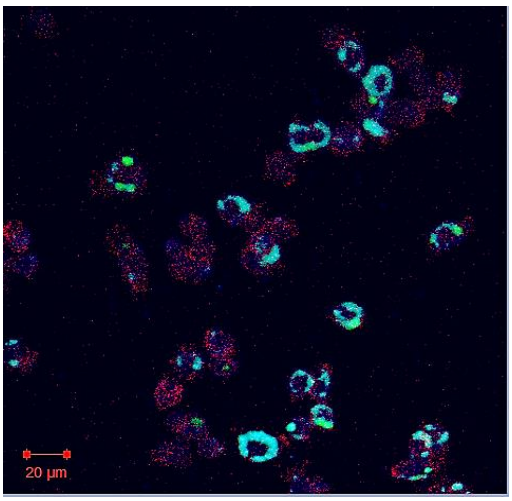

Monocultures:

Air Liquid Interface (ALI) Conditions:

LA-4 cells.

Control.

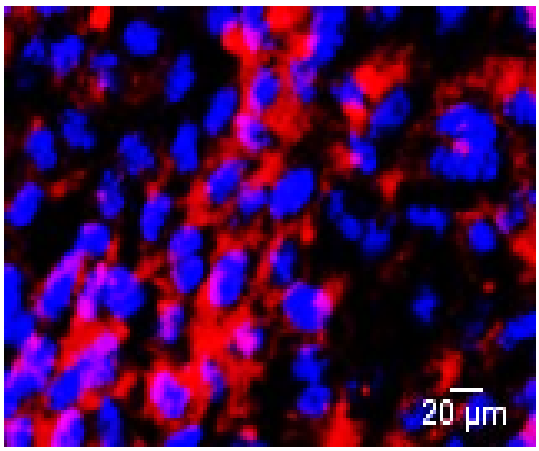

0.1µm PLGA particles

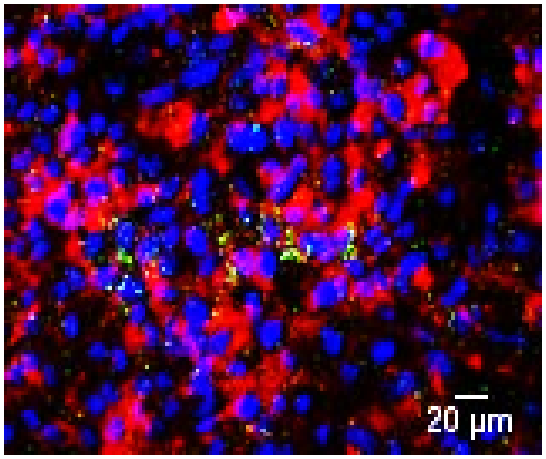

0.5µm PLGA particles

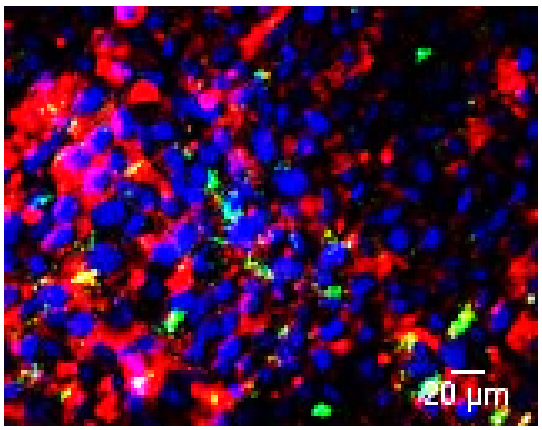

1µm PLGA particles

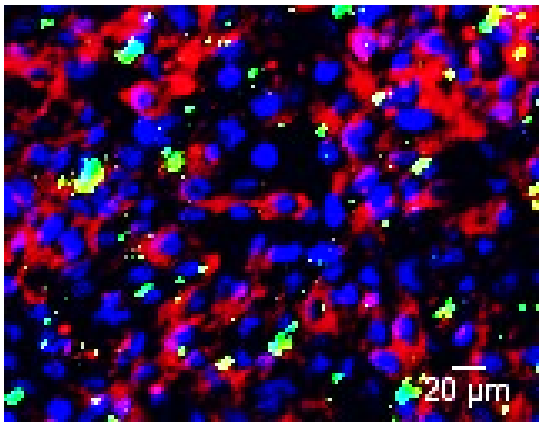

Air Liquid Interface (ALI) Conditions:

MH-S cells

Control

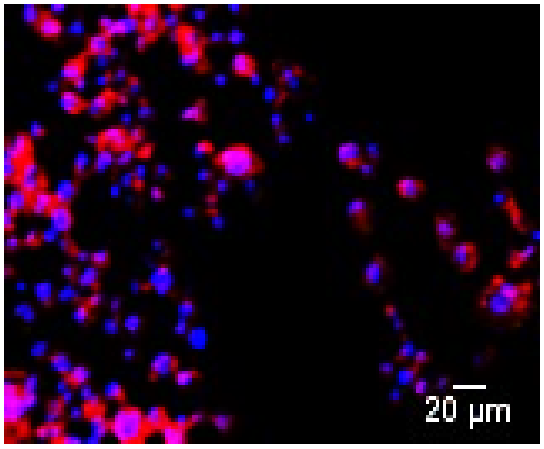

0.1µm PLGA particles

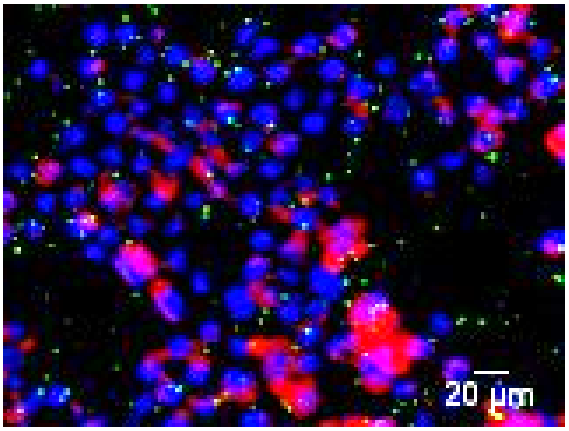

0.5µm PLGA particles

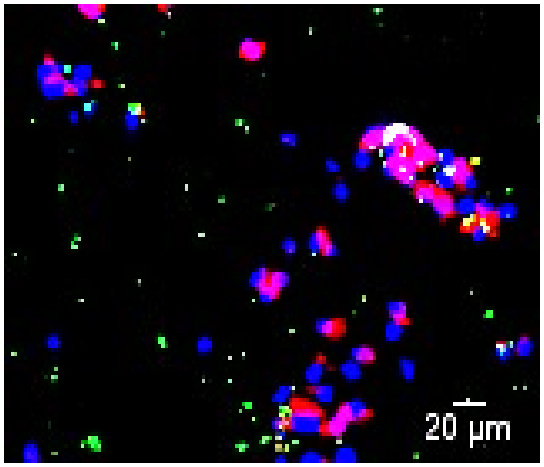

1µm PLGA particles

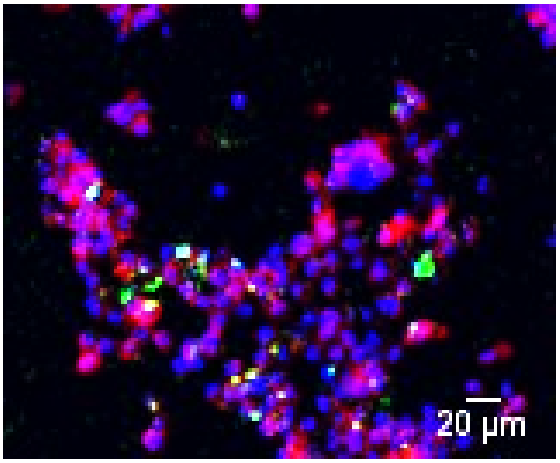

Figure 3-13 Analysis of cellular uptake of 0.1 µm, 0.5 µm, and 1 µm PLGA nanoparticles in monocultures of LA-4 and MH-S cells by confocal microscopy after 24 hours of incubation. Fluorescent images depict the uptake of particles by LA-4 and MH-S cells under

submerged and ALICE-CLOUD monoculture conditions. Stainings: Dapi nuclear staining (Blue), PLGA particles (Green), and F actin staining (red).

Co-cultures:

Submerged Conditions:

LA-4 cells + MH-S cells.

Control

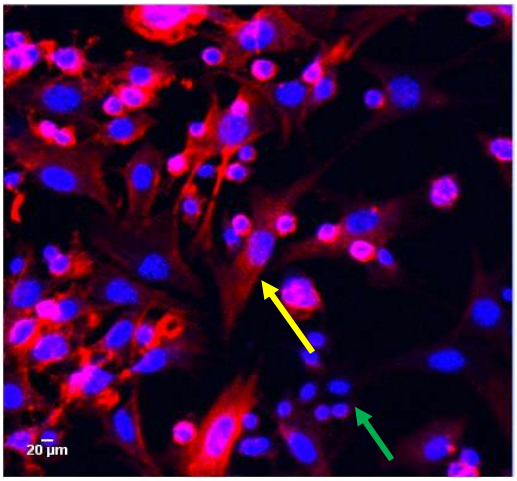

0.1µm PLGA particles

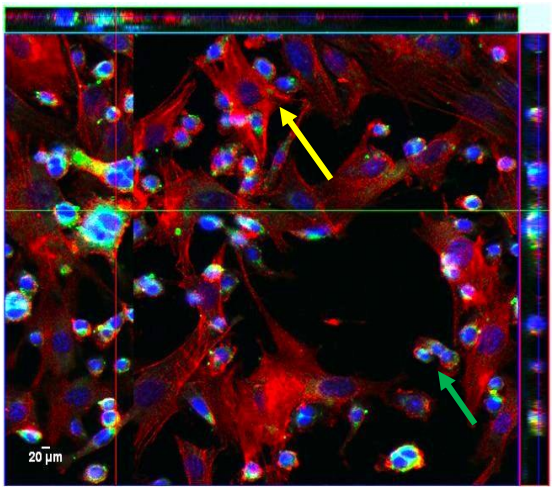

0.5µm PLGA particles

1µm PLGA particles

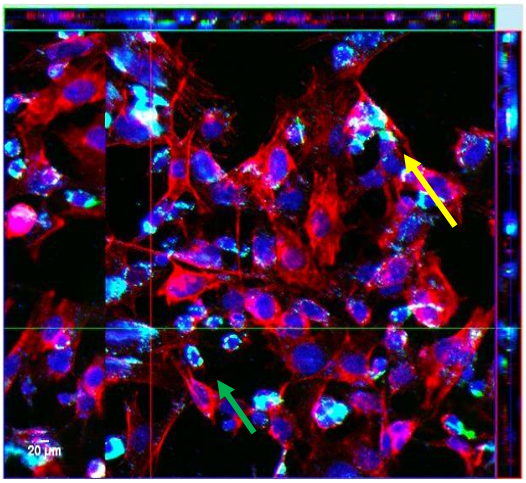

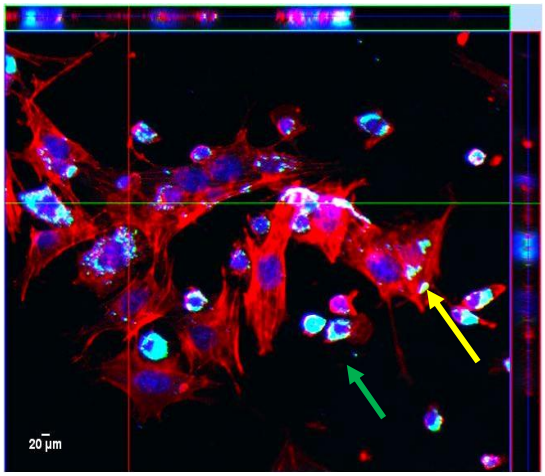

Air Liquid Interface (ALI) Conditions:

LA-4 cells + MH-S cells.

Control

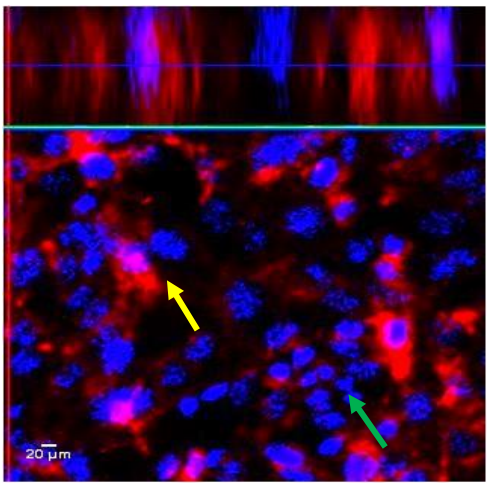

0.1µm PLGA particles

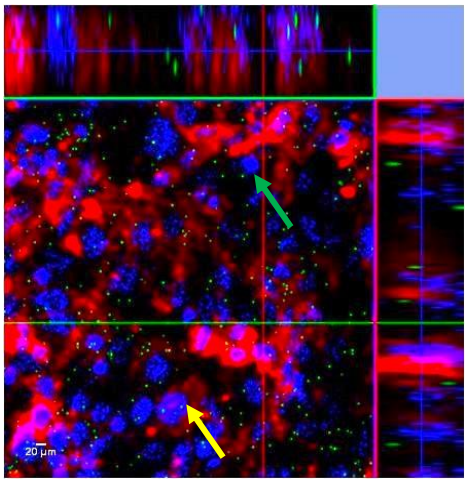

0.5µm PLGA particles

1µm PLGA particles

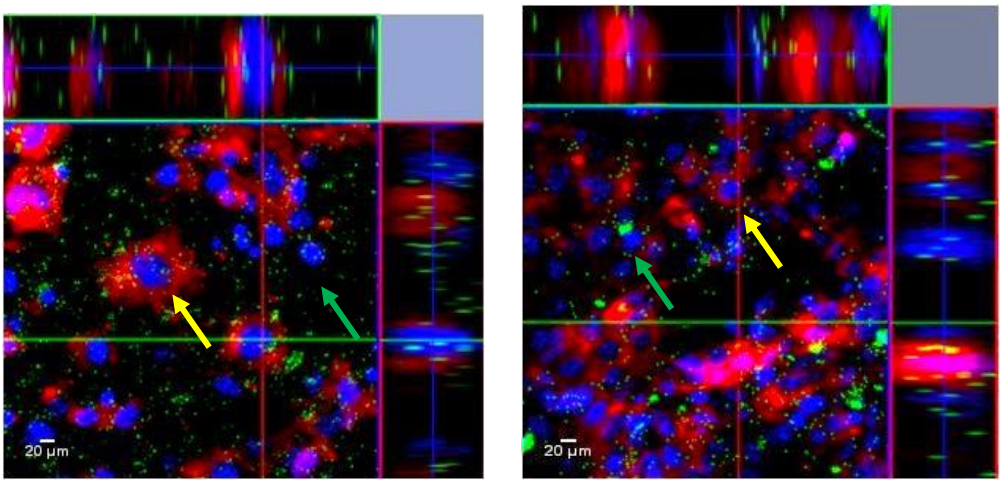

Figure 3-14 Analysis of cellular uptake of 0.1 µm, 0.5 µm, and 1 µm PLGA nanoparticles in co-cultures of LA-4 and MH-S cells by confocal microscopy after 24 hours of incubation. Fluorescent images depict the uptake of particles by LA-4 and MH-S cells under both submerged and ALICE-CLOUD co-culture conditions. In the images, flat oval nuclei representing LA-4 cells are indicated by yellow arrows, while round dark blue nuclei representing MH-S cells are indicated by green arrows. Staining details: DAPI nuclear staining (blue), PLGA particles (green), and F-actin staining (red).

3.2.3 **Effects of PLGA particle exposure on Cell viability and cytotoxicity:**

After exposing monocultures of LA-4 and MH-S cells to PLGA at 10µg/cm2 doses in submerged conditions and 2.7µg/cm2 in ALI conditions, cell viability and cytotoxicity were assessed 24 hours later. Viability was measured using the conversion of WST 1 tetrazolium salts to formazan, which revealed no loss of viability in either the submerged or ALI exposure scenarios (Fig. 3.15a). Furthermore, levels of LDH were used to determine cytotoxicity, and no toxicity was observed in either exposure scenario (Fig. 3.15b). These findings indicate that exposure to PLGA particles did not result in any detrimental effects on cell viability or toxicity in alveolar epithelial and alveolar macrophage cell lines under either submerged or ALI conditions.

a.

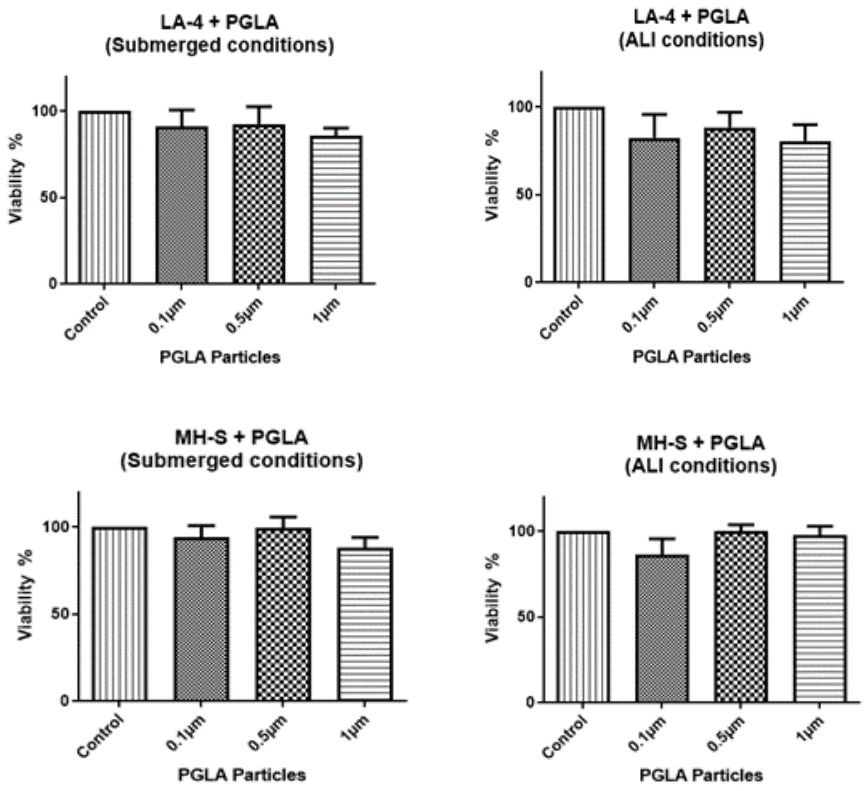
LA-4 + PGLA
(Submerged conditions)
Viability %
100
50
0
Control
0.1µm
0.5µm
1µm
PGLA Particles
LA-4 + PGLA
(ALI conditions)
Viability %
100
50
0
Control
0.1µm
0.5µm
1µm
PGLA Particles
MH-S + PGLA
(Submerged conditions)
Viability %
100
50
0
Control
0.1µm
0.5µm
1µm
PGLA Particles
MH-S + PGLA
(ALI conditions)
Viability %
100
50
0
Control
0.1µm
0.5µm
1µm
PGLA Particles

b.

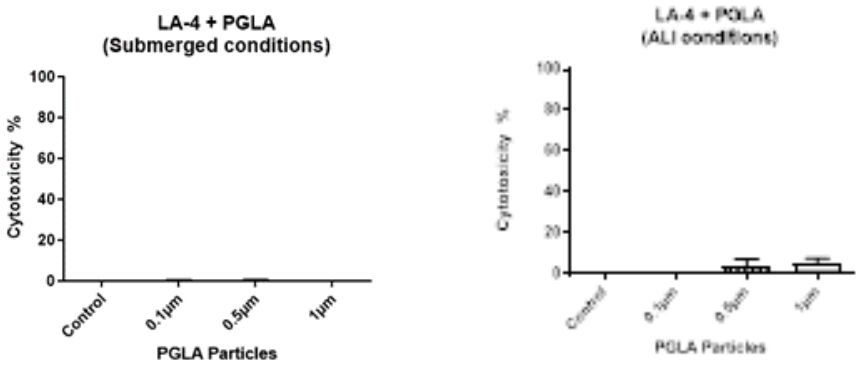
LA-4 + PGLA
(Submerged conditions)
Cytotoxicity %
100
80
60
40
20
0
Control
0.1µm
0.5µm
1µm
PGLA Particles
LA-4 + PGLA
(ALI conditions)
Cytotoxicity %
PGLA Particles

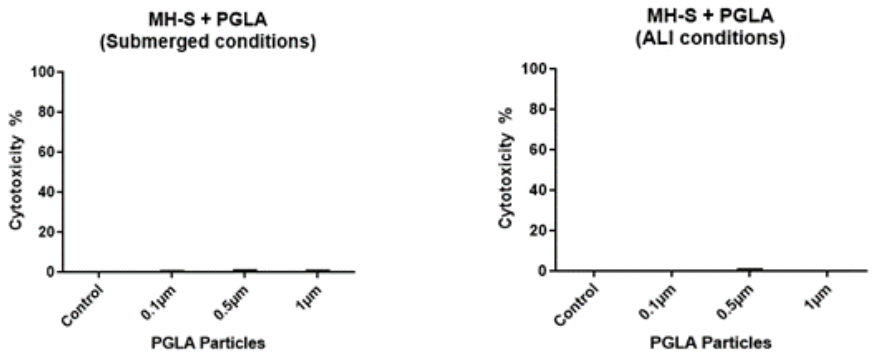

Figure 3-15 Effects of PLGA particles of different sizes on cell viability and cytotoxicity. **a.** WST assay showing viability, and **b**. LDH release from cells (cytotoxicity) compared to positive controls. Data were analyzed using one-way ANOVA, with comparisons to the control group.

3.2.4 Cellular uptake of PLGA particles in an intratracheally instilled mouse model:

24 hours after intratracheal instillation of 50µg of PLGA particles with diameters of 0.1µm and 1µm, mice were sacrificed, and bronchoalveolar lavage (BAL) was performed to assess particle uptake. Analysis of the cellular composition of BAL fluid revealed no increase in the total cell count after 24 hours. However, the neutrophil fraction appeared to be slightly, but not significantly, increased in the case of 0.1 µm particles. The number of lymphocytes was also slightly higher for 0.1µm particles than for the control. The number of macrophages in BALF was unchanged after instillation (as shown in Figure 3.16). Furthermore, no structural changes in the lung epithelium were detected by histological analysis (as shown

in Figure 3.17). In summary, the instillation of PLGA particles did not produce any inflammatory response.

The present study employed flow cytometry of BAL cells and fluorescence microscopy on cytospin-prepared cells to investigate cellular uptake by macrophages. The data for both particle types was normalized by applying a multiplication factor of three to the mean fluorescence intensity (MFI) of 0.1 µm particles to obtain an equivalent MFI value for 1 µm particles. The results revealed that BAL macrophages exhibited uptake of 1µm particles followed by 0.1µm particles, as depicted in Fig. 3.18a. Similarly, fluorescence microscopy with nuclear and actin staining corroborated this particle uptake pattern observed by FACs, as illustrated in Fig. 3.18c. To further examine the particle uptake by alveolar type 2 (AT2) cells, primary AT2 cells were isolated and stained for Epcam marker to obtain a pure AT2 cell population. The results demonstrated that AT2 cells displayed uptake of 0.1µm particles followed by 1µm particles, as shown in Fig. 3.18b. The findings suggest that macrophages preferentially phagocytose bigger particles (1µm) over smaller ones (0.1µm). In contrast, alveolar epithelial cells exhibit significant endocytosis ($p<0.001$) of smaller particles (0.1µm) rather than bigger ones (1µm).

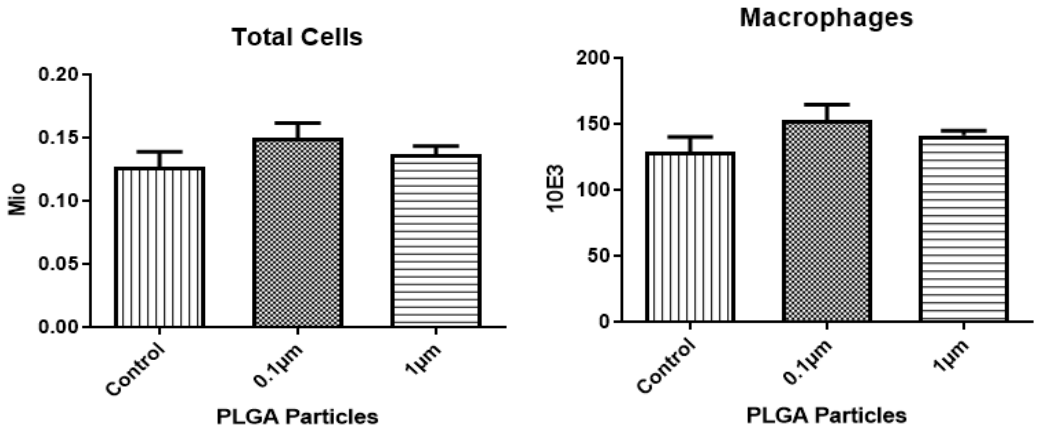

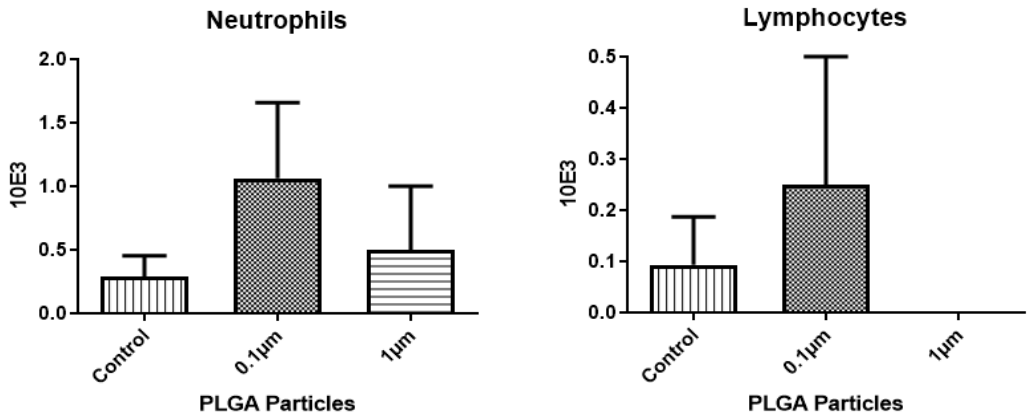

Figure 3-16 Cellular compositions in bronchoalveolar lavage (BAL) fluid 24 hours after intratracheal instillation of 50 µg of 0.1 µm and 1 µm PLGA particles. Data were analyzed using one-way ANOVA, with comparisons made against the control group.

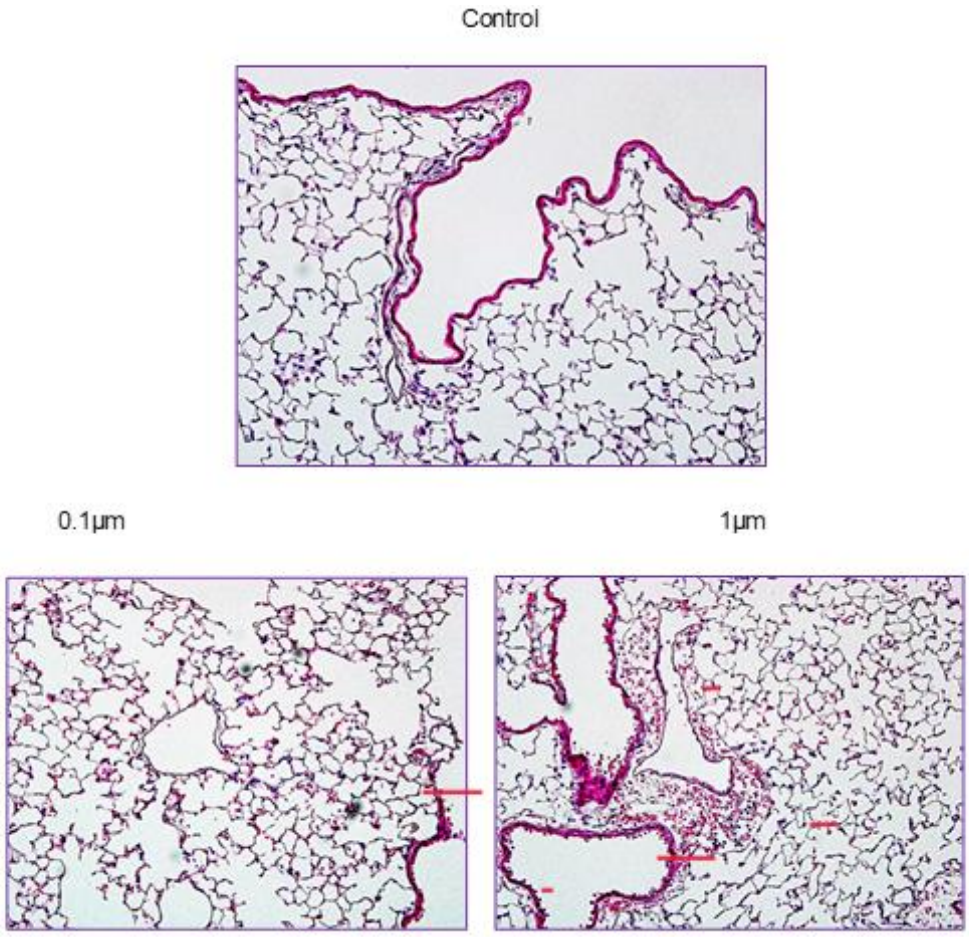

Figure 3-17 Histological images of mice lungs (20x) showing PLGA particles after 24 hours of intratracheal instillation of 50 µg of 0.1 µm and 1 µm PLGA particles.

a.

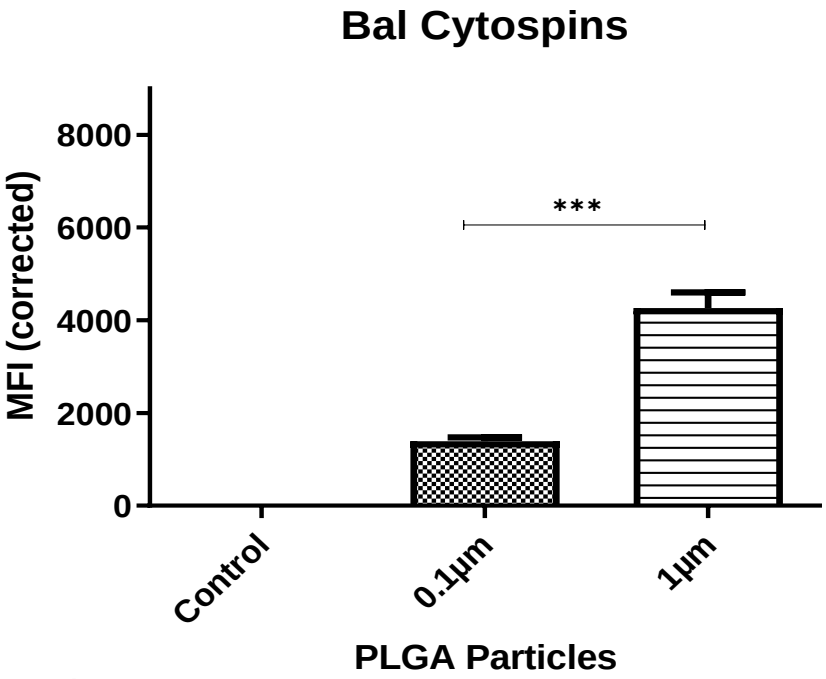

b.

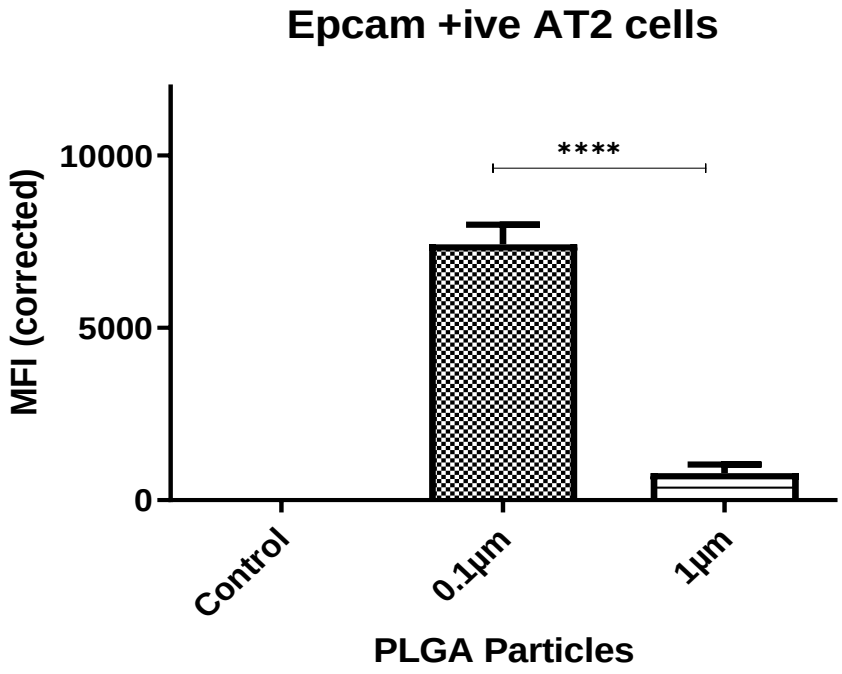

c. BAL Macrophages

Control

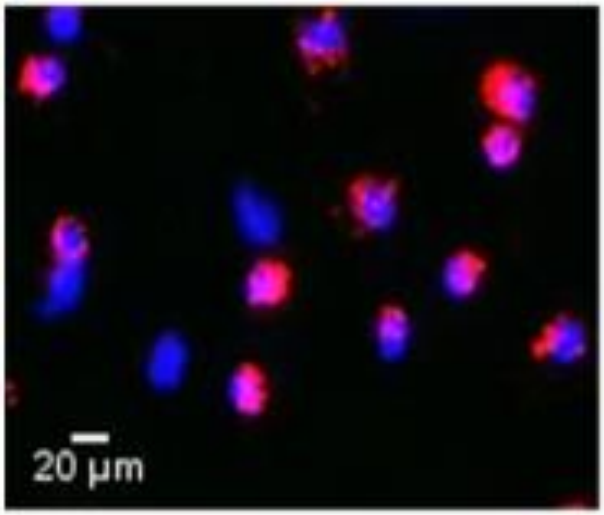

0.1µm PLGA particles

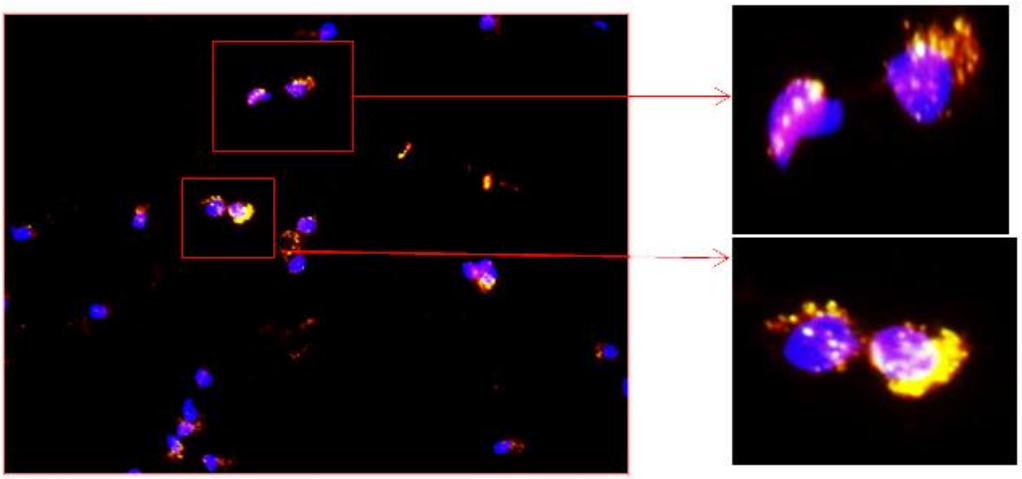

1µm PLGA particles

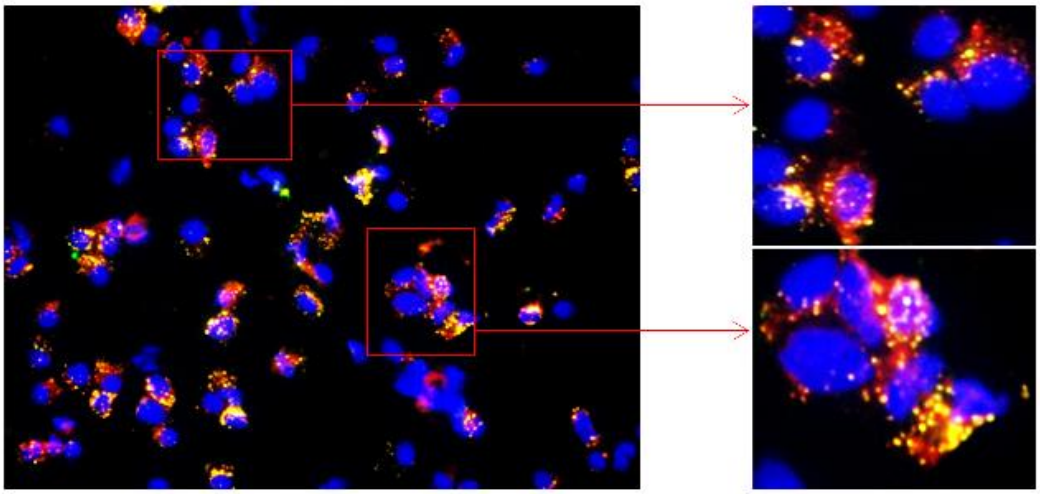

Figure 3-18 Analysis of cellular uptake of 0.1 µm, 0.5 µm, and 1 µm PLGA nanoparticles in mice (C57BL/6J) alveolar epithelial type 2 (AT2) cells and alveolar macrophages by flow cytometry and fluorescence microscopy after 24 hours of intratracheal instillation. Mean fluorescent intensities indicate **a.** uptake of particles by BAL macrophages and **b.** uptake of particles by EpCAM-positive AT2 cells. Data were analyzed by one-way ANOVA, with comparisons made between the groups. **c.** Fluorescence microscopy (20x) images show the uptake of particles in BAL macrophages, with DAPI nuclear staining (blue) and F-actin staining (red).

4. Discussion

4.1 The uptake and toxicity of different sizes and surface-modified PS latex beads by different alveolar cell types in submerged and Air-liquid interface exposure systems

Objective:

This study explores the influence of PS particle size and surface modifications on the uptake and toxicity of various alveolar cells in submerged and air-liquid interface exposure systems. Nanocarrier-mediated drug delivery offers several advantages, including targeted delivery of drugs to specific organs or cells. The lungs are a promising location for targeted drug delivery due to their dense vasculature, low number of drug-metabolizing enzymes, and potential for first-pass effect. [88]. However, before exposing particles to the lungs, it is crucial to understand the pulmonary area's compartments and immune cells to observe how cells interact with particles. This research aims to provide insights into these factors and their effects on nanocarrier delivery to the lungs.

Selection of cell lines:

In line with previous research, my study has utilized widely recognized and established cell lines as the models for alveolar epithelial cell type 2 and alveolar macrophage cell types. Specifically, we have selected Adenocarcinoma human cells (A549) [79], transgenic mouse epithelial cells (MLE-12) [90], and LA-4 cells [91] as our alveolar epithelial cell type 2 models due to their functional characteristics that resemble those of AT II epithelial cells, including their ability to produce surfactant [92]. Additionally, we have chosen MH-S [79], [90] as our alveolar macrophage cell model. By using these established cell lines, I aim to ensure consistency and reliability in my findings and to facilitate comparison and integration with previous and future research in nanocarrier-mediated drug delivery.

Selection of particles:

The lungs have a large internal surface area, making them an attractive target for drug delivery in respiratory disorder treatments [88]. Nanoparticles, such as liposomes, polymers, gold, carbon, micelles, and biological particles, have been developed as promising tools for effective drug delivery to the lungs. However, for their successful use, these nanocarriers must meet specific requirements, including stability, biocompatibility, and biodegradability [89]. In this study, polystyrene particles were chosen to establish a protocol to investigate their uptake and toxicity in different exposure scenarios, as polymers offer several benefits, such as modified surface properties, high drug encapsulation, protection of the drug from degradation, prolonged drug delivery, and long shelf life.

Before exposing the polystyrene particles to cells, it is essential to characterize their physical and chemical properties, including size, shape, surface modifications, and stability. This study used dynamic light scattering (DLS) to confirm the particles' sizes and charges [Fig 3.1].

This thesis discussion focuses on using polystyrene nanoparticles (PS) to investigate the relationship between particle properties, such as size and charge, and their degree of uptake and associated toxicity. Previous studies have shown that surface-modified PS particles exhibit greater uptake than unmodified particles of the same size, potentially due to electrostatic interactions with cell membrane glycoproteins, glycolipids, and receptors [34]. Therefore, in this study, fluorescently labeled PS particles with three different surface modifications and varying sizes were selected to examine the importance of size and surface modification on particle uptake by alveolar epithelial cells.

Hypothesis:

The study utilized two exposure systems, namely, conventional submerged conditions and Air Liquid Interface (ALICE CLOUD), to examine the effect of the exposure system on the cellular response [93]. **The research hypothesized that the response to the particles would depend mainly on their size and surface modification and that the interaction of different cell types with the particles**

would demonstrate their functional role in the alveolar compartment. Previous studies have relied on animal models, which are expensive and time-consuming. To address this, the study utilized in-vitro exposure methods to investigate the particle-cell interactions and their effects on the cellular level [93]. The experiments were conducted at 37°C to avoid inhibiting active processes such as endocytosis, as explained by Tetley et al. (2000) [34].

Uptake of PS particles in Submerged exposure:

The present study used flow cytometry to investigate particle uptake by alveolar epithelial and macrophage cell lines. Three types of surface-modified particles were exposed to the cell lines at two time points, namely 4h and 24h in conventional submerged conditions. The results showed a significant difference in particle uptake between the two-time points, with less uptake observed at 4h compared to 24h. Based on previous studies reporting undetectable particle uptake in AT2 cells after 4h in submerged conditions and slower phagocytosis and endocytosis rates in epithelial cells [34]The authors hypothesized that the particles require more time for AT2 cells to internalize. Therefore, they increased the exposure time to 24h to observe considerable uptake of particles by cells. [94]. Hence, subsequent experiments on polystyrene particle uptake by alveolar epithelial and macrophage cell lines and toxicity were performed only at 24h.

So, the results of additional experiments after 24 hours of exposure in submerged conditions indicated higher uptake of bigger particles of 1 µm carboxyl modified PS (COOH) by alveolar epithelial cell lines, namely A549, MLE 12, and LA4 compared to smaller particles (Fig 3.4, 3.6). This uptake pattern is consistent with other studies reporting the higher uptake of 40nm and 100nm PS COOH particles than of 20nm by A549 cells [95]. Similarly, it has also been observed in the case of silver particles that uptake is higher at 100nm and 50nm than at 20nm by A549 cells [96]. Similarly, in the study conducted by Santos et al. on the effects of transport inhibitors, it has been observed that 200nm COOH PS particles show higher uptake by Hela (Cervical cancer), A549, 1321N1 (brain astrocytoma) cells than by 40nm COOH PS particles at 37C. They have also reported that actin filament and lipid rafts play an important role in the uptake of bigger particles by A549 cells [97]. This uptake pattern may be due to the larger particles having

multiple uptake routes, such as micropinocytosis, clathrin-mediated, and caveolin-mediated. In contrast, smaller particles can diffuse more easily in and out of the cells. This explanation is supported by Frohlich et al.'s uptake study [98].

Claudia et al. [99] and Frolings et al. [13] have reported that macrophages show a greater uptake of CPS particles compared to A549 cells, and COOH PS have ingested to a greater extent in the co-culture of A549 and THP 1 macrophages due to macrophages' preference for COOH PS. Consistent with these findings, our present study indicates that 1 µm carboxyl-modified PS particles are taken up to a greater extent by MHS cells than by epithelial cell lines (Fig. 3.4). This may be attributed to the fact that macrophages are phagocytic cells. Thus, larger PS COOH particles are ingested more than smaller PS COOH particles. Claudia et al. [99] also reported that 20 nm PS particles are less frequently ingested by macrophages than 200 nm particles, and 200 nm PS particles are ingested more frequently by macrophages than epithelial cells. However, Tetley et al. [93] reported contradictory results, where they observed a greater uptake of 50 nm PS particles than of 100 nm particles by epithelial cells and suggested that sedimentation is not a confounding factor when comparing the effect of size on nanoparticle uptake.

This study has also observed a higher uptake of amine-modified particles (PS NH2) by epithelial cells and macrophages (Fig 3.4, 3.6), which suggests that this may be due to the high affinity of PS NH2 particles for the negatively charged surface of the cell membrane. Interestingly, A549 and MLE 12 cells showed higher uptake of smaller APS particles, which was not observed in PS COOH particles. In MHS cells, a higher uptake of 1 µm PS NH2 particles was observed. In contrast, only a small percentage of 0.1 µm particles were detected, likely due to the higher toxicity of smaller particles (Fig 3.7). Flow cytometry did not detect living cells in these conditions. Additionally, the lower uptake of smaller particles in submerged conditions may be due to their colloidal behavior, including agglomeration, diffusion, and sedimentation rates, which could affect nanoparticle uptake behavior. Larger particles tend to sediment faster and have a greater chance of interacting with the cell monolayer, leading to higher internalization rates. This

phenomenon was observed in a study by Limbach et al., where larger ceria particles (320nm) were ingested more readily by lung fibroblasts than smaller particles (25nm), likely due to the slower rate of diffusion and increased agglomeration of smaller particles [100]

Hence, this uptake data showed that particle uptake was influenced by the particle size and surface charge, with bigger particles being more easily internalized and amine-modified particles exhibiting higher uptake due to their surface charge. The study highlights the importance of considering the colloidal behavior of nanoparticles in understanding their uptake behavior in vitro, and the results have implications for the design and development of nanoparticle-based drug delivery systems for respiratory diseases.

Cytotoxicity caused by PS particles in submerged conditions:

Regarding effects caused by particles, we observed that NH2 PS particles are more toxic toward macrophages (Fig 3.7). This could be related to the higher uptake of particles by macrophages compared to epithelial cells due to their phagocytic behavior and charge of amine-modified particles. Similar behavior has been reported by Tetley et al. in their study on TT1 cells, that these particles create holes in the membrane, whereas unmodified and carboxyl-modified PS do not make any holes to rupture the cell membrane. They used TEM imaging to understand amine nanoparticle uptake by macrophages and observed that these are internalized by an active process and can enter the cytosol via lysosomal rupture [34]. In this study, we also found that smaller amine particles are more toxic than bigger ones (Fig 3.7, 3.8), as reported by Ruenraroengsak et al. They showed that 50nm is more toxic than 100nm PS particles. They found a unique observation that APS particles are associated with severe membrane damage and the formation of holes in the alveolar epithelial cells. Using live cell imaging, they showed that PS NH2 particles initiated the nanosized holes in the cell membrane of live human lung epithelial cells [101]. Another study by Leroueil et al. reported the alteration of cell membrane structure by electrostatic attraction between amino surface groups of particles and phospholipids of the cell membrane by transforming the lipid bilayer of the cell to the liquid phase. Our study also observed this toxicity as LDH released from the cells after exposure to PS NH2

particles. They also observed the ability of PS NH2 particles to induce cytokine release from the cells [102]. So, from these results, we can suggest that negatively charged particles would be more suitable for uptake studies instead of using positively charged particles.

We did not observe significant uptake and toxicity in the case of sulfate-modified particles. Few previous studies have examined sulfate particles. In future studies, we could examine their uptake mechanism by cells in detail (Figs. 3.4, 3.6, 3.7).

Hence, the results indicated that a longer exposure time of 24 hours was necessary to observe significant particle uptake by the cells. Additionally, the particles' uptake pattern varied depending on their size and surface charge, with larger particles and particles modified with amine showing higher uptake by the cells. These findings contribute to our understanding of the factors that affect nanoparticle uptake by lung cells, which is important for assessing their potential toxicity and developing strategies for safely using nanoparticles in various applications.

Uptake of PS particles in ALICE CLOUD exposure:

Based on our submerged data, it has been hypothesized that the absence of an air-liquid interface (ALI) leads to colloidal behavior and reduced uptake of particles. To investigate this further, PS particles were exposed to monocultures of cells grown under ALI conditions in the form of aerosols using the ALICE CLOUD Instrument. This exposure method is more physiologically relevant to in vivo conditions in the alveolar region. Lenz et al. demonstrated that the ALICE exposure system allows for uniform, efficient, and dose-controlled deposition of nanoparticles onto cells. The nebulizer membrane pore size limits the size of deposited agglomerates of nanoparticles to approximately 1 µm [103]. We also used a 1µm pore size nebulizer membrane to limit agglomeration during exposure, which we had previously encountered in the submerged exposure system.

To achieve more realistic in vitro testing, it would be advantageous to culture epithelial cells with other cell types, such as macrophages, dendritic cells, endothelial cells, or mast cells. Several studies have established co-culture and triple co-culture systems using ALI exposure to observe particle uptake. However, our exposure experiments were only conducted on monocultures of epithelial and

macrophage cell lines. To our knowledge, no study has investigated the uptake and toxicity of different particle modifications by other cell lines together. After exposing particles to the ALI exposure system in our study, we observed that even smaller particles were taken up by cells, which was not observed in the submerged exposure system (Fig 3.5, 3.6). This indicates that our hypothesis regarding sedimentation, diffusion, and protein effects in the medium may be accurate and that this problem can be resolved by using the ALI exposure system. However, particle exposure under ALI conditions increased toxicity for all cell lines (Fig 3.9).

Hence, the ALICE CLOUD Instrument and ALI exposure system provided a physiologically relevant in vitro model for studying cell particle uptake. The results suggest that particle uptake may be limited by sedimentation, diffusion, and protein effects in the medium in submerged conditions but not in ALI conditions. However, particle exposure under ALI conditions resulted in more significant toxicity for all cell lines.

Cytotoxicity caused by PS particles in ALICE CLOUD conditions:

Numerous prior investigations have examined the impact of particles on the ALI exposure system. For instance, Herzog et al. demonstrated similar effects of silver particles on the coculture of A549 cells, dendritic cells, and macrophages in both ALI and submerged conditions [104]. Furthermore, Lenz et al. observed the activation of the IL-8 promoter in ALI conditions following exposure to bortezomib particles in A549 cells [84]. Another study by Lenz et al. showed that ZnO NPs induced higher levels of the anti-oxidative enzyme HO-1 in A549 cells in ALI conditions relative to submerged conditions [103]. Based on our results and those previously reported, the toxicity of particles may be underestimated in submerged conditions due to the absence of direct contact between the particles and the plasma membrane of cells resulting from the presence of a medium. Consequently, this study suggests that cells cultured in ALI conditions are more physiologically relevant to uptake and cytotoxicity in in vivo conditions, which should be considered in future research.

Conclusion:

In vitro exposure methods have facilitated investigations of particle-cell interactions, obviating the need for expensive and time-consuming animal models. In conclusion, the uptake data indicates that particle size and surface charge significantly influence particle uptake, with larger particles being more easily internalized and amine-modified particles showing higher uptake due to their surface charge. The study emphasizes the need to consider the colloidal behavior of nanoparticles when examining their uptake behavior in vitro. Also, the combination of the ALICE CLOUD Instrument and ALI exposure system presents a suitable in vitro model for investigating cell particle uptake in a physiologically relevant manner. The findings indicate that particle uptake can be hindered by sedimentation, diffusion, and protein effects in submerged conditions but not in ALI conditions. Nevertheless, particle exposure in ALI conditions increased toxicity across all cell lines studied. These findings have important implications for designing and developing nanoparticle-based drug delivery systems for respiratory diseases.

4.2 **The uptake of PLGA particles by alveolar macrophages and epithelial cells depends on the exposure scenario:** Validation of this co-culture setup's uptake pattern of nanoparticles *in vivo* by intratracheal instillation of nanoparticles in mice.

Objective and Hypothesis:

The **objective** of this study was to utilize a co-culture model comprising alveolar epithelial cells and alveolar macrophages to evaluate the uptake of PLGA nanoparticles and to validate the uptake behavior of nanoparticles in the co-culture setup in vivo by administering nanoparticles via intratracheal instillation in mice.

In pulmonary nanomedicine, animal models have been the primary method of investigating the interaction of particles with the lungs for the study of diseases and novel drug development [103] [105]. However, the need to develop an in vitro

screening platform for particle uptake and release as nano-carriers has become apparent. Although co-cultures have been established for studying particle uptake by alveolar cells, no studies have yet compared in vitro established uptake methods to in vivo models. In this study, we exposed fluorescently labeled PLGA particles to targeted alveolar cell lines in monocultures and cocultures under submerged and air-liquid interface exposure scenarios to mimic the physiological state of the lungs and observe the uptake pattern. We then compared this pattern to the uptake of the same particles by alveolar macrophages and AT2 cells in the mouse lungs in vivo. The novelty of this study lies in its examination of particle uptake in vitro and in vivo, which has not been previously explored by using PLGA particles. To achieve this objective, we conducted a study to examine the uptake kinetics of green fluorescently labeled PLGA particles in vitro using alveolar epithelial cells (LA-4) and alveolar macrophages (MH-S) under both submerged and ALICE CLOUD conditions, as well as in vivo using mouse lungs (BAL macrophages and AT2 cells).

The research hypothesized that a co-culture model at ALI conditions incorporating cellular interactions could mimic the efficiency and relevance of the in vivo lung tissue barrier, enhancing the performance of in vitro screening setups compared to simple monocultures.

Selection of particles:

In this investigation, we employed Poly (lactic-co-glycolic acid) PLGA particles due to their widespread use as biodegradable polymers [105][106]. These particles hydrolyze into lactic acid and glycolic acid monomers, which are biologically endogenous and readily metabolized by Krebs' cycle, resulting in minimal toxicity associated with their use for drug delivery [107]. Moreover, the FDA approves these polymeric particles for human drug delivery systems, and they are commercially available in various molecular weights and monomer ratios [107]. Specifically, we used PLGA 50:50 (lactic acid: glycolic acid) copolymer, consisting of an equal proportion of lactic acid and glycolic acid [108], for this study. These spherical particles exhibit a low polydispersity index (PDI) and can be covalently fluorescently labeled without compromising their physicochemical characteristics

[106]. We selected fluorescently labeled PLGA particles of three different sizes, namely, 0.1 µm, 0.5 µm, and 1 µm, for our research.

Selection of cell lines:

Following inhalation, deposited nanoparticles interact significantly with epithelial cells and macrophages in the alveoli to maintain epithelial integrity [106]. It is important to consider the interaction between these cell types to mimic the physiological response for inhalation studies closely. For the current study, we have selected two significant types of lung cells: epithelial cells (LA-4 cell line) and alveolar macrophages (MH-S cell line), as they are commonly exposed to inhaled particles in inhalation therapies. Macrophages are professional phagocytes and utilize phagocytosis to engulf inhaled particles, while epithelial cells ingest particles through endocytosis [109]. As macrophages are positioned on the top of the epithelial layer in the alveolar region of the lung architecture, these two cell types are crucial for developing an in vitro co-culture model of the lung for particle uptake and release [110].

Particle exposure systems:

In this study, we used submerged conditions and ALICE CLOUD for the nebulization of aerosols to monoculture and co-cultures, as it provides an air-liquid interface that is more physiologically related to the lung environment. Although air-liquid interface exposure has become more widely used in recent years, there are no or little studies on the exposure of PLGA particles to monocultures and co-cultures of alveolar epithelial and macrophage cell lines in both submerged and ALICE exposure scenarios and later also compared to the uptake of particles by alveolar epithelial cells and alveolar macrophages of the mouse lung after intratracheal instillation. Therefore, we have designed our study to investigate the uptake pattern by the co-culture in-vitro model of alveolar epithelial cell lines in submerge and ALI and then compared it with the pattern of particle uptake by mouse lung epithelial cells.

Particle uptake:

To enable the application of particles in various exposure scenarios, a concentration of 10µg/cm2 (1:100 dilution) was selected for submerged conditions, representing a concentration of 100µg/mL. For ALICE CLOUD, a nebulizer containing 250µL of particles at a dilution factor of 1:5 was used, resulting in a concentration of 2.7µg/cm2 and a total particle dose of 400µg across the 143cm2 area of the ALI chamber. Additionally, a dose of 50µg was administered via intratracheal instillation to the mouse model. Different concentrations were employed for submerged and ALI conditions due to the disparity in dilution requirements for particle uptake assessment. Specifically, the 1:100 dilution factor in submerged conditions was adequate for detecting particle uptake using flow cytometry. In contrast, a 1:5 dilution was required for ALI conditions due to the insufficient sensitivity of the 1:100 dilution.

In this study, two detection techniques, namely qualitative detection by fluorescence microscopy and quantitative detection by flow cytometry, were employed to investigate the uptake of particles by cells. A comparison of different detection techniques, including plate reader analysis, image analysis, and flow cytometry, was described by Claudia et al. It was found that plate reader analysis and flow cytometry were promising techniques for reliable uptake studies due to their ability to relate uptake signals to total fluorescence. Flow cytometry was superior to image analysis as it allowed more cells to be measured, and particles with different fluorescent intensities could be compared. [112]. Additionally, histograms generated from flow cytometry analysis allowed the estimation of the number of particles per cell based on their mean fluorescent intensities. However, imaging small fluorescent particles (0.1µm) was challenging due to noticeable sensitivity loss.

This study examined particle exposure to LA-4 and MH-S cell lines separately and in co-culture. The co-culture model was established to reproduce the physiological conditions of the lung, like many other studies [111]. The co-culture was implemented using both submerged and air-liquid interface (ALI) conditions, as it is well-established that submerged conditions are less suitable for investigating

aerosol deposition in the air space of the lung. Kletting et al. [110] It was previously reported that macrophages were weakly attached to the epithelial cell surface under submerged conditions, resulting in fewer macrophages on the top of the epithelial cells compared to ALI conditions.

Previously, Rothen et al. provided evidence suggesting that A549 epithelial cells cannot internalize 1µm polystyrene particles after a 1-hour exposure. They recommended prolonging the exposure duration from 1 hour in future investigations, considering that phagocytosis or macropinocytosis may proceed slower in epithelial cells relative to macrophages [109]. In contrast to their observations, our study revealed that LA-4 cells showed significant uptake of 1µm particles compared to 0.1µm in submerged monocultures and cocultures (Fig 3.11, 3.12). However, under air-liquid interface (ALI) conditions, we did not observe this uptake pattern for LA-4 cells; instead, 0.1 µm particles exhibited significant uptake, which aligns with the physiological response of epithelial cells reported by Tetley et al. in 2014 [34]. In contrast, macrophages demonstrated better uptake of 0.5µm and 1µm particles relative to 0.1 µm under submerged monoculture and coculture conditions. In contrast, there was no significant difference in the uptake pattern of both cultures by MH-S cells under ALI conditions (Fig 3.11).

In this study, the possibility of getting a fluorescence signal from surface-attached particles has been negated through the implementation of trypan blue quenching. Research has indicated that the prevalent method of quenching membrane-bound fluorescein-labeled substances in the context of flow cytometry analyses involves the application of trypan blue. This non-permeable dye has been reported to effectively quench the fluorescence of particles adherent to the cell surface. [113].

The present study investigated the potential impact of particles on mitochondrial and cell membrane integrity, as evaluated by the WST and LDH assays, respectively (Fig 3.15). Our findings demonstrate no significant effect of PLGA particles at a 100µg/mL concentration on either measure of cellular function. These results differ from those reported by Grabowski et al. (2013) [106], who found that neutral

PLGA/PVA nanoparticles exerted cytotoxic effects on A549 cells at concentrations exceeding 1mg/mL as assessed by the MTT assay. Such discrepancies could be attributed to variations in particle size and physicochemical properties resulting from differences in production methodology and the higher concentrations employed in the study.

In vivo, particle uptake studies typically employ intratracheal instillation and inhalation of particles as widely accepted methods for observing particle fate [114]. In this investigation, we conducted intratracheal instillation of 50 µg of PLGA particles in mice and subsequently observed particle uptake patterns in BAL macrophages and primary AT2 cells. Our results indicate no discernible changes in tissue architecture or significant alterations in BAL cell numbers were observed 24 hours after intratracheal instillation of 0.1 mm and 1 µm particles. Furthermore, previous research has demonstrated that exposure of mice to 200-250 nm PLGA nanoparticles with neutral, positive, and adverse surface charges did not elicit an inflammatory response, as evidenced by a lack of variations in cellular populations, protein quantity, or expression of cytokines in BAL. [115].

The present study reveals a consistent pattern of particle uptake by primary alveolar type 2 (AT2) cells in an air-liquid interface (ALI) co-culture system. Specifically, larger particles were preferentially internalized by BAL macrophages. In comparison, smaller particles were initially internalized by AT2 cells, followed by the uptake of larger particles that are typically engulfed via phagocytosis by macrophages and endocytosis by epithelial cells. Hence, the study has identified a consistent pattern of particle uptake AT2 cells in an ALI co-culture system. The pattern indicates that BAL macrophages preferentially internalize larger particles, while AT2 cells internalize smaller particles than larger particles (Fig 3.17, 3.18).

Conclusion: Comparison of PLGA uptake by invitro co-cultures and in vivo:

In this study, we have examined the correlation between particle uptake observed in the air-liquid interface (ALI) co-culture system and the in vivo particle uptake of epithelial cells, which aligns with our research hypothesis. However, it should be noted that for the MHS cell line, a distinct pattern of particle uptake was detected

in bronchoalveolar lavage (BAL) macrophages compared to the ALI co-culture system. Specifically, a higher uptake of 0.1µm particles relative to 1µm particles was observed in the MHS cell line. Conversely, BAL macrophages exhibited superior uptake of larger particles compared to smaller particles. We found that the uptake of 0.1µm particles by the LA4 cell line in the ALI co-culture system and AT2 cells was similar. However, for larger particles, the uptake pattern in AT2 cells differed from that in LA4 cells, as the uptake of 1µm particles was insignificant compared to LA4 cells.

	ALI Coculture		**Mouse lung**	
PLGA (µm)	**LA4 cells**	**MH S cells**	**AT 2**	**AM**
0.1	++	++	++	+
1	++	+	+	++

Thus, we conclude that while both exposure systems showed comparable results for smaller particles, their results diverged for larger particles, warranting further investigation in the future. We suggest that such discrepancies may be attributed to cell type or dose, which should be considered in future studies.

In conclusion, we have successfully established a co-culture model of the human epithelial airway and alveolar tissue using ALICE Cloud to mimic PLGA particle uptake. Our model efficiently mimics the lung tissue barrier and provides a more relevant in vitro screening setup than simple monocultures. This approach can reduce, refine, and replace animal experimentation, meeting the need to establish realistic in vitro setups.

References

[1] N. L. Rosi and C. A. Mirkin, “Nanostructures in bio diagnostics,” *Chem. Rev.*, vol. 105, no. 4, pp. 1547–1562, 2005.

[2] V. Wagner, A. Dullaart, A.-K. Bock, and A. Zweck, “The emerging nanomedicine landscape,” *Nat. Biotechnol.*, vol. 24, no. 10, pp. 1211–1217, 2006.

[3] R. A. Freitas Jr, “What is nanomedicine?,” *Nanomedicine Nanotechnol. Biol. Med.*, vol. 1, no. 1, pp. 2–9, 2005.

[4] R. R. Coombs, Nanotechnology in Medicine and the Biosciences. Gordon and Breach, 1996.

[5] S. Lanone and J. Boczkowski, “Biomedical applications and potential health risks of nanomaterials: molecular mechanisms,” *Curr. Mol. Med.*, vol. 6, no. 6, pp. 651–663, 2006.

[6] E. B. Manaia, M. P. Abuçafy, B. G. Chiari-Andréo, B. L. Silva, J. A. Oshiro Junior, and L. A Chiavacci "Physiochemical characterization of drug nanocarriers" Int J Nanomedicine., vol. 12, pp. 4991–5011, 2017.

[7] Mueller, R. Solid lipid nanoparticles (SLN) for controlled drug delivery—A review of the state of the art. *Eur. J. Pharm. Biopharm.* **2000**, *50*, 161–177.

[8] Mueller, R. Lipid nanoparticles: Recent advances. *Adv. Drug Deliv. Rev.* **2007**, *59*, 375–376

[9] M. Mahmoudi, S. Sant, B. Wang, S. Laurent, and T. Sen, “Superparamagnetic iron oxide nanoparticles (SPIONs): development, surface modification and applications in chemotherapy,” *Adv. Drug Deliv. Rev.*, vol. 63, no. 1–2, pp. 24–46, 2011.

[10] G. Pagona and N. Tagmatarchis, “Carbon nanotubes: materials for medicinal chemistry and biotechnological applications,” *Curr. Med. Chem.*, vol. 13, no. 15, pp. 1789–1798, 2006.

[11] M. J. Bessa, F. Brandão, F. Rosário, L. Moreira, A. T. Reis, V. Valdiglesias, B. Laffon, S. Fraga and J. P. Teixeira, "Assessing the in vitro toxicity of airborne (nano)particles to the human respiratory system: from basic to advanced models," Journal of Toxicology and Environmental Health, Part B, vol. 26, no. 2, pp. 67-96, Mar. 2023. [12] S. H. van Rijt, T. Bein and S. Meiners, "Medical nanoparticles for next-generation drug delivery to the lungs," Eur. Respir. J., vol. 44, pp. 765-774, 2014.

[13] D. Patel, K. Sharma, C. S. Chauhan, and G. Jadon, “An overview on the respiratory system,” *Int. J. Adv. Res. Pharm. Bio Sci.*, vol. 3, no. 1, 2013.

[14] A. Patwa and A. Shah, “Anatomy and physiology of respiratory system relevant to anesthesia,” *Indian J. Anaesth.*, vol. 59, no. 9, pp. 533–541, 2015.

[15] Y. S. Khan and D. T. Lynch, “Histology, lung,” 2018.

[16] J. F. Murray, “Pulmonary edema: pathophysiology and diagnosis,” *Int. J. Tuberc. Lung Dis.*, vol. 15, no. 2, pp. 155–160, 2011.

[17] S. Ganesan, A. T. Comstock, and U. S. Sajjan, Barrier function of airway tract epithelium. Tissue Barriers 1: e24997. 2013.

[18] M. J. Evans, L. S. Van Winkle, M. V. Fanucchi, and C. G. Plopper, “Cellular and molecular characteristics of basal cells in airway epithelium,” *Exp. Lung Res.*, vol. 27, no. 5, pp. 401–415, 2001.

[19] A. R. Brody, “The brush cell,” *Am. J. Respir. Crit. Care Med.*, vol. 172, no. 10, pp. 1349–1349, 2005.

[20] I. Drozdov, I. M. Modlin, M. Kidd, and V. V. Goloubinov, “From Leningrad to London: the saga of Kulchitsky and the legacy of the enterochromaffin cell,” *Neuroendocrinology*, vol. 89, no. 1, pp. 109–120, 2009.

[21] Patton, J.S. *Mechanisms of macromolecule absorption by the lungs*. Adv. Drug Deliv. Rev. **1996**,vol:19, pp: 3–36.

[22] Patton, J.S.; Brain, J.D.; Davies, L.A.; Fiegel, J.; Gumbleton, M.; Kim, K.-J.; Sakagami, M.; Vanbever, R.; Ehrhardt, C. *The particle has landed—Characterizing the fate of inhaled. Pharmaceuticals*. J. Aerosol Med. Pulm. Drug Deliv. **2010**, vol: 23, pp: S71–S87.

[23] Tena, A.F.; Clarà, P.C. *Deposition of inhaled particles in the lungs.* Arch Bronconeumol. **2012**, vol. 48, pp. 240–246.

[24] M. Paranjpe and C. C. Müller-Goymann. Nanoparticle-mediated pulmonary drug delivery: A review. Int. J. Mol. Sci. **2014**, vol: 15, pp: 5852-5873.

[25] M. Nassimi *et al.*, “Low cytotoxicity of solid lipid nanoparticles in vitro and ex vivo lung models,” *Inhal. Toxicol.*, vol. 21, no. sup1, pp. 104–109, 2009.

[26] L.F.C. Silva, G. Kasten, C.E.M. de Campos, A.L. Chinelatto, and E. Lemos-Senna, "Preparation and characterization of quercetin-loaded solid lipid microparticles for pulmonary delivery," Powder Technol., vol. 239, pp. 183-192, 2013.

[27] W. Wang, R. Zhu, Q. Xie, A. Li, Y. Xiao, H. Liu, S. Wang, and D. Cui, "Enhanced bioavailability and efficiency of curcumin for the treatment of asthma by its formulation in solid lipid nanoparticles," Int. J. Nanomed., vol. 7, pp. 3667-3677, 2012.

[28] J. Varshosaz, S. Ghaffari, S.F. Mirshojaei, A. Jafarian, F. Atyabi, and F. Kobarfard, "Biodistribution of amikacin solid lipid nanoparticles after pulmonary delivery," BioMed. Res. Int., vol. 2013, pp. 1-8, 2013.

[29] S.V. Mussi, R.C. Silva, M.C. Oliveira, C.M. Lucci, R.B. Azevedo, and L.A.M. Ferreira, "New approach to improve encapsulation and antitumor activity of doxorubicin-loaded in solid lipid nanoparticles," Eur. J. Pharm. Sci., vol. 48, pp. 282-290, 2013.

[30] J.U. Menon, P. Ravikumar, A. Pise, D. Gyawali, C.C.W. Hsia, and K.T. Nguyen, "Polymeric nanoparticles for pulmonary protein and DNA delivery," Acta Biomater., vol. in press, 2014, doi: 10.1016/j.actbio.2014.01.033

[31] K.K. Gill, S. Nazzal, and A. Kaddoumi, "Paclitaxel loaded PEG5000–DSPE micelles as a pulmonary delivery platform: Formulation characterization, tissue distribution, plasma pharmacokinetics, and toxicological evaluation," Eur. J. Pharm. Biopharm., vol. 79, pp. 276-284, 2011. [32] A. Kolte, S. Patil, P. Lesimple, J. W. Hanrahan, and A. Misra, “PEGylated composite nanoparticles of PLGA and polyethyleneimine for safe and efficient delivery of pDNA to lungs,” *Int. J. Pharm.*, vol. 524, no. 1–2, pp. 382–396, 2017.

[33] R. R. Shinde, M. H. Bachmann, Q. Wang, R. Kasper, and C. H. Contag, “PEG-PLA/PLGA Nanoparticles for In-Vivo RNAi Delivery,” *NSTI Nano Tech Calif.*, 2007.

[34] A. J. Thorley, P. Ruenraroengsak, T. E. Potter, and T. D. Tetley, “Critical determinants of uptake and translocation of nanoparticles by the human pulmonary alveolar epithelium,” *ACS Nano*, vol. 8, no. 11, pp. 11778–11789, 2014.

[35] H. Chen, T. Zhao, Y. Dong, J. Zhang, H. Huang, and J. Zhu, "Paclitaxel-loaded poly(glycolide-co-ε-caprolactone)-b-D-α-tocopheryl polyethylene glycol 2000 succinate nanoparticles for lung cancer therapy," Int. J. Nanomedicine, vol. 8, pp. 1947–1957, 2013.

[36] V. Stock *et al.*, "Uptake and effects of orally ingested polystyrene microplastic particles in vitro and in vivo," *Arch. Toxicol.*, vol. 93, no. 7, pp. 1817–1833, 2019.

[37] D. Yoo, K. Guk, H. Kim, G. Khang, D. Wu, and D. Lee, "Antioxidant polymeric nanoparticles as novel therapeutics for airway inflammatory diseases," Int. J. Pharm., vol. 450, pp. 87-94, 2013.

[38] W. L. Backes, "Passive diffusion of drugs across membranes," 2015.

[39] S. Nizzero, A. Ziemys, and M. Ferrari, "Transport barriers and oncophysics in cancer treatment," *Trends Cancer*, vol. 4, no. 4, pp. 277–280, 2018.

[40] N. K. Rajendran, S. S. D. Kumar, N. N. Houreld, and H. Abrahamse, "A review on nanoparticle-based treatment for wound healing," *J. Drug Deliv. Sci. Technol.*, vol. 44, pp. 421–430, 2018.

[41] P. Foroozandeh and A. A. Aziz, "Insight into cellular uptake and intracellular trafficking of nanoparticles," *Nanoscale Res. Lett.*, vol. 13, no. 1, pp. 1–12, 2018.

[42] S. Sahay, D.Y. Alakhova, and A.V. Kabanov, "Endocytosis of nanomedicines," J Control Release, vol. 145, no. 3, pp. 182-195, 2010.

[43] I. Rivolta, A. Panariti, B. Lettiero, S. Sesana, P. Gasco, M. Gasco, et al., "Cellular uptake of coumarin-6 as a model drug loaded in solid lipid nanoparticles," J Physiol Pharmacol, vol. 62, no. 1, pp. 45, 2011.

[44] K. Sandvig, S. Pust, T. Skotland, and B. van Deurs, "Clathrin-independent endocytosis: mechanisms and function," Curr Opin Cell Biol, vol. 23, no. 4, pp. 413-420, 2011.

[45] J. Adler-Moore and R.T. Proffitt, "AmBisome: Liposomal formulation, structure, mechanism of action and pre-clinical experience," J Antimicrob Chemother, vol. 49, pp. 21-30, 2002.

[46] B. D. Chithrani, A. A. Ghazani, and W. C. Chan, "Determining the size and shape dependence of gold nanoparticle uptake into mammalian cells," *Nano Lett.*, vol. 6, no. 4, pp. 662–668, 2006.

[47] S. E. Gratton *et al.*, "The effect of particle design on cellular internalization pathways," *Proc. Natl. Acad. Sci.*, vol. 105, no. 33, pp. 11613–11618, 2008.

[48] A. Banerjee, J. Qi, R. Gogoi, J. Wong, and S. Mitragotri, "Role of nanoparticle size, shape and surface chemistry in oral drug delivery," *J. Controlled Release*, vol. 238, pp. 176–185, 2016.

[49] C. Liu, J. Shi, Q. Dai, X. Yin, X. Zhang, and A. Zheng, "In-vitro and in-vivo evaluation of ciprofloxacin liposome for pulmonary administration," Drug Dev. Ind. Pharm., pp. 1-7, 2013. doi: 10.3109/03639045.2013.858740

[50] S. Li and N. Malmstadt, "Deformation and poration of lipid bilayer membranes by cationic nanoparticles," *Soft Matter*, vol. 9, no. 20, pp. 4969–4976, 2013.

[51] D. Hühn *et al.*, "Polymer-coated nanoparticles interacting with proteins and cells: focusing on the sign of the net charge," *ACS Nano*, vol. 7, no. 4, pp. 3253–3263, 2013.

[52] J. Todoroff and R. Vanbever, "Fate of nanomedicines in the lungs," *Curr. Opin. Colloid Interface Sci.*, vol. 16, no. 3, pp. 246–254, 2011.

[53] E.D. Hood, M. Chorny, C.F. Greineder, I.S. Alferiev, R.J. Levy, and V.R. Muzykantov, "Endothelial targeting of nanocarriers loaded with antioxidant enzymes for protection against vascular oxidative stress and inflammation," Biomaterials, vol. 35, pp. 3708-3715, 2014.

[54] J. C. Lay, M. R. Stang, P. E. Fisher, J. R. Yankaskas, and W. D. Bennett, “Airway retention of materials of different solubility following local intrabronchial deposition in dogs,” *J. Aerosol Med.*, vol. 16, no. 2, pp. 153–166, 2003.

[55] J. Rejman, V. Oberle, I.S. Zuhorn, and D. Hoekstra, "Size-dependent internalization of particles via the pathways of clathrin- and caveolae-mediated endocytosis," Biochem. J., vol. 377, pp. 159-169, 2004.

[56] A. Woods *et al.*, “In vivo biocompatibility, clearance, and biodistribution of albumin vehicles for pulmonary drug delivery,” *J. Controlled Release*, vol. 210, pp. 1–9, 2015.

[57] L. Yang, L. Shang, and G.U. Nienhaus, "Mechanistic aspects of fluorescent gold nanocluster internalization by live HeLa cells," Nanoscale, vol. 5, pp. 1537-1543, 2013.

[58] L. Yang, F. Stockmar, N. Azadfar, and G.U. Nienhaus, "Intracellular thermometry by using fluorescent gold nanoclusters," Angew Chem Int Ed Engl, vol. 52, pp. 11154-11157, 2013.

[59] X. Jiang, J. Dausend, M. Hafner, A. Musyanovych, C. Röcker, K. Landfester, V. Mailänder, and G.U. Nienhaus, "Specific effects of surface amines on polystyrene nanoparticles in their interactions with mesenchymal stem cells," Biomacromolecules, vol. 11, pp. 748-753, 2010.

[60] O. Lunov, T. Syrovets, C. Loos, J. Beil, M. Delacher, K. Tron, G.U. Nienhaus, A. Musyanovych, V. Mailänder, K. Landfester, and T. Simmet, "Differential uptake of functionalized polystyrene nanoparticles by human macrophages and a monocytic cell line," ACS Nano, vol. 5, pp. 1657-1669, 2011.

[61] J.C. Sung, B.L. Pulliam, and D.A. Edwards, "Nanoparticles for drug delivery to the lungs," Trends in Biotechnology, vol. 25, pp. 563-570, 2007.

[62] H. Yuan, C.-Y. Chen, G. Chai, et al., "Improved transport and absorption through the gastrointestinal tract by PEGylated solid lipid nanoparticles," Molecular Pharmaceutics, vol. 10, pp. 1865-1873, 2013.

[63] S.H. van Rijt, T. Bein, and S. Meiners, "Medical nanoparticles for next-generation drug delivery to the lungs," The European Respiratory Journal, vol. 44, pp. 765-774, 2014.

[64] E. Fröhlich and C. Meindl, "In Vitro Assessment of Chronic Nanoparticle Effects on Respiratory Cells," Nanomaterials - Toxicity and Risk Assessment, 2015, http://dx.doi.org/10.5772/60701

[65] T. Mosmann, “Rapid colorimetric assay for cellular growth and survival: application to proliferation and cytotoxicity assays,” *J. Immunol. Methods*, vol. 65, no. 1–2, pp. 55–63, 1983.

[66] L. A. Dailey *et al.*, “Investigation of the proinflammatory potential of biodegradable nanoparticle drug delivery systems in the lung,” *Toxicol. Appl. Pharmacol.*, vol. 215, no. 1, pp. 100–108, 2006.

[67] R. U. Janicke, M. L. Sprengart, M. R. Wati, and A. G. Porter, “Caspase-3 is required for DNA fragmentation and morphological changes associated with apoptosis,” *J. Biol: Chem.*, vol. 273, no. 16, pp. 9357–9360, 1998.

[68] G. Koopman, C. P. Reutelingsperger, G. A. Kuijten, R. M. Keehnen, S. T. Pals, and M. H. Van Oers, “Annexin V for flow cytometric detection of phosphatidylserine expression on B cells undergoing apoptosis,” 1994.

[69] O. Sorg, “Oxidative stress: a theoretical model or a biological reality?,” *C. R. Biol.*, vol. 327, no. 7, pp. 649–662, 2004.

[70] B. M. Babior, “Phagocytes and oxidative stress,” *Am. J. Med.*, vol. 109, no. 1, pp. 33–44, 2000.

[71] J. Kelley, “Cytokines of the lung,” *Am Rev Respir Dis*, vol. 141, no. 3, pp. 765–788, 1990.

[72] B. Trouiller, R. Reliene, A. Westbrook, P. Solaimani, and R. H. Schiestl, “Titanium dioxide nanoparticles induce DNA damage and genetic instability in vivo in mice,” *Cancer Res.*, vol. 69, no. 22, pp. 8784–8789, 2009.

[73] E.-J. Park, J. Yi, K.-H. Chung, D.-Y. Ryu, J. Choi, and K. Park, “Oxidative stress and apoptosis induced by titanium dioxide nanoparticles in cultured BEAS-2B cells,” *Toxicol. Lett.*, vol. 180, no. 3, pp. 222–229, 2008.

[74] K. Bhattacharya, M. Davoren, J. Boertz, R. P. Schins, E. Hoffmann, and E. Dopp, “Titanium dioxide nanoparticles induce oxidative stress and DNA-adduct formation but not DNA-breakage in human lung cells,” *Part. Fibre Toxicol.*, vol. 6, no. 1, pp. 1–11, 2009.

[75] M. S. Cartiera, K. M. Johnson, V. Rajendran, M. J. Caplan, and W. M. Saltzman, “The uptake and intracellular fate of PLGA nanoparticles in epithelial cells,” *Biomaterials*, vol. 30, no. 14, pp. 2790–2798, 2009.

[76] A. D. Lehmann, N. Daum, M. Bur, C.-M. Lehr, P. Gehr, and B. M. Rothen-Rutishauser, “An in vitro triple cell co-culture model with primary cells mimicking the human alveolar epithelial barrier,” *Eur. J. Pharm. Biopharm.*, vol. 77, no. 3, pp. 398–406, 2011.

[77] J. Geys *et al.*, “In vitro study of the pulmonary translocation of nanoparticles: a preliminary study,” *Toxicol. Lett.*, vol. 160, no. 3, pp. 218–226, 2006.

[78] M. I. Hermanns, R. E. Unger, K. Kehe, K. Peters, and C. J. Kirkpatrick, “Lung epithelial cell lines in coculture with human pulmonary microvascular endothelial cells: development of an alveoli-capillary barrier in vitro,” *Lab. Invest.*, vol. 84, no. 6, pp. 736–752, 2004.

[79] B. M. Rothen-Rutishauser, S. G. Kiama, and P. Gehr, “A three-dimensional cellular model of the human respiratory tract to study the interaction with particles,” *Am. J. Respir. Cell Mol. Biol.*, vol. 32, no. 4, pp. 281–289, 2005.

[80] B. Rothen-Rutishauser, L. Müller, F. Blank, C. Brandenberger, C. Mühlfeld, and P. Gehr, “A newly developed in vitro model of the human epithelial airway barrier to study the toxic potential of nanoparticles,” *ALTEX-Altern. Anim. Exp.*, vol. 25, no. 3, pp. 191–196, 2008.

[81] C. Brandenberger *et al.*, “Effects and uptake of gold nanoparticles deposited at the air-liquid interface of a human epithelial airway model,” *Toxicol. Appl. Pharmacol.*, vol. 242, no. 1, pp. 56–65, 2010.

[82] B. Rothen-Rutishauser *et al.*, “Direct combination of nanoparticle fabrication and exposure to lung cell cultures in a closed setup as a method to simulate accidental nanoparticle exposure of humans,” *Environ. Sci. Technol.*, vol. 43, no. 7, pp. 2634–2640, 2009.

[83] A. J. Ghio, L. A. Dailey, J. M. Soukup, J. Stonehuerner, J. H. Richards, and R. B. Devlin, “Growth of human bronchial epithelial cells at an air-liquid interface alters the response to particle exposure,” *Part. Fibre Toxicol.*, vol. 10, no. 1, pp. 1–8, 2013.

[84] A.-G. Lenz *et al.*, “Efficient bioactive delivery of aerosolized drugs to human pulmonary epithelial cells cultured in air-liquid interface conditions,” *Am. J. Respir. Cell Mol. Biol.*, vol. 51, no. 4, pp. 526–535, 2014.

[85] S. Upadhyay and L. Palmberg, “Air-liquid interface: relevant in vitro models for investigating air pollutant-induced pulmonary toxicity,” *Toxicol. Sci.*, vol. 164, no. 1, pp. 21–30, 2018.

[86] S. van Riet *et al.*, “In vitro modeling of alveolar repair at the air-liquid interface using alveolar epithelial cells derived from human induced pluripotent stem cells,” *Sci. Rep.*, vol. 10, no. 1, pp. 1–12, 2020.

[87] A. A. Pezzulo *et al.*, “The air-liquid interface and use of primary cell cultures are important to recapitulate the transcriptional profile of in vivo airway epithelia,” *Am. J. Physiol.-Lung Cell. Mol. Physiol.*, vol. 300, no. 1, pp. L25–L31, 2011.

[88] F. Blank *et al.*, “Interaction of biomedical nanoparticles with the pulmonary immune system,” *J. Nanobiotechnology*, vol. 15, no. 1, pp. 1–9, 2017.

[89] S. Dhanasekaran, “SMART Drug Based Targeted Delivery: A New Paradigm for Nanomedicine Strategies,” *Int. J. Immunother. Cancer Res.*, vol. 1, no. 1, pp. 008–012, 2015.

[90] S. H. Van Rijt *et al.*, “Applicability of avidin protein coated mesoporous silica nanoparticles as drug carriers in the lung,” *Nanoscale*, vol. 8, no. 15, pp. 8058–8069, 2016.

[91] S. H. Sim *et al.*, “Innate immune responses of pulmonary epithelial cells to Burkholderia pseudomallei infection,” *PLoS One*, vol. 4, no. 10, p. e7308, 2009.

[92] K. A. Wikenheiser *et al.*, “Production of immortalized distal respiratory epithelial cell lines from surfactant protein C/simian virus 40 large tumor antigen transgenic mice.,” *Proc. Natl. Acad. Sci.*, vol. 90, no. 23, pp. 11029–11033, 1993.

[93] P. Ruenraroengsak and T. D. Tetley, “Differential bioreactivity of neutral, cationic and anionic polystyrene nanoparticles with cells from the human alveolar compartment: robust response of alveolar type 1 epithelial cells,” *Part. Fibre Toxicol.*, vol. 12, no. 1, pp. 1–20, 2015.

[94] B. Rothen-Rutishauser *et al.*, *Nanomed.*, vol. 9, no. 5, pp. 607–621, 2013, doi: 10.2217/nnm.13.24.

[95] T. dos Santos, J. Varela, I. Lynch, A. Salvati, and K. A. Dawson, *PLoS One*, vol. 6, no. 9, p. e24438, 2011, doi: 10.1371/journal.pone.0024438.

[96] M. Wu, H. Guo, L. Liu, Y. Liu, and L. Xie, “Size-dependent cellular uptake and localization profiles of silver nanoparticles,” *Int. J. Nanomedicine*, vol. 14, p. 4247, 2019.

[97] T. Dos Santos, J. Varela, I. Lynch, A. Salvati, and K. A. Dawson, “Effects of transport inhibitors on the cellular uptake of carboxylated polystyrene nanoparticles in different cell lines,” *PloS One*, vol. 6, no. 9, p. e24438, 2011.

[98] C. Meindl, K. Öhlinger, V. Zrim, T. Steinkogler, and E. Fröhlich, “Screening for effects of inhaled nanoparticles in cell culture models for prolonged exposure,” *Nanomaterials*, vol. 11, no. 3, p. 606, 2021.

[99] M. Claudia, O. Kristin, O. Jennifer, R. Eva, and F. Eleonore, “Comparison of fluorescence-based methods to determine nanoparticle uptake by phagocytes and non-phagocytic cells in vitro,” *Toxicology*, vol. 378, pp. 25–36, 2017.

[100] L. K. Limbach *et al.*, “Oxide nanoparticle uptake in human lung fibroblasts: effects of particle size, agglomeration, and diffusion at low concentrations,” *Environ. Sci. Technol.*, vol. 39, no. 23, pp. 9370–9376, 2005.

[101] P. Ruenraroengsak *et al.*, “Respiratory epithelial cytotoxicity and membrane damage (holes) caused by amine-modified nanoparticles,” *Nanotoxicology*, vol. 6, no. 1, pp. 94–108, 2012.

[102] P. R. Leroueil, S. Hong, A. Mecke, J. R. Baker Jr, B. G. Orr, and M. M. Banaszak Holl, “Nanoparticle interaction with biological membranes: does nanotechnology present a Janus face?,” *Acc. Chem. Res.*, vol. 40, no. 5, pp. 335–342, 2007.

[103] A. G. Lenz *et al.*, “A dose-controlled system for air-liquid interface cell exposure and application to zinc oxide nanoparticles,” *Part. Fibre Toxicol.*, vol. 6, no. 1, pp. 1–17, 2009.

[104] F. Herzog *et al.*, “Mimicking exposures to acute and lifetime concentrations of inhaled silver nanoparticles by two different in vitro approaches,” *Beilstein J. Nanotechnol.*, vol. 5, no. 1, pp. 1357–1370, 2014.

[105] F. Emami, S. J. Mostafavi Yazdi, and D. H. Na, “Poly (lactic acid)/poly (lactic-co-glycolic acid) particulate carriers for pulmonary drug delivery,” *J. Pharm. Investig.*, vol. 49, no. 4, pp. 427–442, 2019.

[106] N. Grabowski *et al.*, “Toxicity of surface-modified PLGA nanoparticles toward lung alveolar epithelial cells,” *Int. J. Pharm.*, vol. 454, no. 2, pp. 686–694, 2013.

[107] S. Kumari, S. Swetha, and S. Mayor, *Cell Res*, vol. 20, pp. 256–275, 2010, doi: 10.1038/cr.2010.19.

[108] F. U. Amin, S. A. Shah, H. Badshah, M. Khan, and M. O. Kim, “Anthocyanins encapsulated by PLGA@ PEG nanoparticles potentially improved its free radical scavenging capabilities via p38/JNK pathway against Aβ1–42-induced oxidative stress,” *J. Nanobiotechnology*, vol. 15, no. 1, pp. 1–16, 2017.

[109] D. A. Kuhn *et al.*, “Different endocytotic uptake mechanisms for nanoparticles in epithelial cells and macrophages,” *Beilstein J. Nanotechnol.*, vol. 5, no. 1, pp. 1625–1636, 2014.

[110] S. Kletting *et al.*, “Co-culture of human alveolar epithelial (hAELVi) and macrophage (THP-1) cell lines.,” 2018.

[111] C. Endes *et al.*, “An in vitro testing strategy towards mimicking the inhalation of high aspect ratio nanoparticles,” *Part. Fibre Toxicol.*, vol. 11, no. 1, pp. 1–13, 2014.

[112] M. Claudia, O. Kristin, O. Jennifer, R. Eva, and F. Eleonore, “Comparison of fluorescence-based methods to determine nanoparticle uptake by phagocytes and non-phagocytic cells in vitro,” *Toxicology*, vol. 378, pp. 25–36, 2017.

[113] S. Vranic *et al.*, “Deciphering the mechanisms of cellular uptake of engineered nanoparticles by accurate evaluation of internalization using imaging flow cytometry,” *Part. Fibre Toxicol.*, vol. 10, no. 1, pp. 1–16, 2013.

[114] E. Fröhlich and S. Salar-Behzadi, “Toxicological assessment of inhaled nanoparticles: role of in vivo, ex vivo, in vitro, and insilico studies,” *Int. J. Mol. Sci.*, vol. 15, no. 3, pp. 4795–4822, 2014.

[115] N. Grabowski *et al.*, “Surface coating mediates the toxicity of polymeric nanoparticles towards human-like macrophages,” *Int. J. Pharm.*, vol. 482, no. 1–2, pp. 75–83, 2015.

[116] T. Stoeger, C. Reinhard, S. Takenaka, A. Schroeppel, E. Karg, B. Ritter, J. Heyder, and H. Schulz, "Instillation of Six Different Ultrafine Carbon Particles Indicates a Surface Area Threshold Dose for Acute Lung Inflammation in Mice," Environmental Health Perspectives, vol. 114, no. 3, pp. 328-333, Mar. 2006.

Acknowledgments

I would like to begin by expressing my sincere gratitude to the German Academic Exchange Service (DAAD) for awarding me a scholarship to pursue my PhD studies. Their financial support has allowed me to pursue my academic and research goals, and I am deeply grateful for this opportunity.

I am also grateful to my supervisor, Prof. Dr. rer. nat. Silke Meiners, Dr. Tobias Stöger, and Prof. Dr. rer. nat. Markus Rehberg, for their invaluable guidance and mentorship throughout my PhD research. Their expertise, insightful feedback, and unwavering commitment have shaped my research and academic growth.

I want to acknowledge the Institute of Lung Biology and Disease at Helmholtz Zentrum Munich for providing the necessary facilities and resources for my research. The state-of-the-art equipment, technical support, and collaborative environment have enabled me to conduct my experiments and achieve my research objectives.

I would also like to thank the Munich Medical Research School (MMRS) and CPC Research School for admitting me and granting me the opportunity to pursue my PhD degree. Their support, networking opportunities, and scientific events have been instrumental in advancing my academic and professional goals.

Finally, I would also like to extend my heartfelt thanks to my colleagues, husband, parents, family, and friends for their unwavering support and encouragement throughout my academic journey. Their love, patience, and understanding have been my source of strength during challenging times, and I am forever indebted to them.

Affidavit

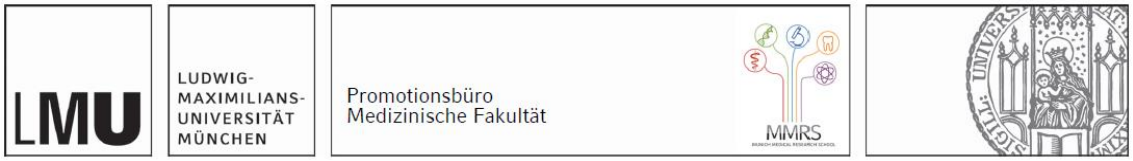

Affidavit

Ishaque, Mehwish
_____
Surname, first name

_____
Street

_____
Zip code, town, country

I hereby declare that the submitted thesis entitled:

Nanocarriers for cell-specific targeting in the lung and development of an in vivo validated in-vitro screening platform of drug uptake and release

……

It is my own work. I have only used the sources indicated and have not made unauthorized use of the services of a third party. Where the work of others has been quoted or reproduced, the source is always given.

I further declare that the dissertation presented here has not been submitted in the same or similar form to any other institution for the purpose of obtaining an academic degree.

2.10.2025 _____ Mehwish _____

place, date Signature doctoral candidate

Confirmation of congruency

LMU LUDWIG-MAXIMILIANS-UNIVERSITÄT MÜNCHEN

Promotionsbüro
Medizinische Fakultät

MMRS

Confirmation of congruency between printed and electronic version of the doctoral thesis

Ishaque, Mehwish
Surname, first name

Street

Zip code, town, country

I hereby declare, that the submitted thesis entitled:

Nanocarriers for cell-specific targeting in the lung and development of an in vivo validated in-vitro screening platform of drug uptake and release

……

is congruent with the printed version both in content and format.

Munich, 2.10.2025
place, date

Mehwish
Signature doctoral candidate